

# 'Predicting the degradation of surface pavement due to raveling'

## ***Graduation Thesis***

### *Colophon*

Final presentation date '03-07-2017'

### *Personal information*

Name J.H. (Jens) Boersma  
Student ID 0831067  
Email address j.h.boersma@student.tue.nl

### *Graduation committee*

Chairman Prof.dr.ir B. (Bauke) de Vries  
Supervisor dr. G.Z. (Gamze) Dane  
2<sup>nd</sup> supervisor dr. ing. P.J.H.J. (Peter) van der Waerden  
Supervisor of the company Ing. P. (Pieter) van Dueren den Hollander (Heijmans)

### *Institute*

University Eindhoven University of Technology  
Faculty Faculty of the Built Environment  
Department Construction, Management and Engineering



## Table of Content

Preface.....	5
Summary .....	6
Samenvatting.....	8
Abstract .....	11
Interview with experts .....	11
1 Introduction.....	13
1.2 Problem Definition research and Research design .....	14
1.3 Expected results .....	15
2. Literature study .....	17
2.1 ‘Design, Build, Finance, and Maintain’ contracts in The Netherlands .....	17
2.2 Porous asphalt concrete.....	18
2.3 Environmental impact and traffic loads .....	19
2.4 Statistical methods of external factors that have an impact on the degradation of surface pavement .....	21
2.5 Conclusion .....	23
3. Theoretical Framework .....	25
3.1 The datasets that are implemented in the model .....	25
3.1.1 Dataset surface pavement .....	26
3.1.2 Traffic intensity dataset.....	26
3.1.3 Temperature dataset.....	26
3.1.4 Visual inspections .....	27
3.2 FME model design .....	31
3.2.1 Process description model design FME.....	31
3.3 Analyzing manipulated data and making assumptions.....	33
3.4 Best-fit curve .....	35
3.5 Monte Carlo simulation method .....	36
3.6 An overview of the process of producing the prediction the risk over time model .....	37
4. Results of the Model .....	41
4.1 Results of the complete dataset and the impact of cold weather on the surface pavement with the ‘Heijmans’ approach .....	41
4.1.2 Impact of traffic on surface pavement.....	41
4.2.3 The impact of cold weather and traffic intensity combined .....	42
4.3 Fatigue failure ratio over time.....	46
4.3.1 Results of the complete dataset and the impact of cold weather on the surface pavement due to plotting the fatigue failure ratio over time.....	46

4.3.3	Impact of traffic and cold weather on surface pavement because of plotting fatigue failure ratio over time .....	48
4.4	Best-fit curve .....	51
4.5	'Monte Carlo' simulation.....	54
4.5.1	Case study project 'A12 VEG' .....	55
4.6	Summary Results.....	56
5.	Conclusions.....	59
6.	Discussion and recommendations .....	61
6.1	FME model.....	61
6.2	predicting the risk model .....	61
6.3	Monitoring surface pavement.....	62
6.4	'Quality' of the surface pavement.....	63
6.5	Archiving the data .....	63
6.6	The impact of the parameters traffic intensity and cold weather .....	63
	Reverences .....	65
	Appendix A .....	70
	Appendix B .....	75
	Appendix C .....	76
	Appendix D .....	77
	Appendix E.....	79
	Light 'TI' .....	80
	Light 'TI', 'T-extreme' >20 days .....	81
	Light 'TI', 'T-extreme' > 30 days .....	82
	Moderate 'TI' .....	83
	Moderate 'TI', 'T-extreme' > 20 days .....	84
	Moderate 'TI', 'T-extreme' > 30 days .....	85
	Heavy 'TI' .....	86
	Heavy 'TI', 'T-extreme' > 20 days .....	87
	Heavy 'TI', 'T-extreme' > 30 days .....	88
	Appendix F.....	89
	Appendix G .....	93

## Preface

This thesis for the MSc. Programme Construction Management & Engineering was written during the academic year of 2016-2017. I remember when I first stepped into the office of the supervisor of my graduation committee, dr. G.Z. (Gamze) Dane at mid-summer of 2016. That I had subject for my graduation thesis and I needed to clarify my subject. Gamze did not know anything about asphalt but gave here blessing if I could show her that I really wanted to do this subject. At that moment I had meetings with ing. Pieter van Dueren den Hollander to make a probability model for degradation of asphalt construction over time, because 'Heijmans' wanted to predict the degradation curve of the asphalt. We came up with the idea to construct a database and with this database, I could produce a prediction model. I started at 'Heijmans' in the beginning of September 2016.

The last 8 months I have been working on this thesis. In the beginning, it was not easy to scope the research problem and to produce a valid database. But, it was interesting, fun, and have learned a lot about how to handle data. During the process, I have learned how to pick the right data, merge data, and analyzing data. Furthermore, I have learned a lot about how to produce prediction models. I want to thank sincerely 'Heijmans' for having me. Furthermore, I want to thank my graduation committee for having the faith in me and that I could do it. And last but not least I want to thank my brother MSc. Quinten Boersma who has helped me during the process of this thesis. I sometimes felt lost and he always inspired me and gave me good feedback during the process.

Jens Boersma,  
Rosmalen/Utrecht,  
April 2017

## Summary

In the Netherlands, a shift from traditional contract to maintenance contracts has taken place in the infrastructural sector. Therefore, contractors want to know how their product behaves over time. Due to the new contract forms, the contractors are responsible for the design, construction, financing, and maintenance of a project through these maintenance contracts. This implies that following this new contract design, the contractors, and no longer Rijkswaterstaat, are now responsible for the risks involved with a project.

Having to work with this new contract format, contractors have an increasing interest in risk assessment regarding the degradation of asphalt and especially porous asphalt concrete (PAC). PAC is widely used as a surface pavement for highways due to its properties. Present, about 90% of the highways are provided with a PAC construction, this will increase in the future. PAC characteristic is that noise pollution decreases due by traffic. Furthermore, it is easier to drain water than dense asphalt concrete (DAC). These properties are caused by the fact that PAC constructions have a higher percentage of air voids. The disadvantage of PAC surface pavement is that it degrades faster over time. Furthermore, predicting the degradation risk over time of the surface pavement is at this moment not accurate.

Literature research shows that traffic loading and environmental factors have the largest effect on degradation risk on PAC over time. These factors often cause a type of damage called 'raveling'. Raveling is caused by the fact that the granule is forced-out from the binder. This is because the binder loses its flexibility over time due to traffic loading and environmental impact.

This research focusses on how to predict the degradation caused by raveling. According to laboratory research, predicting what the degradation risks are for a longer time on PAC surface pavement due to sampling, is difficult. Therefore, in this study, a statistical method has been chosen to make a more accurate prediction of asphalt degradation over time. The question for that matter is; 'To what extent is it possible to predict the risk factor of excavation that affects the degree of degradation of asphalt on the highways in the Netherlands, based on external factors that affect the fatigue difference of the top layer?'

The predictive model has been developed by combining different empirical data sets and plotting them over time. These data sets include; construction dates of the existing surface pavements of all highways in the Netherlands, type of asphalt, traffic loading in the Netherlands, local weather data, and the state of the asphalt through visual inspections.

To merge the data sets, the software program 'Feature Manipulation Engine' (FME) has been used. This program is used to link information with each other. Asphalt is divided into 100-meter tiles. The following information is linked to the 100-meter tiles subjects: Construction date, date of inspection, the number of days exposed to cold days colder than  $-10\text{ C}^{\circ}$ , the state of the asphalt at the time of inspection, and the traffic load that the 100-meter tile was exposed to during the life-cycle of the pavement. Furthermore, according to the literature truck traffic has the highest impact on the degradation on the surface pavement. Therefore, only the driving lanes that are used by truck traffic are used for this research.

The data acquired in this research shows significant scattering. Therefore, we applied a filtering technique in order to properly analyze the data. With this filtering technique, the correlation between environmental impact and traffic load over the time of degradation was analyzed. The data shows that these variables have a significant impact on the degradation of asphalt and that the amount of scattering increases over time. The data also shows that the traffic load has a bigger impact with respect to the effects of cold weather. However, the scattering, most likely caused by the initial state (quality) of the surface pavement remained. This implies that the produced plots and applied filtering technique were not accurate enough to produce a prediction model. Therefore, we have chosen to plot the measured data differently. In these new figures, we have chosen to plot moment where the asphalt has degraded so much that it no longer meets the requirements of the contract (fatigue failure). These plots filter out the scattering. The results show that traffic loading still has more impact than cold weather. The datasets which depict the impact of weather and traffic load together show no clear difference with respect to the datasets which only show the effects of traffic intensity.

This way of plotting is used to produce a best-fit curve. In order to produce the best-fit curve, the cumulative beta distribution (cumulative distribution function (CDF)) is used. The fatigue failure ratio is easy to implement in the model. Furthermore, CDF is flexible and has a natural curve. The CDF model has been adapted as best-fit by means of a regression analyzes. In this research, we assess the standard deviation of the measured data with the predictive model, using a moving average. This calculated error is then used in order create a Monte Carlo simulation which captures the scattering in the data. Furthermore, in all datasets, this error is greater than the difference between the scenario of 'only traffic loading' and the scenarios of 'traffic loading combined with cold weather'. These scenarios were implemented in a Monte Carlo simulation model to simulate the risk of fatigue failure ratio over time.

The conclusion of the research depicts that the prediction model can predict that when the traffic load increases the risk of fatigue failure ratio over time increases. And that traffic loading has a more significant impact on the risk on fatigue failure ratio than cold weather.

## Samenvatting

Doordat er in Nederland een verschuiving heeft plaats gevonden van traditionele contract vormen naar onderhoudscontracten in de branche van de civiele uitvoering willen aannemers beter weten wat hun product is en hoe het zich gedraagt over de tijd. Dit komt door dat aannemers de verantwoordelijkheid krijgen over het ontwerp, bouwen, financieren, en het onderhouden van een project door deze onderhoudscontracten. Rijkswaterstaat legt de risico's door deze contractvormen bij de aannemer.

Dit onderzoek focust zich op het feit dat aannemers willen weten hoe de degradatie risico's lopen van asfalt en dan met name zeer open asfalt beton (ZOAB). ZOAB wordt namelijk veel gebruikt als toplaag voor snelwegen door de eigenschappen. Op dit moment is ongeveer 90 % van de snelwegen voorzien van ZOAB en dit zal alleen maar meer worden. ZOAB heeft namelijk als eigenschap dat het geluid reducerend werkt. Verder kan het gemakkelijker water afvoeren dan dicht asfalt beton (DAB). Deze eigenschappen komt omdat er grotere holle ruimte in ZOAB zitten. Het nadeel van ZOAB is dat het sneller degradeert en men niet accuraat kan voorspellen wanneer de vervangen dient te worden.

Verkeersbelasting en milieubelasting zijn volgens de literatuur externe factoren die invloed hebben op het degraderen van ZOAB over de tijd. Deze factoren veroorzaken vaak een type schade genaamd 'rafeling'. Rafeling ontstaat doordat het granulaat loslaat van de bindmiddel. Dit komt omdat het bindmiddel zijn flexibiliteit verliest over de tijd door verkeersbelasting en de milieubelasting.

Dit onderzoek wil aan de hand van de externe factoren die invloed hebben op het degraderen van ZOAB wat het schade type veroorzaakt 'rafeling' te kunnen voorspellen. Dit is gedaan door eerst te kijken naar wat de literatuur hier over zegt. Volgens laboratorium onderzoek is het niet accuraat te voorspellen wat de degradatie risico's zijn over een langere tijd voor ZOAB monsters uit het veld. Daarom, is er in dit onderzoek een statistische methode gekozen om een nauwkeurigere voorspelling te kunnen maken van degradatie van asfalt over de tijd. De vraag die daar bij speelt is; 'In hoeverre is het mogelijk om de risicofactoren van rafeling te voorspellen die de afbraakgraad van de toplaag van asfalt op de snelwegen in Nederland beïnvloeden, op basis van externe factoren die invloed hebben op het vermoeidheidsverschil van de toplaag?'

Het voorspellende model is ontwikkeld doormiddel van verschillende empirische datasets samen te voegen en deze te plotten over de tijd. Deze datasets bevatten aan legdatums over de aanwezige toplagen van alle snelwegen in Nederland, type asfalt, verkeersbelasting in Nederland, weergegevens van weerstations, en de kwaliteit van asfalt doormiddel van visuele inspecties.

Om de datasets samen te voegen het software programma 'Feature Manipulation Engine'(FME). Dit programma is gebruikt om informatie aan elkaar te linken. Asfalt is opgedeeld in 100 meter vakken. Aan deze vakken is de volgende informatie gelinkt; aanleg datum, datum van inspectie, aantal dagen dat de 100 meter vakken zijn bloot gesteld aan koude dagen kouder dan  $-10^{\circ}\text{C}$ , de kwaliteit van het asfalt, en de verkeersbelasting waar het 100 meter vak is aan bloot gesteld.

Voor het onderzoek alleen de rijbanen waar vrachtwagen verkeer gebruik van maakt is gebruikt omdat volgens de literatuur de vrachtwagens de meeste en het snelst schade aanrichten bij de toplaag van de asfalt constructie. Bij het analyseren van de data is er naar voren gekomen dat er een grote spreiding is in de gemeten data over de tijd. Daarom is er eerst gekozen om te kijken doormiddel van een filtering techniek te kijken over er correlatie tussen milieubelasting en verkeersbelasting met degradatie over de tijd. Hierin kwam naar voren dat dat zichtbaar is maar de spreiding bleef groot en bleef toe nemen over de tijd. Ook al, kan men zeggen dat verkeersbelasting een grotere impact heeft op de degradatie van asfalt over de tijd dan de weerbelasting de spreiding bleef te groot om een accurate voorspellingsmodel te kunnen maken met deze weergaven van de gemeten data te plotten. Om deze spreiding er uit te kunnen filteren hebben we gekozen om er anders naar te kijken en de gemeten data anders te plotten. Er is gekeken wanneer het asfalt zo erg gedegradeerd is dat het niet meer voldoet aan de eisen van het contract (vermoeidheidsuitval). Er is gekozen om de gemeten data te plotten als vermoeidheidsprobleemverhouding over de tijd, om de spreiding er uit te filteren. Hier komt naar voren dat verkeersbelasting nog steeds meer impact heeft dan weersbelasting maar dan zonder de spreiding. Ook is er gekeken wat de impact is van als de twee factoren zijn samengevoegd. Hierin, is geen duidelijke significantie waargenomen.

Deze manier van plotten is daarna gebruikt waarschijnlijkheidsmodel te produceren. Om dit te produceren de cumulatieve bèta distributie (cumulatieve distributie functie(CDF)) is gebruikt omdat de vermoeidheidsuitval is geplot als ratio en om zijn flexibele natuurlijke eigenschappen. Het CDF model is er als best fit ingepast doormiddel van een regressie analyse. De laatste stap in het proces is aangenomen dat de waarschijnlijkheidsmodellen waar zijn maar wel een standaardfout mee te nemen. Omdat de standaardfout groter is dan het verschil tussen de scenario's van alleen verkeersbelasting en als de weersbelasting is toegevoegd in het scenario. Is er gekozen om alleen de verkeersbelasting scenario's te gebruiken om in een Monte Carlo simulatie te stoppen.

Uit het waarschijnlijkheids simulatiemodel kan worden geconcludeerd dat als de verkeersbelasting toeneemt het risico op vermoeidheidsuitval eerder plaats vind over de tijd. En dat verkeersbelasting een significantere impact heeft op het risico op vermoeidheidsuitval dan weers impact.



## Abstract

In The Netherlands new contract forms have emerged. Rijkswaterstaat (RWS) is the executive agency of 'Ministry of Infrastructure and Environment' and is in charge of the infrastructural national network in the Netherlands. RWS wanted to shift the risks of projects from RWS to the contractors because contractors have the knowledge to construct and manage projects. Due to this new development, contractors need to shift their focus from merely construction of the motorways to construction and maintenance of the motorways. This means that contractors needed to understand how the pavement construction of the motorways behaves during its life-cycle. Therefore, contractors want to know what the life-expectancy is of pavement constructions, and in particular the surface pavement. Raveling is one of the main damage types that causes degradation on the surface pavement in The Netherlands on motorways. Currently, there are no practical models or tools available for understanding the risks of maintaining a surface pavement. However, Heijmans has a method which empirically assesses this risk. This research will use this method called 'Heijmans life-cycle management'. This research focuses on producing an empirical database with a software tool called 'the Feature Manipulation Engine (FME)'. This tool is used to merge different datasets into one database. With this database, two filtering techniques are produced which can assess the degradation risk. The first technique involves plotting the degradation of the surface pavement over a lifetime and the second technique depicts the fatigue failure ratio of the surface pavement over a lifetime. With plotted data of fatigue failure ratio over time, a probability beta distribution curve is constructed to produce a probability 'Monte Carlo; simulation model to predict fatigue failure ratio of surface pavement. The results show that the first plotting technique shows too much scattering over time in order to produce a predictive model. The second, however, is in able to filter out the scattering and can be used for the predictive model. The results also show the effects of cold weather is neglectable with respect to the impact of traffic loading. Finally, our predictive model shows that high traffic intensity results in a rapid increase in failure at 4.8 years, in moderate traffic intensity this moment occurs at 5.6 years and for low traffic intensity this moment occurs at 7.1 years.

## Interview with experts

To optimize the argumentation of different subjects in this thesis, various experts have been consulted. These experts are consulted because of the lack of literature. .... The first expert that has been consulted is Arthur Taming. He works at Heijmans at the Department of Heijmans infra asset management and acquisition as a project manager. He is an expert in the topic contract forms. The second expert that is consulted is Wouter Heijser. He works at Heijmans as well at the Department of Heijmans infra road construction as an Advisor. He is an expert in the topic of PAC constructions. The third expert that is consulted is Rob Kuppeveld. He works at Heijmans at the Department of Heijmans infra road construction as an advisor as well. He is an expert in the topic visual inspections. The last expert that has been consulted is Teun Schutte. He works at Heijmans as well at the Department Heijmans infra management and maintenance as a project manager. He is an expert in risk management. In Appendix B you will find all the interviews.



## 1 Introduction

Rijkswaterstaat (RWS) is the executive agency of 'Ministry of Infrastructure and Environment' in charge of the infrastructural national network in the Netherlands. RWS is responsible for construction and the maintenance of the national road network of The Netherlands. RWS is not the stakeholder that does the construction and maintenance by themselves of the road networks, but the physical with respect to construction and maintenance are executed by contractors. This way of working is recorded in 'The Uniform Administrative Conditions for the Execution of Works 1989 (UAV, 1989)'. This is a standard agreement between a client and the contractor that is used in the construction industry. It regulates a contractor building contract between parties. Furthermore, the UAV regulates the contractual relationship between the client and the contractor. This relationship form is called a 'traditional' relationship. In this form, the client asks a contractor to be responsible for the construction of a project or maintenance of a project.

Today, maintenance for the surface pavement construction has a high priority for RWS. Therefore, divers maintenance contracts exist between RWS and contractors for maintaining surface pavement constructions (A. Tameling, personal communication. March 16, 2017). RWS wants to achieve long-term quality of infrastructural projects, lower the costs and time overruns (D.J.R. (Dirk-Jan Rijke) Vinke, 2013). Moreover, RWS wants to cut the cost in their own organization and deliver more quality at their core tasks. Therefore, RWS created a new credo '*markt, tenzij*' (the market unless). This credo means that RWS shifted the traditional tasks like construction, maintenance of infrastructural projects to the private market. To realize this shift, a new contract form was used: Design, Build, Finance, and Maintenance (DBFM) (Eversdijk & Korsten, 2009). This implies that it is important for contractors to understand the degradation behavior of asphalt during its life-cycle.

In The Netherlands, Porous asphalt concrete (PAC) is the main used mixture of surface pavement, significantly. The major reason for this widespread use is that PAC has the ability to significantly reduce the noise level that is produced by cars, and trucks tires at speeds higher than 50 km/h. PAC is a cheaper solution to reduce traffic noise than other options, like noise barriers. The noise reduction is done, due to the high population density. Furthermore, people live very close to the main roads in The Netherlands (Hagos, 2008). Therefore, due to the properties of PAC, more than 90 % of the highways in The Netherlands has a surface pavement constructed these days (Y. Zhang, van de Ven, Molenaar, & Wu, 2016).

The aging of the PAC mixture surface layer is due to entering of oxygen, light, and water into the pavement construction. This causes changes in the properties of the binder (Francken, L., Vanelstraete, A., and Verhasselt, 1997), which leads to durability issues by which the mixture will be more sensitive to traffic and climatic loading (L. T. Mo, Hurman, Wu, & Molenaar, 2007). The dominant damage type that influences the degradation of the surface pavement is called 'raveling' (Miradi, 2004b). 'Raveling' is a type of failure where the aggregate particles get loose of the adhesion composition of bitumen and aggregate. The failure mechanism is due to the axle load in a combination of the stress of the tires that scull on the surface layer of the pavement (L. T. Mo, Hurman, Wu, & Molenaar, 2008). Furthermore, environmental load and quality of the PAC construction due to construction are important factors (Hagos, 2008).

Laboratory aging methods on surface pavement do not simulate field aging of PAC constructions. The results show that laboratory aging is not capable of simulating more than 3 years of field aging. The UV light + humidity cannot be simulated in respect to field aging (Hagos, 2008).

The aim of this research is to predict the influence of the two parameters traffic load and environmental load on PAC surface pavement by producing a statistical probability model over time based on empirical data. According to Henning and Roux (2012), there are no long-term statistical performance models that can predict the influence of traffic load and environmental load over time on the deterioration of the PAC surface pavement (Henning & Roux, 2012). The model that they developed, could only predict raveling due to traffic loading. In this model, no environmental load was included. Opara and all (2016) established to produce an environmental load predictive model in a statistical way (Opara, Skakuj, & Stöckner, 2016). By monitoring the PAC surface pavement during winter and summer, these authors have produced a probability model for raveling. This thesis will aim to merge the two parameters and will make a new probability model.

## 1.2 Problem Definition research and Research design

The maintenance part of DBFM contract is a crucial part for contractors. Contractors want to map the life-cycle of, the surface pavement. This will give the contractors a better view of the degradation curve of surface pavement and is it possible to lower the risk for the contractor. To do so, it is important for contractors to understand the life-cycle of the surface pavement, so the contractors can predict the lifecycle of the surface pavement. The parameters 'environmental impact', 'traffic intensity', and 'quality of the asphalt', plays a crucial role in the life-cycle of the surface pavement construction. To the lack of empirical data 'quality of the asphalt' is not included in this research. In this research, we try to an extent whether it is possible to predict the risk factor of raveling and its influence on the degradation curve of the surface pavement highways within The Netherlands. We will focus on the influence of external factors such as climate impact and traffic intensity. Therefore, the research question will be:

*'Wich external factors have the highest impact on raveling that influences the degradation curve of surface pavement at highways in The Netherlands? And what is the risk impact of the external factors on the fatigue failure of the surface pavement?'*

To do so, a database is constructed, with empirical data. In this database, the following factors need to be implemented; a spatial dataset of all the PAC surface pavement highways in The Netherlands, local weather forecast, traffic intensity, and visual inspection on the surface pavement. The last dataset is provided by a contractor 'Heijmans'. Heijmans who does visual inspections on surface pavements. Experts from this contractor add a degradation value to the surface pavement according to the matrix DWW-Wijzer. Heijmans then have their own matrix, called 'Heijmans life-cycle management'. This matrix is based on an analyzing technique called 'Failure mode, effects, and criticality analysis'(FMECA). This FMECA model can transform the 'DWW-Wijzer' value into a risk value. These two matrixes will be explained in the next chapter 'Conceptual framework'. Furthermore, there also will be sub-questions answered during this research thesis;

- *'Which of external factors have according to the literature the most impact?'*
- *'Which of external factors have according to the risk model the most impact?'*

### 1.3 Expected results

The expected results of this research are to produce a prediction model that can predict the risk of fatigue failure over time on surface pavement caused by independent variables traffic load and environmental impact (cold weather). This will be realized by merging spatial datasets and plot the spatial datasets over time. The dataset is then the input for a simulation model. The output of the simulation model will produce a risk model of fatigue failure over time for different scenarios.



## 2. Literature study

This chapter depicts an overview of recent developments in the literature. The overview discusses the development a maintenance contract named ‘Design, Build, Finance, and Maintain’. Furthermore, the mechanical failure mechanism ‘raveling’, and the influences that cause this failure. The last overview that will be described is the development of statistical models of degradation on the surface pavement.

### 2.1 ‘Design, Build, Finance, and Maintain’ contracts in The Netherlands

This subchapter describes the use of Build, Design, Finance, and Maintain (DBFM) contracts in The Netherlands. As earlier mentioned, RWS is a key player that is the executive agency of ‘Ministry of Infrastructure and Environment’, and is in charge of the infrastructural national network in the Netherlands. The combination of all four disciplines is a unique way of working with a private-public partnership (PPP). A DBFM contract is initiated by RWS, however, RWS does not fully specify the demands of the project. The contract form forces RWS to describes the requirements on a functional level. This gives the private party the necessary space to design a solution that meets the functional requirements (see figure 2.1) (Vervoort, 2013). Furthermore, during the design phase, the private party also should take into account the construction, finance, and, maintenance phases of the project. This is due to, that the private party must settle the complete project that generally lasts between twenty and thirty years (Vervoort, 2013). This means the DBFM contract form, shifts the traditional tasks to the private party. The private party is then responsible for the design, construction, finance, and the maintenance of the project. This mains that RWS has contact with just one party who is responsible for the complete realization and maintenance of the project. RWS advantage of the DBFM contract form is with complex planning issues the controlling of time, money, risks, and reduce uncertainties (Eversdijk & Korsten, 2009).

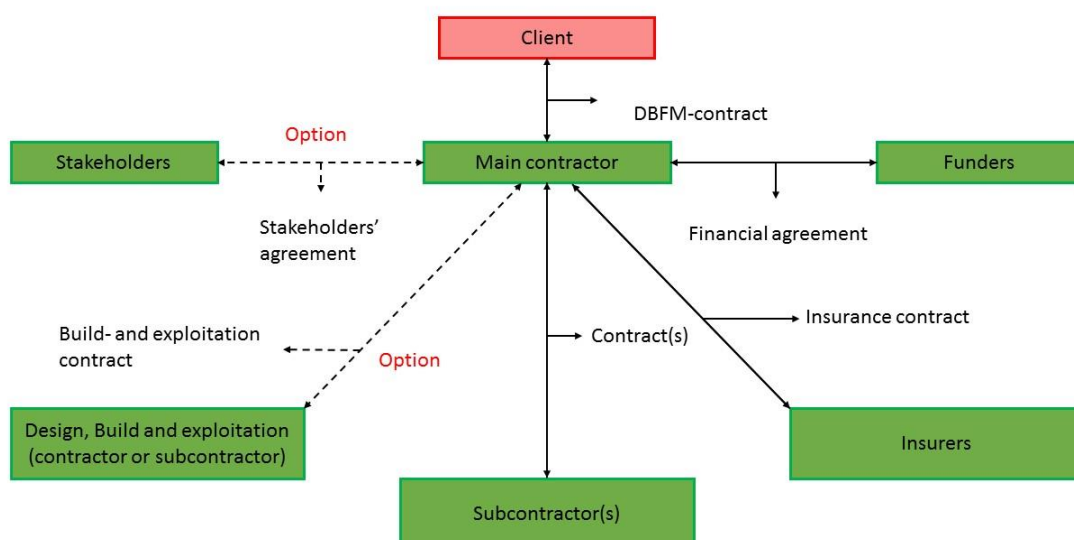


Figure 2.1: Scheme plot of key players in a DBFM contract (syndeks, 2017)

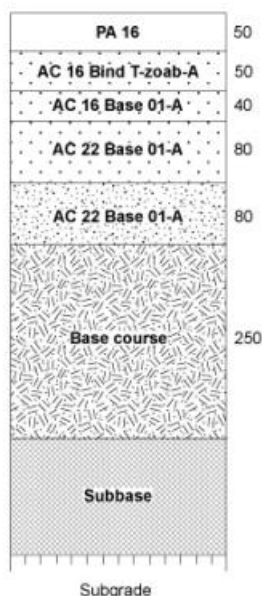
The combination of design, construct, finance, and maintenance of a project is for private parties a new way of working. With traditional contracts, different disciplines tendered separately. This means that there was no impulse for contractors to invest in optimal life-cycle in cost assessment, like in material use, process, and asset management, etc. (Eversdijk & Korsten, 2009).

Due to lack of impulse, before the DBFM contracts were introduced, the maintenance part of the contract is essential for the contractor to a DBFM contract (A. Tameling, *Personal conversation*, March 16, 2017). The investment of the design and construction need to be in optimal balance with life-cycle of the project, so the contractor has the optimal maintenance cost during the contract period.

To find the optimal balance in the life-cycle of the project during the contract period, empirical data need to be collected to predict the life-cycle of the surface pavement. So that, the risk for a contractor during the maintenance period can be minimized. The problem is that contractors do have empirical data collected but do not have a structured database. Therefore, a dataset needs to be constructed to driven predictions about life-cycle of the surface pavement (A. Tameling, *Personal conversation*, March 16, 2017).

## 2.2 Porous asphalt concrete

Asphalt (or bitumen in the European Union (EU)) is a residual product from the non-destructive distillation of crude oil. Asphalt is mainly used in paving the roads (Abraham, 1938).



Until the 1980s asphaltic surfaces were laid directly on sand beds. After the 1980s foundations were being used to reduce the asphalt thickness. The pavement construction of the highways nowadays usually consists of 30 centimeters of asphalt (four layers of dense asphalt with a PAC construction that is used as a surface layer) (see figure 2.2). The asphalt layers are stabilized on a foundation of the aggregate mix. Highways that are constructed in the past, usually have an approximate thickness of 40 centimeters (Nijssen, Wilfred A M G, Marc J.A. Stet, Wim A. Kramer, n.d.). As earlier mentioned in The Netherlands, PAC is the main used mixture of surface pavement, due to the abilities of noise reduction. Moreover, compare the PAC mixture to dense asphalt concrete (DAC) mixtures, who have not these abilities, due to the air voids in the mixture. DAC mixtures contain an air void percentage between 3 and 5 %. PAC mixtures though have an air void percentage between 20 and 27 %. Due to the dense

Figure 2.2: Standard asphalt paving construction in the Netherlands (Nijssen, Wilfred A M G, Marc J.A. Stet, Wim A. Kramer, n.d.).

a mixture of DAC, the binder film thickness covering the aggregates is thicker. The result of this covering of the aggregates has an influence on the aging of the surface layer of the pavement construction (Kandhal & Chakraborty, 1996).

The aging of the PAC mixture surface layer is due to entering of oxygen, light, and water into the pavement construction. This causes changes in the properties of the binder (Francken, L., Vanelstraete, A., and Verhasselt, 1997), which leads to durability issues by which the mixture will be more sensitive to traffic and climatic loading (L. T. Mo et al., 2007). The binder or also called bituminous mortar is a mixture of a filler, fine sand fraction, and bitumen (Hagos, 2008). The aging of the binder has an influence on the lifecycle of the PAC surface pavement. The average service life is lower than the average service life of DAC.

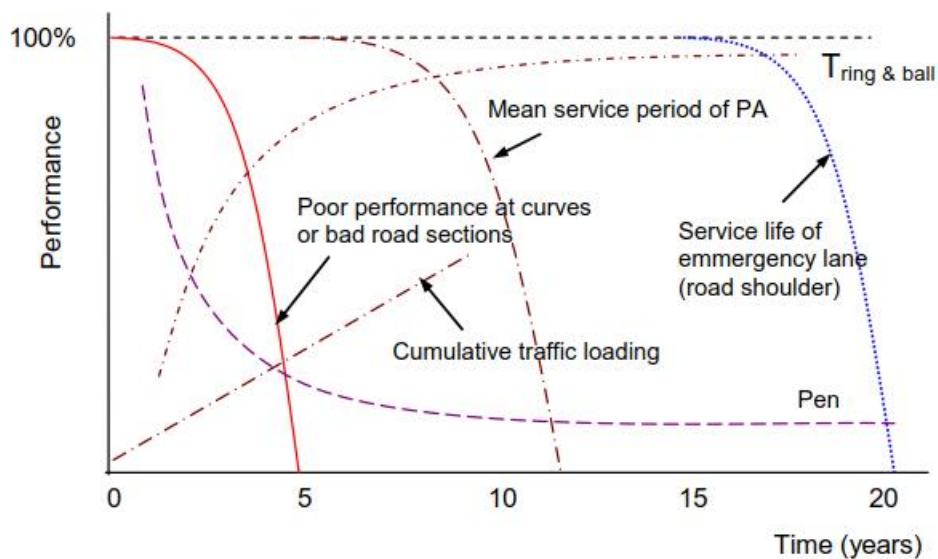


Figure 2.3: Schematic description of the degradation curve of PAC (Hagos, 2008).

Figure 2.3 shows a degradation curve of a PAC surface pavement construction. The curves are performance lines and display the lifecycle of the surface pavement construction. The dominant damage type that influences the degradation of the surface pavement is called ‘raveling’ (Miradi, 2004b). ‘Raveling’ is a type of failure where the aggregate particles get loose of the adhesion composition of bitumen and aggregate. The failure mechanism is due to the axle load in a combination of the stress of the tires that scull on the surface layer of the pavement (L. T. Mo et al., 2008). The bituminous mortar binding absorbs the high traffic load as displayed in, figure 2.5. The plot exposes a situation before the load and when the load appears. This failure mechanism is a very common failure in PAC constructions ((L. Mo, Huurman, Wu, & Molenaar, 2014), (for a brief overview of other damage types see Appendix A)). Furthermore, up to 90 percent of the fatigue failures of the surface layers of PAC is raveling (Opara et al., 2016). Therefore, when raveling is initiated on the pavement the deterioration appears rapidly (see figure 2.4).

### 2.3 Environmental impact and traffic loads

According to M. Huurman et al (2010), the highest impact of environmental loading factor on the degradation of the road surface is a low temperature. This low-temperature influences

raveling in two ways. First, the presence of salt brine, which depresses the freezing point below zero, causes a cycle of constant freezing and un-freezing. This leads to the frequent exertion of mechanical forces in the surface pavement construction. The second influence is mainly caused by the decrease of relaxation potential of aged mortar of the PAC construction. The binder of the surface pavement is getting more brittle during aging (M. Huurman, Mo, & Woldekidan, 2010). Furthermore, according to Miradi (2004a), the pavement construction will become more sensitive to cold days when the asphalt ages. Huurman et al (2010) discovered that when the bitumen ages and the temperature drop to -10 °C the stress on the bitumen increases significantly. Therefore, they argued that the relaxation behavior of bituminous mortars degrades as temperatures decreases.

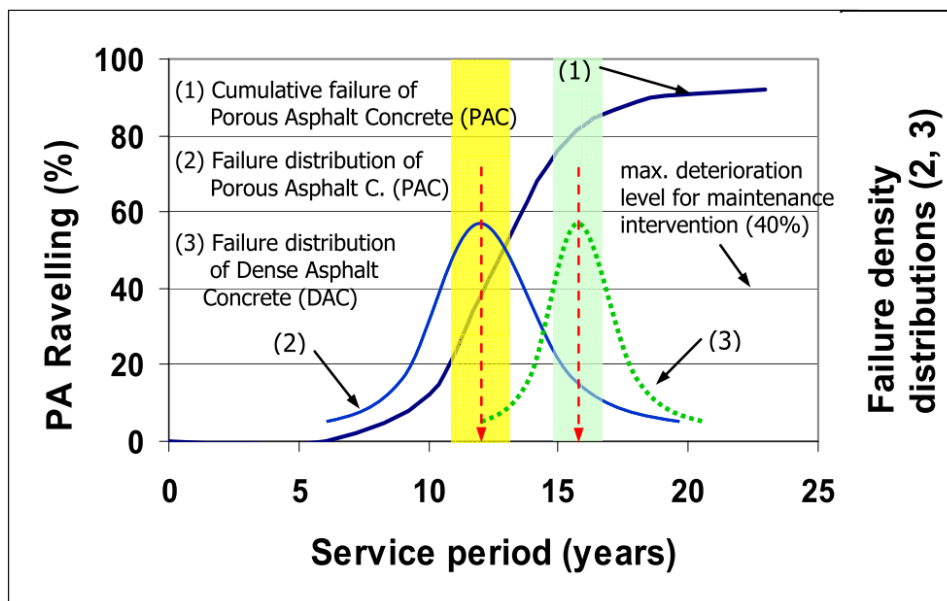


Figure 2.4: Schematic plot of PAC performance relative to dense asphalt (Hagos, 2008).

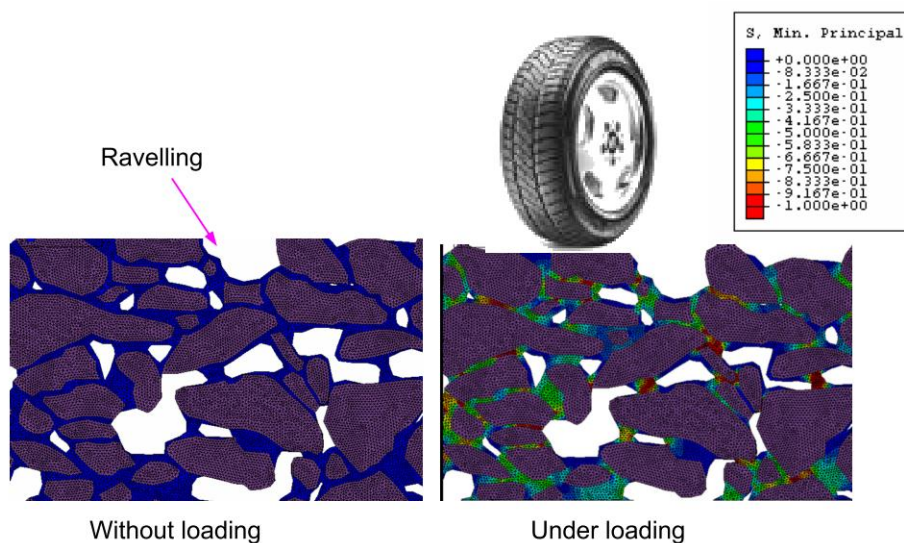


Figure 2.5: The effect of loading on a PA structure (R. M. Huurman, Mo, & Medani, 2007).

Traffic load has by far the highest impact on fatigue damage ('raveling') and it is depended on the use. Traffic load is divided into two influential groups, named heavily loading lanes and lightly loaded lanes (Vervoort, 2013). This research is focusing on the heavily loaded lanes due to the fact that these lanes show by far the most raveling. Commercial trucks with an axel loads of 100kN cause the most degradation on the surface pavement (M. Huurman et al., 2010). The mechanism of the failure on the pavement is the combination of stresses that occurs just after a tire passes over a particle (L.T. Mo et al (2007) (see figure 2.5). At that moment, minor tension in combination with shear stress is affecting the contact area. Based on these studies it can also be said that the bitumen in the pavement becomes more sensitive to tire stresses during aging as well as with colder temperatures.

Another important factor which is of significant impact on the bad performance of PAC surface pavement construction is poor workmanship during construction (Hagos, 2008). These authors showed that, for poorly constructed asphalt, the binder ages faster, and therefore, has an influence on the aging of the PAC construction. The lifespan of PAC can be low as 4 years (Hagos, 2008) (see figure 2.3). The binder ages faster due to a virility of factors (Hagos, 2008);

- Variations during the production of the asphalt mixture;
- Segregation of the aggregates and dripping off of the mortar during transportation and construction of the surface pavement mixture;
- Poor control of temperature during construction;
- Moisture issues in asphalt mixture due to the environment (Opara et al., 2016).

In this thesis, the focus will not be on the external factors of the quality of the asphalt during construction time due to the lack of empirical data.

## 2.4 Statistical methods of external factors that have an impact on the degradation of surface pavement

As earlier mentioned, laboratory experiments are not capable of accurately simulating PAC field aging for more than 3 years. Variables like UV light and humidity cannot be simulated in respect to field aging (Hagos, 2008) (L. T. Mo, Huurman, Wu, & Molenaar, 2011).

Therefore, this research is aiming to make use of a statistical approach in order to predict the degradation of the surface pavement because of raveling. According to D. Bouwmeester at al, (2004) a probability approach will provide better life-cycle information on surface pavements with respect to normal deterministic laboratory methods. This is because of a few advantages; the most prominent one being is that we can investigate how raveling is influenced by each variable. This is possible due to the factors that are directly accounted in the model (Opara et al., 2016). Furthermore, the statistical approach can quantify the importance of different factors, and relationships between these factors. This approach is done by using an exploratory analyzing method. The approach produces an overview of the dataset, such as distributions and apparent relationships between the traffic load and time factors (Henning & Roux, 2012). The datasets contain spatial data such as age surface pavement, surface pavement type, traffic network (traffic load), location surface pavement, and the condition of

the surface pavement. The datasets showed by Opara et al., (2016) contain spatial data, air temperature, the cause of the degradation of the pavement, surface pavement type, location, and the condition of the pavement. The statistical models that are developed by Opara et al (2016) and Henning & Roux (2012) try to capture the influence of traffic load and environmental load separately.

Opara et al., (2016) and Henning & Roux (2012) used a linear regression approach in order to produce a probability. This approach shows a better understanding of the overall data composition, such as distributions and apparent relationships between variables and “what-if” analyses. In this research, we will make use of a regression model as well, due to the fact that a regression model can capture relationships between variables such as traffic loading and environmental impact.

Henning & Roux (2012) probability results show that the probability of raveling is 0.5 at 6 years because of traffic loading (see figure 2.6). Furthermore, they find out that low volume roads ravel faster than high volume roads. This is opposite what they expected. Therefore, in this research will make use of 3 groups of traffic loading; light, moderate, heavy, to capture this expectation and combine this traffic loading with environmental loading.

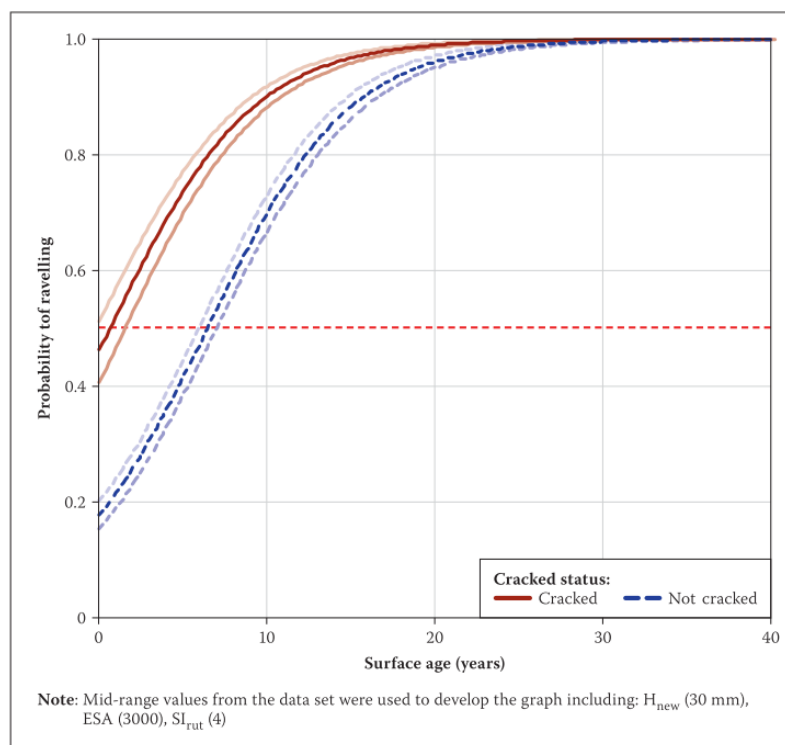


Figure 2.6: Predicting raveling initiation for PAC surface pavement (Henning & Roux, 2012)

In this research, we try to combine the impact of cold weather and traffic intensity in one risk model. Furthermore, according to Henning & Roux (2012), it is clear that there is a common need to understand the risk of failure more than know the deterioration over time. Therefore, this research is trying to capture this understanding by making use of the ‘visual inspections. The visual inspections are performed in respect with the ‘DWW-wijzer’ that is developed by RWS (Doorduijn et al., 1994). The development of the classification system is established due to expert consultancy. The experts developed the tool by means of visual inspections. Due to,

the lack of experience and knowledge, the experts did not add weight factors to classify the damages. Their recommendation in 1994 was to analyze whether it was necessary to add weight factors to the classification tool. This could lead to a more accurate classification tool (Doorduyn et al., 1994). 'Heijmans' developed such a tool in 2012 and added weight factors to the model by using the FMECA method (*T. Schutte, personal communication. March 14, 2017*). The model is used to plot risk of fatigue failure over time (see Chapter 4, Results).

## 2.5 Conclusion

In the first section of this chapter, the DBFM contract form and their impact on contractors who operate in the infra technical environment are explained. Due to the new contract form, the risk of finance and maintenance of the projects shift from the client to contractors (Eversdijk & Korsten, 2009). Therefore, contractors want to reduce risks during maintenance of infrastructural projects. Due to, the lack of knowledge of surface pavement behavior during their life-cycle the focus of the contractors is to map the degradation of surface pavement over time.

In The Netherlands, 90 % of the surface pavement is carried out in PAC construction (Hagos, 2008). The performance over time of the PAC pavement is lower than DAC pavement constructions (Hagos, 2008). Therefore, contractors want to know what the average lifespan is of PAC pavement constructions and what is the impact of external factors on the life span of the pavement construction. External factors like environmental load and traffic load have a significant impact on degradation (M. Huurman et al., 2010).

This research is focusing on to produce a statistical risk of fatigue failure over time model for PAC surface pavement. This will be realized by making use of a statistical approach. In the method that is used is the classification system of RWS the base. The classification will be linked to the surface pavement as well the impact of external factors such as environmental factors and traffic loading. Due to, the fact that these factors have the most impact on the degradation of the surface pavement (Vervoort, 2013)(M. Huurman et al., 2010). Furthermore, these external factors are separate observed and analyzed with statistical methods (Henning & Roux, 2012)(Opara et al., 2016). In this research, the aim is to combine these external factors and produce a prediction risk model with above independent variables in the model.



### 3. Theoretical Framework

In this chapter, the theoretical framework will be described. Figure 3.1 shows the methods that are used for achieving the goal for producing a prediction model for raveling over time. To realize this prediction model, empirical data is needed to structure the model. As was described in the previous section, different variables are responsible for the fatigue failure of raveling, which is: Traffic intensity, environmental impact, quality of the construction phase of surface pavement, and aging of the surface pavement.

As earlier mentioned not all important factors can be implemented in the model. For instance, because of the lack of empirical data, the quality of the construction phase of the surface pavement is not included. Furthermore, this initial parameter is believed to be of significant impact on the degradation of asphalt (Kuennen, 2013). However, monitoring of initial asphalt quality during the construction phase is still under development (*W. Heijsser, personal communication. March 13, 2017*). Unfortunately, surface pavement that is monitored is too young to include in the model (*W. Heijsser, personal communication. March 13, 2017*).

Therefore, factors that are included in the model are traffic intensity, environmental impact, and aging of the surface pavement (see figure 3.1).

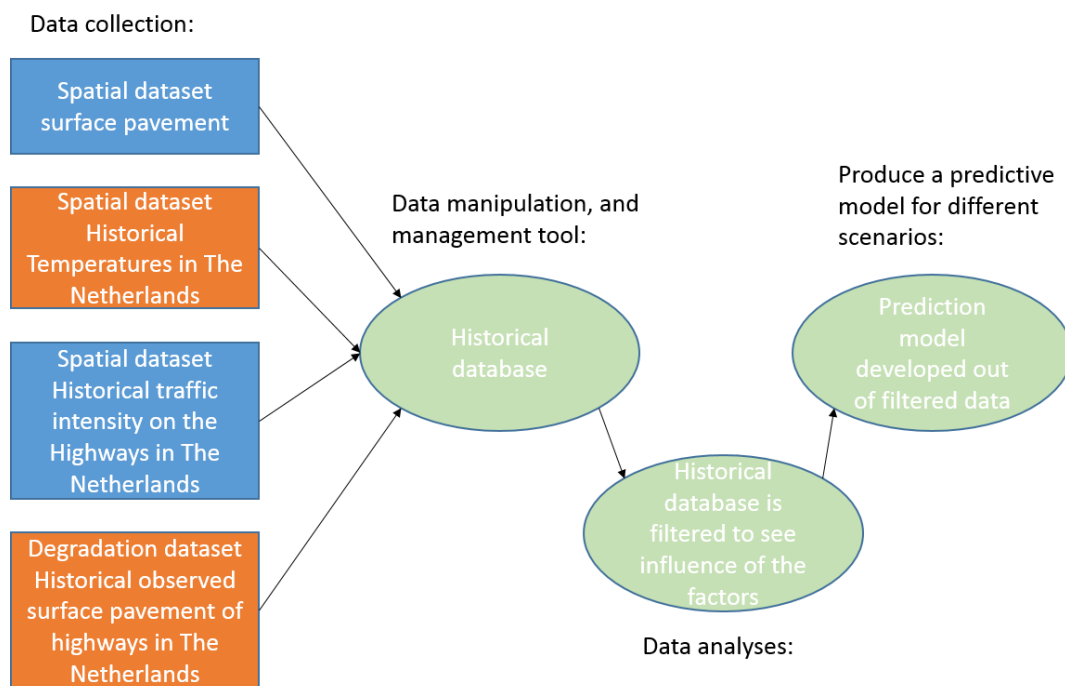


Figure 3.1: Scheme conceptual framework description (data approach)

#### 3.1 The datasets that are implemented in the model

This subchapter is about the different datasets that are used to produce a merged dataset that will be used to make a prediction model. In the datasets that are used variants independent and dependent variables will be collected to produce this prediction model. The following subchapters will be about the datasets that are collected for the management and manipulation tool; surface pavement of all the highways in The Netherlands, a spatial dataset

of the independent variable environmental impact, a spatial dataset of the independent traffic intensity, and the visual inspections of the dependent variable of the surface pavement.

### 3.1.1 Dataset surface pavement

The dataset of the spatial surface pavement is called 'KernGIS'. This dataset contains the national road system of The Netherlands and is a geographic information system (GIS) based in ArcGIS. The product of KernGIS is a digital map in which, objects are exposed as points, lines, or polygons. This dataset is updated every year. This research is using the last update from 01-09-2016 (Rijkswaterstaat, 2016b). The attributes of the objects are displayed in a table when the user clicks on the object. These attributes show; date of construction, pavement type, driving direction, location, and hector-values. Due to these abilities, the dataset can be used for analyzing. The use, of KernGIS, is primarily to manage the maintenance of the national motorways and national waterways. Furthermore, KernGIS is used to source the Network Information System (NIS), for RWS. So, RWS can manage the performance of their administrative tasks (Rijkswaterstaat, 2017).

### 3.1.2 Traffic intensity dataset

The data of the traffic loading on the highways is collected by RWS as well. The dataset is called (Dutch: INTensiteit op WEgVAKken (INWEVA)), (Rijkswaterstaat, 2016a). Approximately 3000 road sections are stored in the dataset. In these road sections, the traffic intensity is monitored. The rest of the road sections have been estimated according to traffic models. The scope was to measure the intensity of the traffic is all the carriage lanes, access ramps and exits, parallel lanes, and connection roads. The dataset produces a yearly mean per section. The set is further disaggregated in working days and weekdays. Furthermore, is the set disaggregated in morning-, evening period and vehicle classes (light, average and heavy). The dataset is updated every year and is available since 2012 (Rijkswaterstaat, 2016a).

The vehicle class that is used for this research is heavy traffic. Vehicles that belong in this classification are eleven meters in length or more and have an axle load of 100 kN per axle or more. In the software tool, INWEVA this class is expressed as 'L3'. This assumption is chosen due to the literature (M. Huurman et al., 2010). This 'L3' class is according to the literature the cause of raveling of the surface pavement. Furthermore, the lane where the heavy traffic generally travels is the outer lane. Therefore, is the scope narrowed down to only the outer lane of the highway.

### 3.1.3 Temperature dataset

The dataset of the environmental temperature in The Netherlands is derived from Royal Netherlands Meteorological Institution (Dutch: Koninklijk Nederlands Meteorologisch Instituut (KNMI)). KNMI is an institution that is forecasting the weather, monitoring the weather, climate, air quality and seismic activities (Koninklijk Nederlands Meteorologisch Instituut, 2016). KNMI collects all the data in their data center. The weather is monitored in The Netherlands by 325 weather stations. The first monitoring was done on 01-01-1901 in 'De Bilt'. The weather station is still monitoring till this present day. The weather stations are monitoring different parameters, such as maximum temperature, lowest temperature, wind

speed, hours of sunshine, air pressure, and humidity. The scope of the monitoring will be narrowed to the lowest temperatures, because lowest temperatures have the highest impact on degradation on the surface pavement according to Huurman et al., 2010. Therefore, the model will make use of days that have a temperature  $-10\text{ C}^\circ$  or lower (Opara et al., 2016). Figure 3.2 displays an example of 2 weather stations, called 'Eindhoven' and 'De Bilt', which show the amount of days that exposes temperatures that have  $-10\text{ C}^\circ$  or lower in a year. In this model 24 weather stations are included, which are located all over The Netherlands.

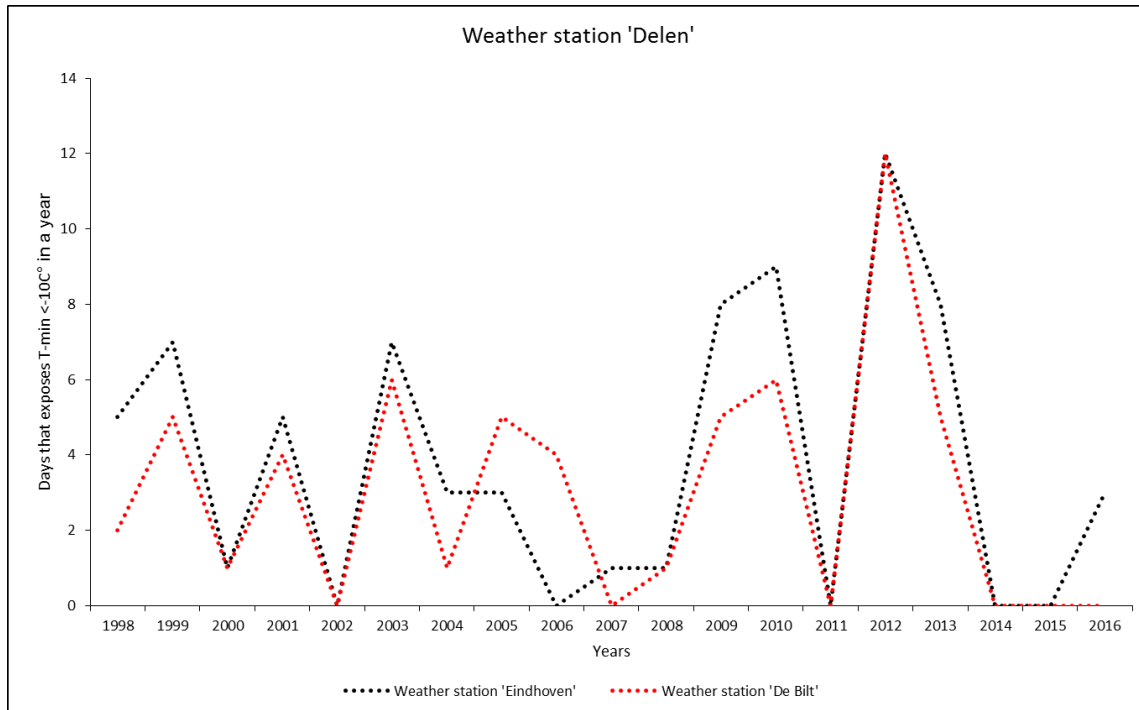


Figure 3.2: Graph where 2 weather station displays the amount of days in a year, where the temperature is below  $-10\text{ C}^\circ$ .

### 3.1.4 Visual inspections

The most important dataset that will be added to the model is the 'visual inspections'. This dataset contains the state of the surface pavement. The dataset contains the following data; inspection dates, degradation classification, hector-value, driving direction, lane, the cause of degradation (if there is degradation), and location. The visual inspections are produced by 'Heijmans'. Due to, the change of the contract forms the contractors are responsible for the visual inspections. The visual inspections are mainly done behind a monitor. A third party called 'Cyclomedia' provide the footage for inspecting the surface pavement. This footage is executed by car, with on top a  $360^\circ$  camera. However, the problem of the visual inspections is that 'Heijmans' inspect the surface pavement once. This provides the problem that a tile of surface pavement is not monitored during its life-cycle. This is because that contractors work behavior is more in respect to the older traditional contract forms. Therefore, there is no monitored measured dataset that can be used for this research (R. Kuppeveld, personal communication. March 13, 2017). However, if you use all different data points you can produce a degradation curve. This technique will be further explained in the subchapter '3.3 analyzing manipulated data and making assumptions'.

The visual inspections are produced according to instructions of RWS. RWS provides an instruction manual that is called DWW-wijzer (Appendix C, DWW-wijzer). In this document ‘DWW-Wijzer’ is a guideline, how to locate and to classify damage.

The damages are classified into three severity grades (see figure 3.3), light damage (classified as 1), moderate damage (classified as 2), and serious damage (classified as 3). Next, is the scale of the severity grade that is categorized, the motorway is divided into 100-meter lane tiles. These 100-meter lane tiles are on the left side inspected as on the right side of the motorway. These tile than is classified. The scale of the damage is classified in three groups, small scale (classified as A), limited scale (classified as B), large scale (classified as C). For this research, raveling is the type of damage that is used for the model. The group that is classified as ‘1’, shows a damage type where 6-10 % of the first layer of granules has been forced-out (per square meter), the second group, shows a damage type where 11-20% of the first layer of granules has been forced-out (per square meter), the third class shows a damage type where more than 20 % of the first layer of granules has been forced-out (per square meter).

Damage	Severity grade		
	1 Light damage	2 Moderate damage	3 Serious damage
Ravelling On PAC surface pavement (per m <sup>2</sup> from lane)	6-10% of the original granules in the surface pavement are forced-out.	11-20% of the original granules in the surface pavement is forced-out.	> 20% of the original granules in the surface pavement is forced-out.
Damage	Scale of the severity grade		
	A Small scale	B Limited scale	C Large scale
Ravelling (% length of a 100 metre tile)	<15%	15 till 25%	>25%

Figure 3.3: ‘DWW-Wijzer’ table that is used for classifying raveling damage.

The scale of the damage is measured in percentages as well, but then in a tile of 100-meters. This means, how often does the severity of the damage occur in the 100-meter tile. The first classification is ‘A’, the size of the raveling is then less than 15 % of the tile that show damage. The second classification is ‘B’, the size of the raveling is then between 15 and 25 % of the tile that show damage. The last classification is ‘C’, the size of the raveling is more than 25 % of the tile that show damage. Furthermore, an important part is that RWS demands that after ‘2B’ the tile needs to be maintained. The higher classification is there to show the priority of maintaining the tile.

The problem with this classification system is the risk factor of maintenance of the tile is not included. This means that classification is not chronological. When the damage is classified as ‘1A’ it does not mean that the next step over time is ‘1B’, ‘1C’, ‘2A’, ‘2B’, etc. in chronological order. This means that there needed to be a more chronological classification to capture the degradation of the asphalt over time.

Therefore, ‘Heijmans’ has produced a tool that captures the risk factor over time. they developed a model to understand the risk of the degradation that was exposed during the visual inspection. This model translates the classification into a risk factor that can capture when the tile needs to be maintained. In the model, two methods are included, known as

‘Failure Modes, Effects and Criticality Analysis’ (FMECA), and ‘reliability, availability, maintainability, and safety’(RAMS). These two methods are combined in a model, that can provide a risk factor to the ‘9’ classifications of the DWW-Wijzer. This model is used for the probability model due to, the fact that this model adds causes to the degradation classification (the following subchapters will explain the model (*T. Schutte, personal communication. March 14, 2017*)).

#### 3.1.4.1 FMECA method

Failure Modes, Effects and Criticality Analysis (FMECA) was originally developed by United States military (US Department of Defence, 1949). This method is designed to analyze possible failure modes for a product or process. Because of this method, the risk can be estimated with those failure modes. The method can rank problems in terms of importance. Furthermore, the method can find the most serious concerns using identify and carry out corrective actions (Bertolini, Bevilacqua, & Massini, 2006). FMECA is designed to have a bottom-up approach. This approach can break down any system (product and/or production process). FMECA breaks the system down into fundamental components. The method can detect all possible failure modes and the effects on the components. In this analyze of the failure modes, the modes give the information (US Department of Defence, 1949):

- The model breaks the system in a hierarchical matter, into subsystems and final items;
- The model makes a list and description for the process/product that analyzes any failure or generic malfunctioning;
- It classifies the probability, harshness, and detectability of all the failure modes that present themselves;
- The part Criticality Analysis (CA), ranks all failure in order of priority.

In order to decrease the impact of risk of potential failures, corrective actions can be taken. This is done by checking the effectiveness of interventions and compare the CA to the solutions that can be implemented. The evaluation of the failure mode can be achieved, using two different approaches ((Pelaez & Bowles, 1994), (Bowles & Peláez, 1995)). The first approach is called Criticality number (CN), the second approach is called Risk Priority Number. To choose, from one of these approaches, a traceability system needs to be implemented and managed. This involves labeling several problems, that have the highest priority related to the information. Furthermore, the choice that is documented, recorded, and recovered, according to a material management flow system.

#### 3.1.4.2 RAMS method

RAMS is a method that is a collection of techniques that can provide for target a prediction of the performance of the required system. It is an indicator that can be both used qualitative and quantitative, to the degree that the system, or the subsystems, and components that are included in that system. It predicts the reliability of the function as well specifies, both availability and safety of the system. The method is frequently used in the construction industry. Due to, the investment costs that have a higher priority than the performance of the building system. According to, the authorities, reliability, and more availability of the national motorway network has a high priority (Al-Jibouri & Ogink, 2009).

3.1.4.3 Heijmans FMECA-RAMS model

The method FMECA and RAMS are merged together in a model. Figure 3.4 shows the model that ‘Heijmans’ had developed. This model transforms the ‘classification’ of the ‘DWW-Wijzer’ into a risk number. On the left side of figure 3.4, the FMECA model is explained. On the right side, the RAMS model is described.

**Heijmans FMECA model**

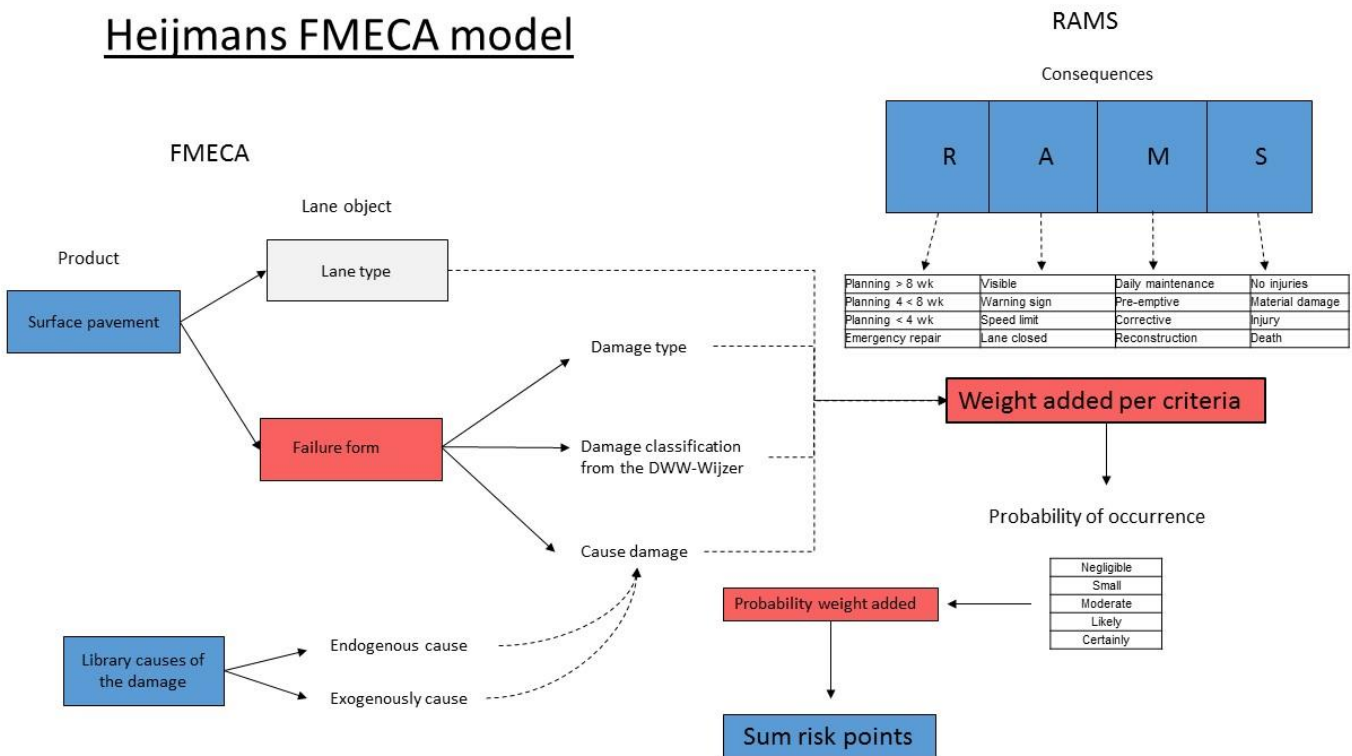


Figure 3.4: Scheme of the Heijmans FMECA model (Heijmans, 2012)

The FMECA model breaks the product down (surface pavement) into sub-systems, which describes the process of failure. The first subsystem is the lane type which is important, because of the difference in road use. The sub-system ‘Failure form’ breaks down as well, at which, the three arrows indicate the three failure forms, which are; the damage type (in this research it will be ‘raveling’), the classification of the DWW-Wijzer, and the cause of the damage. The cause of the damage is stored in a library of the model. There are two groups of causes endogenous, and exogenous. Exogenous causes are causes that do not have their origin through fatigue. For example, a traffic accident which causes damage to the surface pavement, or consolidation of the foundations of the pavement. Endogenous causes have their origin on fatigue (T. Schutte, personal communication. March 14, 2017). For example, the bitumen in the surface pavement is getting fatigued due to the number of vehicles that have been passing by. After this process, the RAMS model adds weight to the failure. These weights are based on consequences if the failure will not be maintained or on the consequences when the failure will be maintained. Next, the weight of the probability occurrence will be added. Figure 3.4 also shows a risk number (Sum risk points). Table 3.1 depicts the index system with the ‘risk sum points’ into life expectancy that used for analyzing the results of the FME model. RWS though wants according to the new contract form that surface pavement needs to be maintained at 2B/2C. Therefore, in this research, the fatigue failure point is settled at 21 points.

Due to, the fact that ‘Heijmans’ is using the ‘DWW-Wijzer’ and developed a model that includes fatigue degradation the model is used for plotting the degradation curve over time.

Damage classification into Heijmans risk points for the truck lane do to ravelling			
DWW-wijzer damage degree	Sum risk points	Chance to reconstruct	Expected life span
1A, 1B, 1C	5	Negligible	Functional remaining life span > 4 years
2A	12	Negligible	Functional remaining life span > 4 years
2A	18	Minimal	Functional remaining life span 2-4 years
2B	21	Minimal	Functional remaining life span 2-4 years
2C	28	Minimal	Functional remaining life span 2-4 years
3A	40	Moderate	Functional remaining life span 1-2 years
3B	55	Serious	Functional remaining life span 0-1 year
3C	70	Catastrophique	Instant need to maintaine

Table 3.1: Translation table of the ‘DWW-wijzer’ into Heijmans expected life span surface pavement.

### 3.2 FME model design

This research is making use of the software tool ‘Feature Manipulation Engine’(FME). FME is a software tool that is a platform for connecting spatial data between geometric and a digital format (see figure 3.5). FME was invented to be used with spatial data (GIS), computer-aided design (CAD), and raster graphics (Safe Software Inc., 2015). FME assist with the transformation of spatial data into the diversity of formats, data models, and a tool to the depository for transmission to end users.

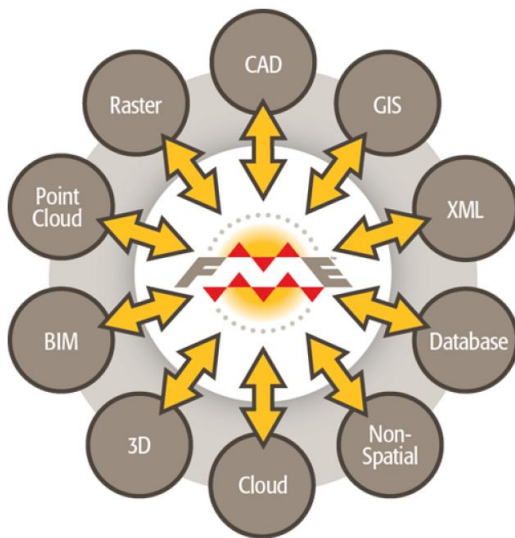


Figure 3.5: Scheme of the FME engine that supports different data types and data formats (Safe Software Inc., 2015).

#### 3.2.1 Process description model design FME

FME is used to manipulate the four datasets that are mentioned above. The Process phases of the model are described in figure 3.6. The aim of the FME model is to produce a file where all the data that is needed to produce a prediction model.

### FME scheme model

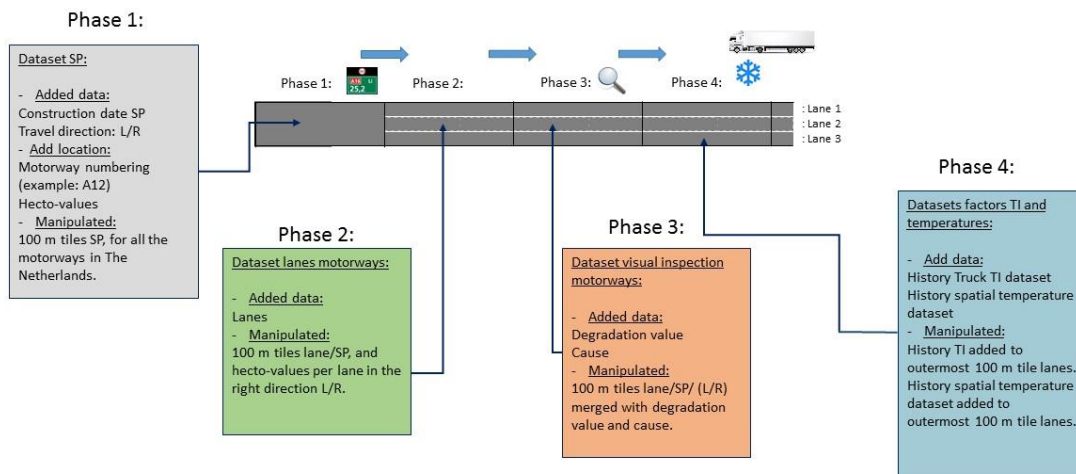


Figure 3.6: FME scheme model of the process cycle

*Phase 1: create 100-meter tiles.*

For this ‘phase,’ The spatial dataset ‘KernGIS’ is used. The aim in this ‘phase’ is to produce 100-meter tiles with information of the surface pavement (SP). In ‘KernGIS’ the SP are archived as spatial unorganized slabs, that can be kilometers long. These slabs needed to be clipped into smaller 100-meter tiles (see figure 3.6, phase 1). To realize the tiles the hecto-values were used to make perpendicular lines between the ‘left’ hecto-value and the ‘right’ hecto-value. This line is laid over the slabs of the surface pavement, so the slabs could be clipped. Furthermore, FME is used to filter out the dense asphalt concrete SP’s, which are not being used for the prediction model. The model produced for every tile the type of SP, the hector-value, construction date, location, motorway numbering, and left (L) or right (R) travel direction.

*Phase 2: create 100-meter lane-tiles.*

In this ‘phase’ the 100-meter tiles needed to be clipped into smaller lane tiles (See figure 3.3, phase 2). To realize the lane tiles a spatial dataset of all the motorways of the lanes were included into the model. These lanes than needed to clip the big 100-meter SP tiles into smaller lane SP tiles. In this process, the starting point of the hector-value and the end point of the hector-value of the tile was manipulated and added to the model. This was needed for merging the Excel files of the visual inspections. The cells in the visual inspection files have a start point (hecto-value ‘A’) and an end point (hecto-value ‘B’). the model needs to understand that these values have to correlate with the spatial start point (hecto-value ‘A’ spatial) and end point (hecto-value ‘B’ spatial) of the spatial model in FME. Due to this realization, the model now had the information of all lane tiles with the PAC SP, what the start point and the end point of the tile was, and if the tile was left or right traveling direction.

*Phase 3: Merge information from excel visual inspection files to spatial data tiles.*

In this 'phase' the aim was to merge the excel cells with information of 'degradation value', 'cause value' of the degradation, lane number, and visual inspection date, this information needed to be added to the proper spatial 100-meter lane tiles of the FME model. Because of the construction date and the visual inspection date, the model had the information of the age of the tiles, 'degradation value', and the 'cause value' per tile.

*Phase 4: add information 'traffic intensity' and local weather forecast to the lane tiles.*

In the last 'phase' two spatial datasets were added. The historical spatial of th'TI' of trucks were added to the outer lane tile of the highways, and the temperature of the weather station dataset was added to the outer lane tiles as well. Now the model had the information of, what the number of past trucks per day was, and had a historical weather table of 20 years of temperature data.

### 3.3 Analyzing manipulated data and making assumptions

The output of the FME model is used to make analyses. The output of the model is plotted in a graph (see figure 3.7). The technique of the analyses is shown in Appendix D as a flow chart. The Y-axis is displayed as the 'Heijmans' FMECA risk points, the X-axis is a timeline in days. The timeline exposes the lifecycle of the 100-meter tiles. Every 100-meter tile is plotted as a blue dot. Do to, the lack of monitoring all the data points are unrelated data points from each other.

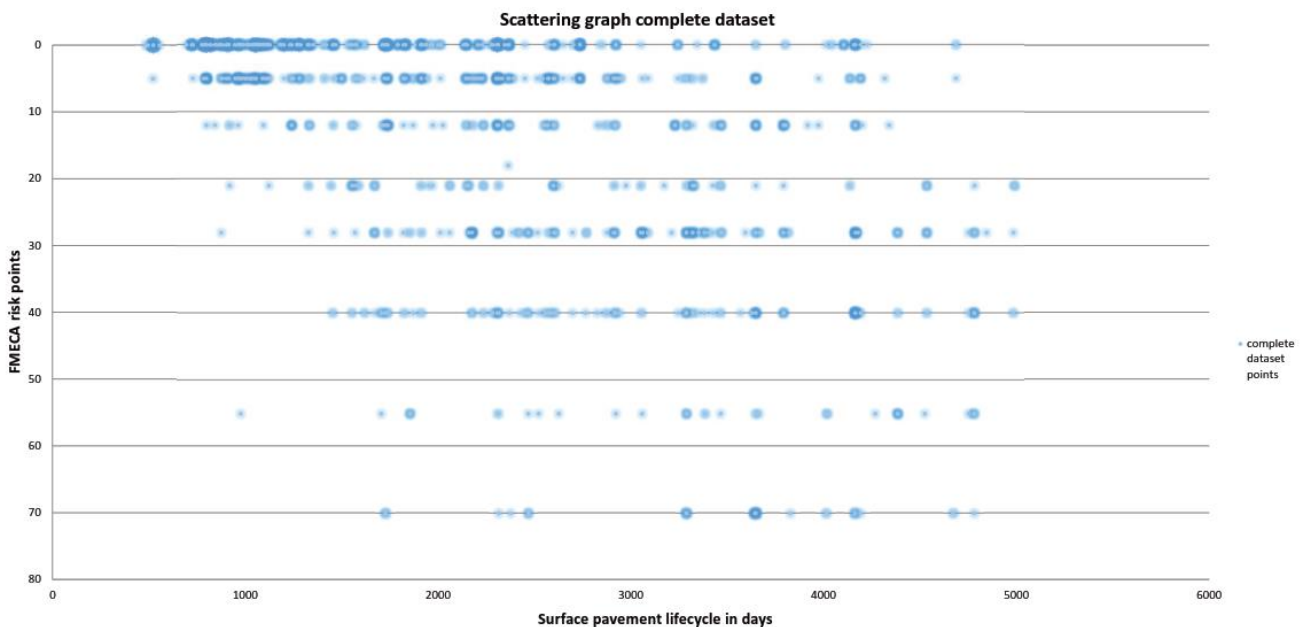


Figure 3.7: Scattering graph of the complete output dataset of the FME model

Information of 1 data point consists of			
Code-Highway	Driving direction	Hecto value from	Hecto-value until
A12	Right	114.7	114.8
Used to find the nearest weatherstation			
Age surface pavement in days	State of the pavement	Cause state pavement	Risk points
2350	2A	REN1	12
X-axis			Y-axis
Trucks that pas by per day	Amount of days that data point is exposed to -10 °C		
3561 (moderate)	25		
Filtering technique	Filtering technique		
IF statement	IF statement		

Table 3.2: output FME model, information stored in a measured data point

The data points that are plotted in the graph (see figure 3.7) consists of; location, life-cycle (time in days), the state of the surface pavement, cause of the degradation of the pavement, FMECA risk points, the independent variables traffic intensity and amount of days that the data point is exposed to -10C° (see table 3.2).

The range of the scattering that is plotted in the graph has a high variation (see figure 3.7). Due to, this high variation it is difficult to make a prediction model. To capture the impact of the independent variables ‘traffic intensity (TI) and ‘temperatures below -10 C° a filtering technique is used.

To understand the impact of the two different parameters, groups are created. For the independent variable ‘TI’ three groups are created; light ‘TI’ (from 0 to 2100 trucks that passing by per day), moderate ‘TI’ (from 2100 to 4200 trucks that are passing by per day), and heavy ‘TI’ (from 4200 to 6300 trucks that are passing by per day). The three groups are classified in this way, because the highest number of trucks that are observed in the dataset, this number is around 6300. To simplify the model, not too many groups are created, this is because of the amount of data points (approximately 3300 data points). Due to the lack of measured data, this classification was chosen.

The impact of the parameter ‘T-extreme’ is organized differently. The process of the observation what the impact of this independent variable is a different filtering technique used. The filtering is done by a ‘more than’ technique. The data points that were exposed to ‘more than’ 20 days and ‘more than’ 30 days were included in the model. This technique was chosen because the observations showed that under 20 days the impact of the independent variable ‘T-extreme’ was not mentionable, and ‘more than’ 40 days the lack of measured data, not a good plot could be produced.

Another crucial point for analyzing the data is to capture the scattering. The solution for this problem is to divide the dataset into grouped datasets. This is done through creating ‘time-steps’ of 250 days. All the data points who occurs in the concerned time-step is assigned to the concerned ‘time-step’ group. The time-step of 250 days is selected because the oldest life-cycle data points are approximately 5000 days. Furthermore, the time-steps cannot be divided more because of the amount of data points. Due to the observation, the grouped datasets would be too small, and then the randomness would get the upper hand. Furthermore, the

grouped datasets that display a dataset smaller than 10 data points will be excluded. This is as well done because of, the randomness that occurs when there are less than 10 data points.

For plotting the results, the 'Heijmans FMECA risk point' approach is used. This approach is to produce an average degradation 'Heijmans FMECA risk point' over time. Furthermore, the standard deviation of the average risk point of a time-step measured dataset is used to provide a more accurate perception of the degradation risk of the surface pavement. In the second act, fatigue failure ratio is plotted over time. This fatigue failure ratio will be expressed in percentages. In every time-step, the amount of measured data that display fatigue failure will be expressed in percentage. The data that show 0 damage will be plotted as well in percentages. The downside of plotting the fatigue failure ratio is that the factor degradation is not included. The fatigue failure ratio over time will be producing a prediction of risk over time model and not a probability model for degradation over time. However, this way of plotting filters out the scattering of the measured data, because of the translation from risk-points into a risk ratio over time (D. Bouwmeester; M. Huurman; F. Tolman, 2004). For the fatigue failure ratio over time, a best-fit curve and a simulation model are produced to make a prediction of risk over time model.

### 3.4 Best-fit curve

This subchapter briefly describes a best-fit model of fatigue failure ratio. To produce such a model, a prediction risk distribution needs to be used. There are many distributions, like the Weibull distribution, Gamma distribution, and Beta distribution. These distributions are related to each other and are infect a family of distributions. This is due to the fact that all these distributions have one or more shape parameters. Because of these shape parameters, a distribution can take a variety of shapes. This depends on the value of the shape parameters (National Institute of Standards and Technology, 2013). The distributions conduct naturally and are used for its properties. The distribution is flexible and can be applied to limited random variables to intervals of finite length in a wide variety of disciplines it is been used for the variability of soil properties, like asphalt (Haskett, Pachepsky, & Acock, 1995), (Lira, Jelagin, & Birgisson, 2013). For producing the best-fit model the beta distribution is used. The cumulative beta distribution function (Pearson, 1916) (also called incomplete beta function ratio) is used due to the fact that the output (x time in days) of the function is between 0 and 1. The X-axis 'time in days' can easily transformed into normalized time/time(max) due to fact that the cumulative beta distribution has an output between 0 and 1. The maximum time of the pavement life-cycle plotted in all the histograms is 5000 days. due to, the fact that the time-steps are 250 a normalized time can be implemented in the model  $250/5000 = 0.05$ . Furthermore, to normalize the maximum time the following steps are needed,  $5000/250 = 20$ ,  $20 \cdot 0.05 = 1$ . The Weibull and Gamma distribution do not have this property. It is therefore difficult to transform the x-axis into normalized time. The function of the cumulative beta distribution is shown by the equation figure 3.7. Furthermore, figure 3.8 is an example of the distribution and depicts 4 models for understanding. The parameter  $\alpha$  influence the lower part of the shape of the curve and the parameter  $\beta$  has an influence on the upper part of the shape of the curve as is shown in figure 3.8.

$$F(x) = I_x(\alpha, \beta) = \frac{\int_0^x t^{\alpha-1}(1-t)^{\beta-1} dt}{B(\alpha, \beta)} \quad 0 \leq x \leq 1; \alpha, \beta > 0$$

Figure 3.7: Function of the cumulative beta distribution

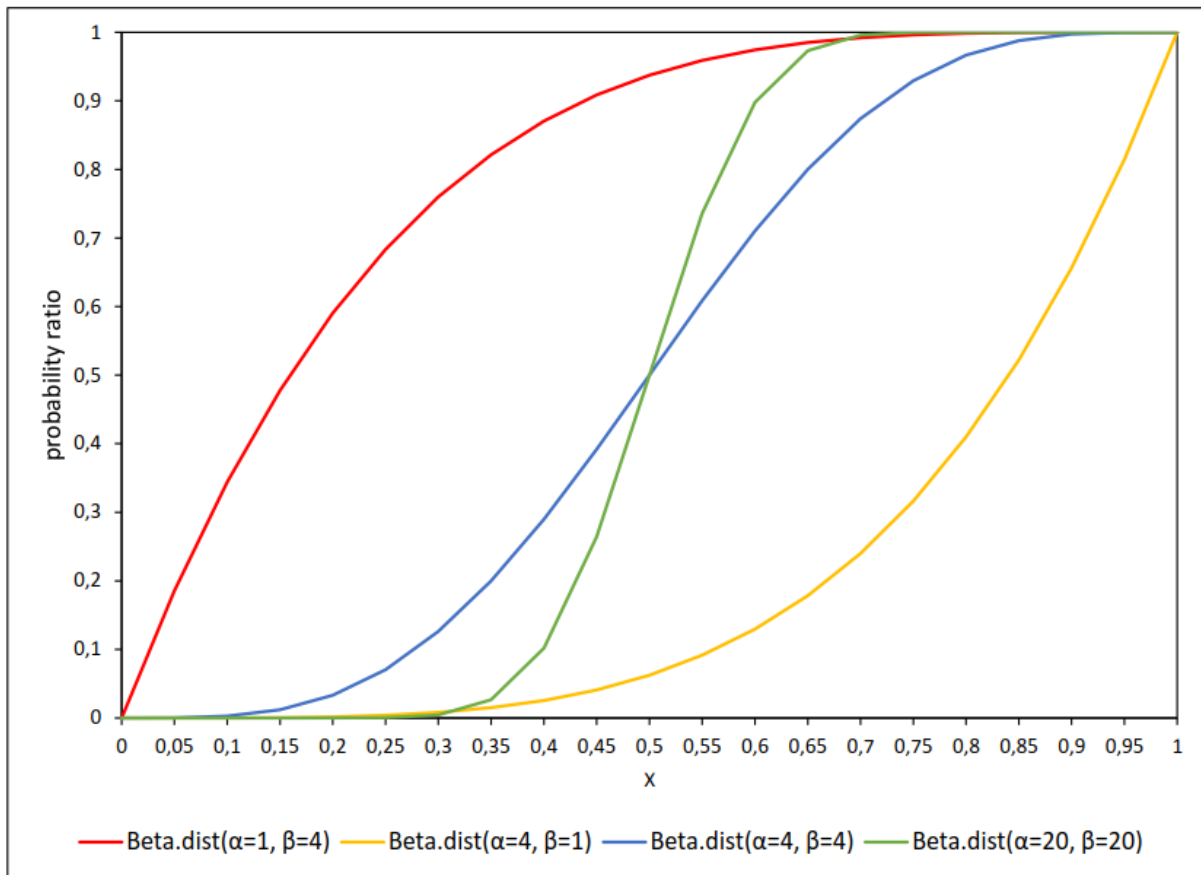


Figure 3.8: Example of 4 cumulative beta distribution probability models

In order to find the best-fit curve out of the measured data, a linear regression analysis is produced. The linear regression analysis is used because the beta distribution can take every shape or form that is needed to produce a best-fit curve (Razali & Wah, 2011). The cumulative beta distribution (cumulative distribution function (CDF)) is fitted in the measured data by finding the highest coefficient of determination ( $R^2$ ). This is done by hand with trial and error. The result is a scenario that will be the input for the simulation. For every impact of the independent variables, a scenario is produced. For further detail see Appendix E.

### 3.5 Monte Carlo simulation method

To simulate the scenarios that are produced by the best-fit models for predicting the risk of fatigue failure over time, a simulation model is produced. To simulate the risk of fatigue failure over time different simulation models can be used, like a Monte Carlo or Stochastic simulation. A Stochastic simulation though can only be used with a linear best-fit model and will lead to change the best-fit curve into a linear model (D. Bouwmeester; M. Huurman; F. Tolman, 2004). The Monte Carlo simulation model can be used for high scattered data and easily being implemented in Excel (A. Chen & Chen, 2016) (Ching & Wang, 2016). Furthermore, the Monte Carlo simulation is a method that can be used for modeling of real-life systems, such as a complex road network, transport of neutrons, or the evolution of the stock market. In essence,

‘natural’ objects appear randomly during the life-cycle. The setting of the Monte Carlo technique is to repeat the experiment many times in the model, to produce a quantity of interest using the ‘Law of Large Numbers’ (Kroese, Brereton, Taimre, & Botev, 2014)

### 3.6 An overview of the process of producing the prediction the risk over time model

This subchapter describes the process of producing the ‘prediction of the risk on fatigue failure over time’ model (see figure 3.9). The process started with collecting and/or manipulate the four datasets; surface pavements of all the highways in The Netherlands, visual inspections with the state of the 100-meter tiles, truck traffic intensity per day, and 18 years of measured cold days lower than -10 C°. the four datasets were separately putted in the FME model (see figure 3.6). The second step in the process was to merge and manipulate the four datasets together in a FME model. The output of the FME model was an Excel sheet with information of the location, state, age, independent variable ‘TI’, and independent variable ‘T-extreme on the 100-meter tile surface pavement (see table 3.2). For understanding the impact of the two independent variables an IF-statement filtering technique is used to produce plots of a degradation curves (see figure 3.10 and Appendix D). But because of the scattering of the measured data, a new technique was developed. The new technique can plot the fatigue failure ratio over time (see the tables in Appendix F, where the tables are produced from degradation risk points to fatigue failure ratio). Than the same IF-statement filtering technique was used to observe the impact of the two independent variables. With this new technique, the scattering can be captured because the measured data can be expressed in ratio over time.

With the new plots a best-fit curve is produced for the impact of different independent variables, as earlier mentioned with the beta distribution (see Appendix E). The best-fit curves can now be used as scenarios for the input of the simulation model, as mentioned earlier the Monte Carlo method is used to produce the simulation model (see Appendix G). The output of the simulation is a model that can predict the risk of fatigue failure over time on surface pavement. The results of this process are described in the next chapter.

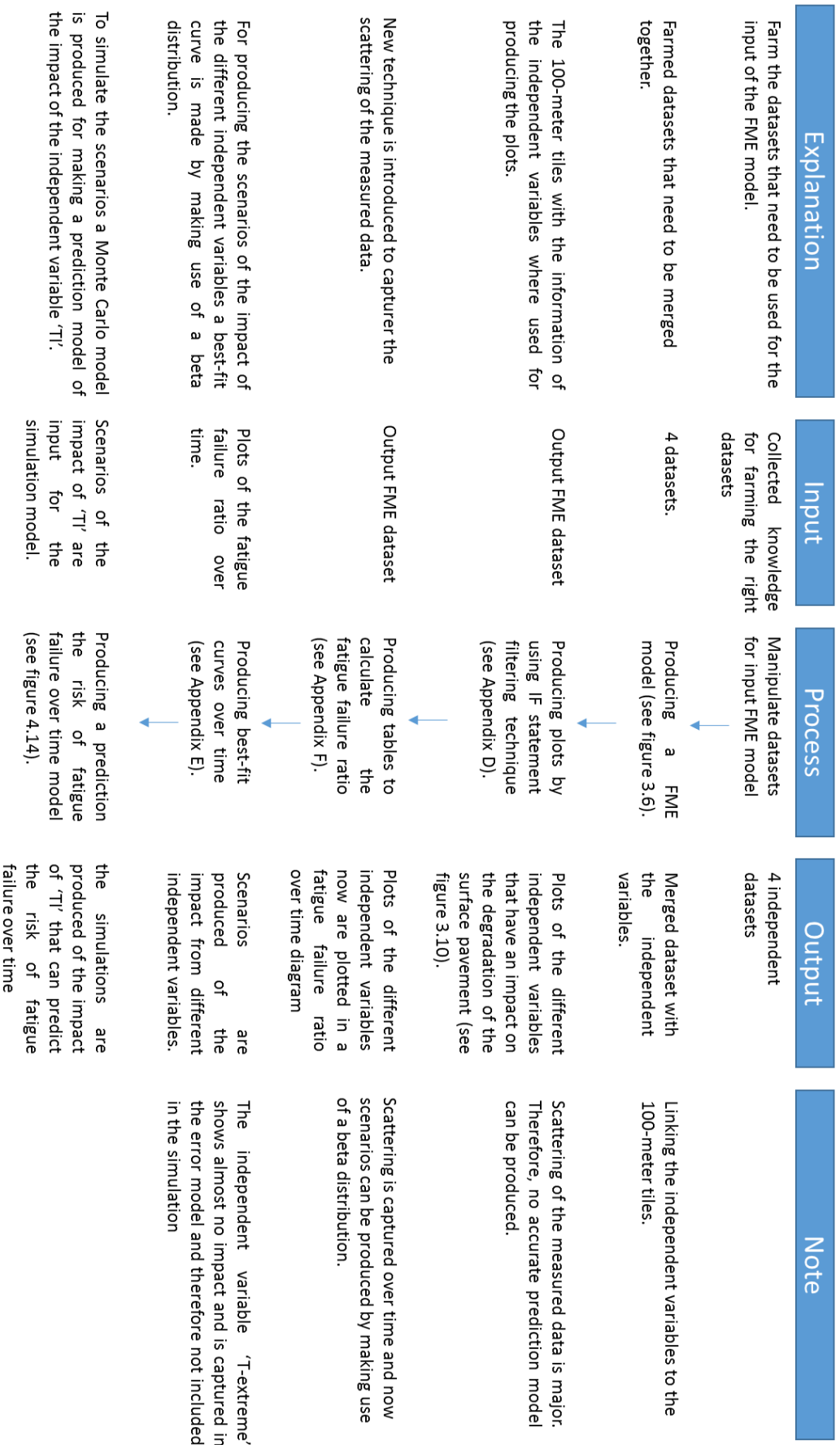


Figure 3.9: An overview of the complete process of producing the prediction of the risk of fatigue failure over time model.

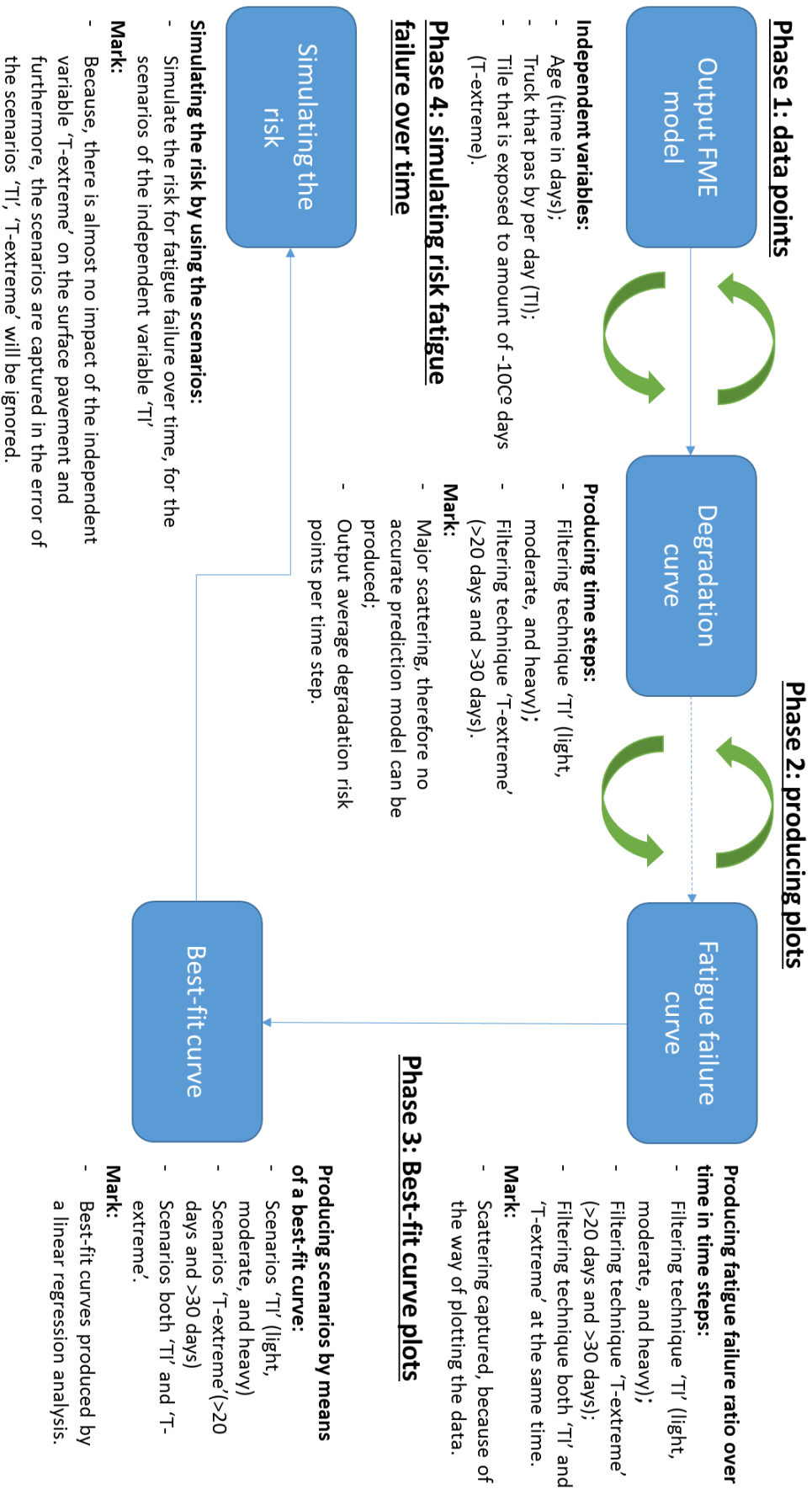


Figure 3.10: A detailed flowchart of the process from the moment of the output of the FME model, producing a prediction the risk of fatigue failure over time model.



## 4. Results of the Model

This chapter describes the acquired results from the output of the FME model. The output is analyzed in Excel. The filter technique that is described in subchapter ‘Analyzing manipulated data, and making assumptions’ is used to compare the different impacts of the independent variables. The independent variables that are used, the amount of extreme cold days during the lifecycle of the surface pavement (T-extreme), and the independent variable traffic intensity (TI) are described in the following subchapters; 3.1, and 3.2 the approach of model ‘Heijmans FMECA model’ is used. Subchapter 3.3 the same ‘Heijmans FMECA model’ is used. However, due to the scattering of the dataset, a different way of describing the dataset is used. The fatigue failure ratio and 0 damage ratio is depicted to capture the scattering. Section 3.4 the results of the best-fit curve by using a beta distribution will be described. The last subchapter 3.5 will use the beta distribution scenario model to simulate a case study by making use of a ‘Monte Carlo’ simulation model.

### 4.1 Results of the complete dataset and the impact of cold weather on the surface pavement with the ‘Heijmans’ approach

In figure 4.1 3 graphs can be observed. 4.1a shows the degradation curve for the ‘complete dataset’. This figure depicts that as the surface pavement ages the amount of damage increases. The orange bars show the amount of data decreases as the surface pavement ages. The critical FMECA fatigue failure mark is set at a value of 21 points and is shown by the horizontal gray line. The graph shows clearly as the time increases the amount of measured damage increases. However, due to the decrease in data points the standard deviation (shown by the error bar) increases over time as well. Figure 4.1b and c display the filtered versions of the complete dataset. Filtering is done on the number of extremely cold days (‘T-extreme’ > 20 days and ‘T-extreme’ > 30 days). These figures show a similar result with respect to the complete dataset. Therefore, one could argue that a slight increase in the amount of cold days has minimal effects on the ‘Heijmans’ FMECA degradation curve. Furthermore, changing the amount of cold days to > 30 days does not show significant changes. Overall all three figures depict that the critical values are reached at approximately 2750 days. Although, slight changes are observed by the impact of extreme temperatures.

#### 4.1.2 Impact of traffic on surface pavement

Figure 4.2 show in three graphs the impact of the independent variable ‘TI’. Figure 4.2a exposes the degradation curve due to the influence of light ‘TI’. As figure 4.1 the same trend can be observed, when surface pavement ages the amount of damage increases. The orange bars though show a slight increase of data as the surface pavement ages. However, due to the filtering technique, a large group of data is filtered out and the decrease of data is huge. The standard deviation though shows a slighter decrease over time compared to the complete dataset. Therefore, one could argue that the slighter decrease represents a more homogeneous data set. Overall due to the lack of data a critical value cannot be observed, however, the trend shows that this will be later in the life-cycle of the pavement in comparison with the complete dataset.

The moderate 'TI' is displayed in figure 4.2b. this figure shows a fairly similar result with respect to the 'complete dataset'. The graph clearly depicts that over time the data decreases and the standard deviation increases. Furthermore, a slight decrease of data is observed. Overall the figure shows that the critical value is reached at approximately 3250 days.

Figure 4.2c shows the impact of a heavy traffic intensity on the degradation of the surface pavement. Due to the filtering, this figure depicts a significant drop the amount of data points (Histogram figure 4.2c). The general trend within the degradation curve shows that the critical value of 21 is reached at an earlier stage in the life-cycle of the pavement with respect to the data shown in figure 4.1a (complete dataset). The increase in standard deviation of the data over time is also fairly similar. Although the decrease in the amount of data points is large, the decrease in the standard deviation over time and the fact that all measured results show values below the critical value, suggests that the traffic intensity has quite a significant impact on the life-cycle of a pavement. Therefore, this curve suggests that the average lifetime of a road pavement enduring a high 'TI' is approximately 2000 days.

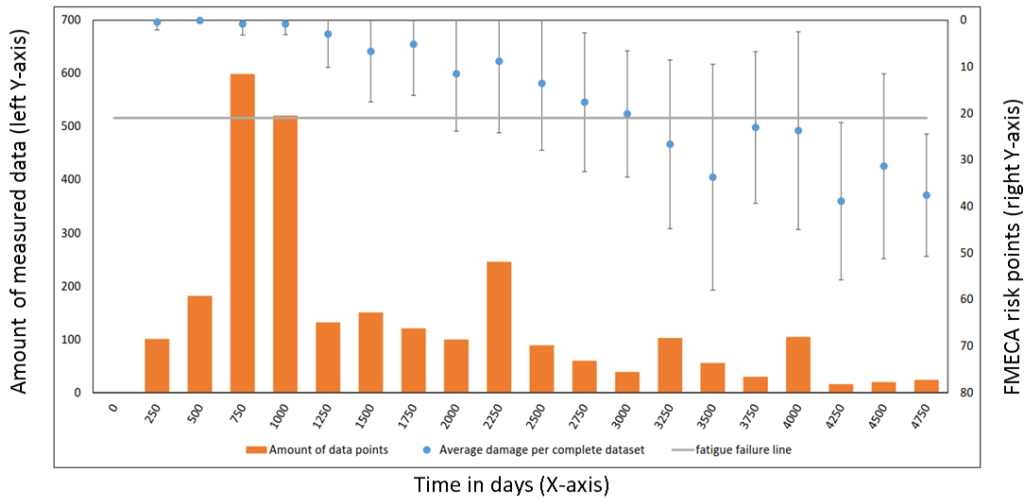
#### 4.2.3 The impact of cold weather and traffic intensity combined

Figure 4.3 displays the impact of the independent variables 'TI' and 'T-extreme' > 30 days combined. Due to, the filtering technique the lowest amount of data with respect to figure 4.1 and 4.2 can be observed. The green dots represent the impact of only 'TI'. Figure 4.3a depicts the impact of light traffic intensity in combination with cold weather. The figure exposes in the early stage of the life-cycle practically no measured data. Therefore, it is difficult to analyze the data. The data that is measured though show no significance with cold weather.

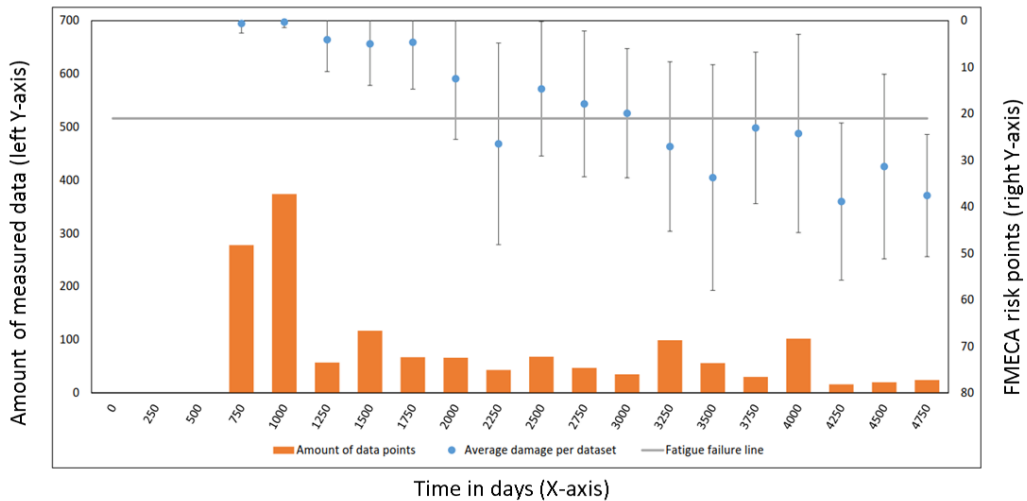
Figure 4.3b depicts the impact of moderate traffic intensity in combination with cold weather more than 30 days. As figure 3.3a no significant impact can be observed by the impact of cold weather. The degradation curve shows a fairly similar degradation trend with respect to figure 4.2a. The amount of data though has severely degraded in comparison with this figure. Overall no impact can be observed.

The influence of heavy traffic intensity in combination with cold weather more than 30 days is displayed in figure 4.3c. Because of the extreme filtering, this figure depicts a significant drop in the amount of data points in respect with figure 4.2c. However, the measured data show that the critical value is reached at an earlier stage in the life-cycle of the pavement in contrast with figure 4.2c. Although the decrease in the amount of data points is large, the fact that all measured results show a bigger drop of values below the critical value, suggests that the cold weather variable has quite a significant impact on the life-cycle of a pavement. Therefore, this curve suggests that the average lifetime of a road pavement enduring a high 'TI' in combination with cold weather is less than 2000 days.

### 4.1a Complete dataset



### 4.1b Impact 'T-extreme' >20 days



### 4.1c Impact 'T-extreme' >30 days

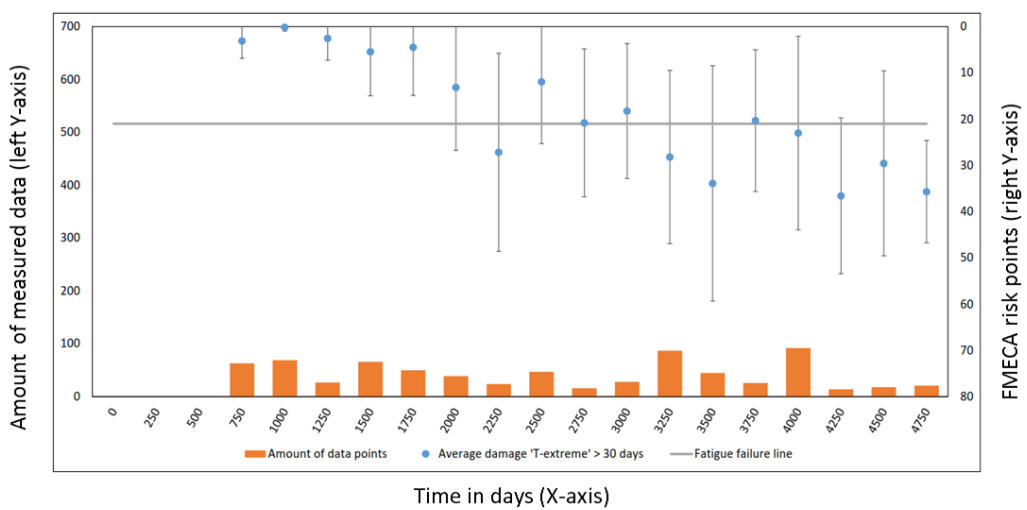
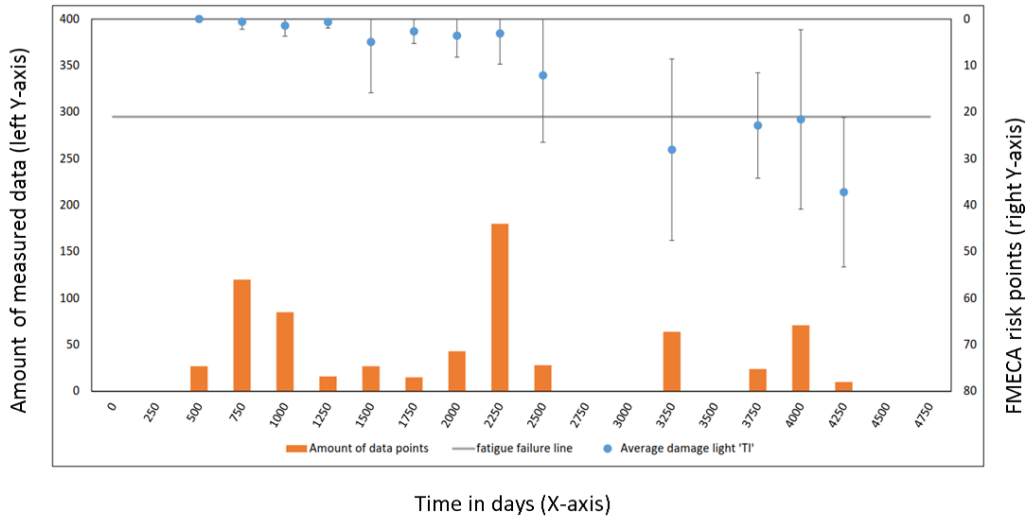
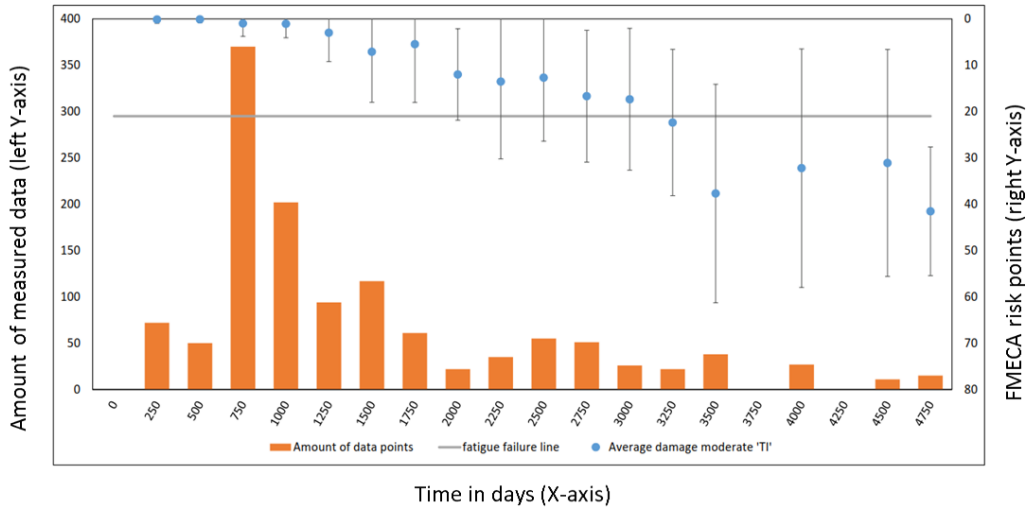


Figure 4.1: graphs complete dataset, and impact extreme cold days, with an average degradation curve of surface pavement.

### 4.2a Light 'TI'



### 4.2b Moderate 'TI'



### 4.2c Heavy 'TI'

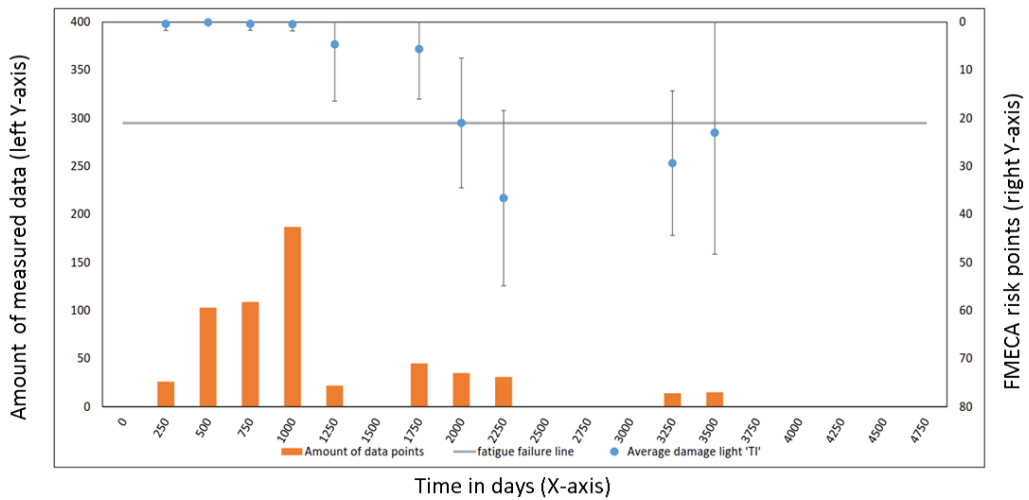
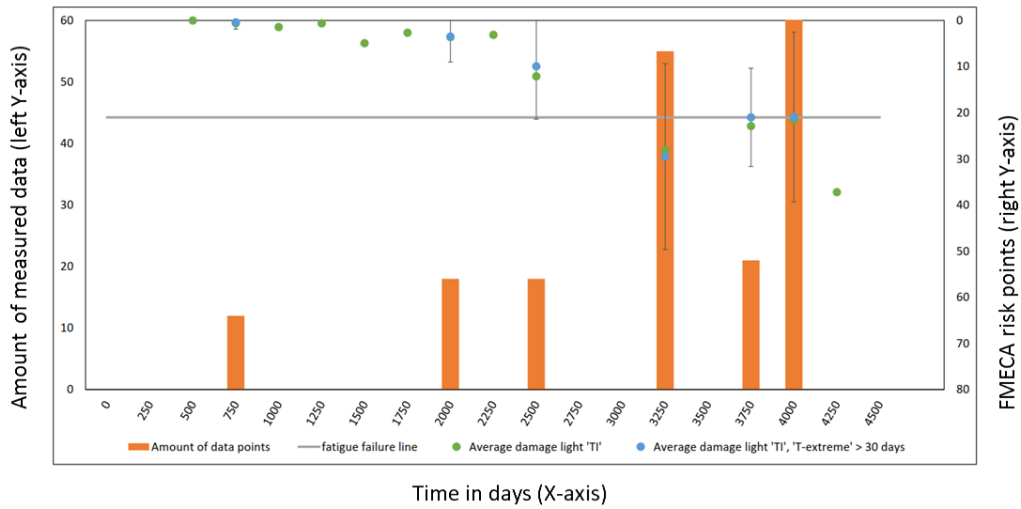
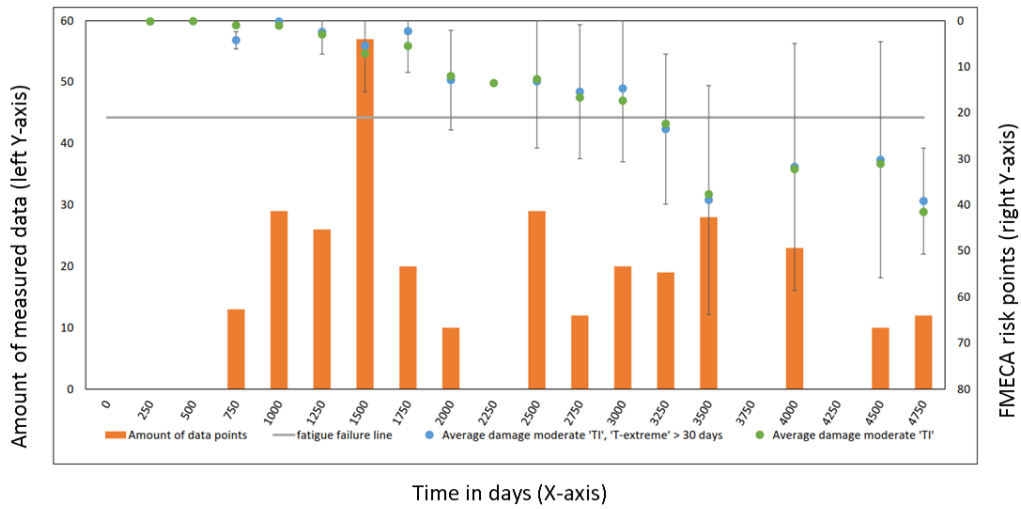


Figure 4.2: graphs, the impact of light, moderate, and heavy 'TI' of trucks on the degradation of the surface pavement.

### 4.3a Light 'TI' and 'T-extreme >30 days



### 4.3b Moderate 'TI' and 'T-extreme >30 days



### 4.3c Heavy 'TI' and 'T-extreme >30 days

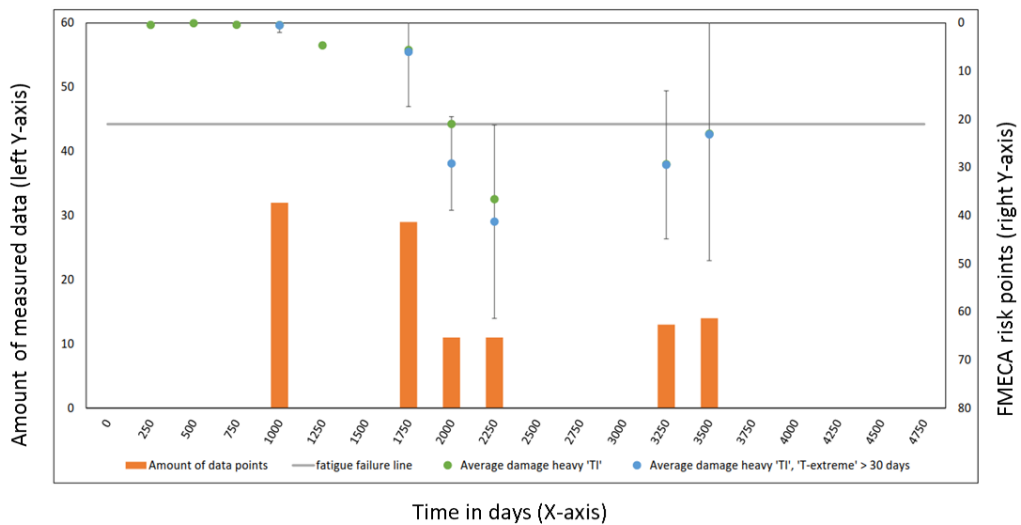


Figure 4.3: graphs, the impact of light, moderate, and heavy 'TI' of trucks on the degradation of the surface pavement.

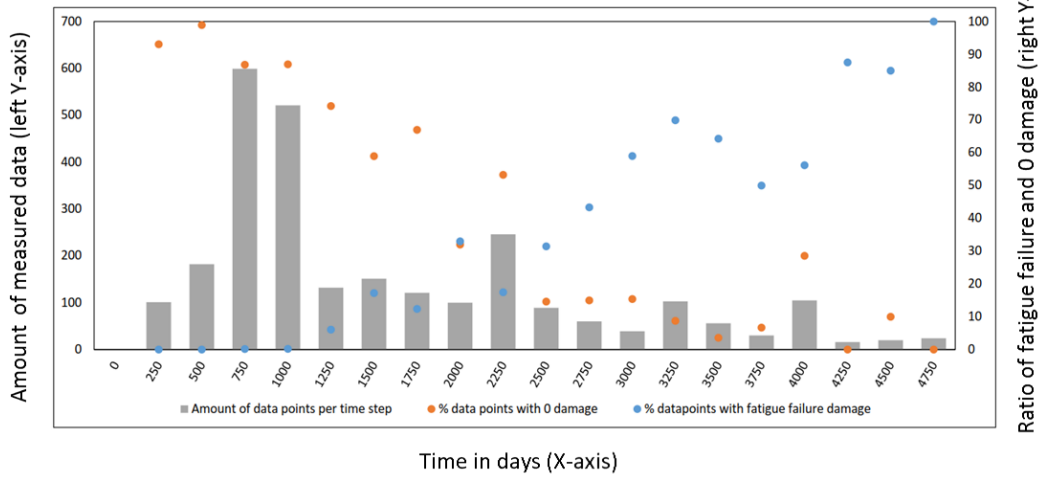
### 4.3 Fatigue failure ratio over time

This subchapter describes the measured data plotted as fatigue failure ratio and 0 damage ratio. Due to, the significant increase of the standard deviation in general a poor reliable prediction model can be produced. Appendix E shows the tables that are used to produce the histograms of the fatigue failure ratio histograms. This way of plotting 2 major measured data groups can be separated from each other. the 0 damage ratio group is approximately 2/3 of the measured dataset. Overall this way of plotting a more reliable prediction model can be produced.

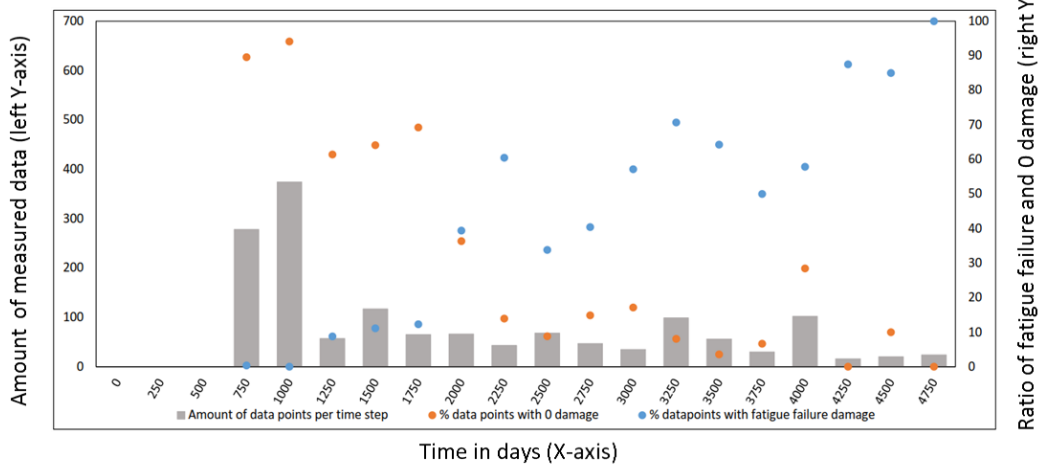
#### 4.3.1 Results of the complete dataset and the impact of cold weather on the surface pavement due to plotting the fatigue failure ratio over time

In figure 4.4 three histograms can be observed in the complete dataset and impact of cold weather. Figure 4.4a shows the fatigue failure ratio (blue dots) for the complete dataset and 0 damage ratio (orange dots). This figure depicts that as the surface pavement ages the fatigue failure ratio increases and the 0 damage ratio decreases. This trend is also observed in respect with figure 4.1a. Furthermore, the measured data indicates that when the fatigue failure ratio starts to increase the 0 damage ratio starts to decrease. Figure 3.1b and c represent the filtered versions ('T-extreme' > 20 days and 'T-extreme' > 30 days) of the complete dataset. These figures show a different result with respect to the complete dataset. The fatigue ratio is increasing more rapid in the early stage of the measured data. After this early stage, the trend starts to follow the trend of figure 4.1a. Furthermore, the 0 damage ratio starts to decrease in the early stage of the measured data with respect of the complete dataset. Like, the fatigue failure ratio, the 0 damage ratio start after the early stage period to follow the trend of the complete dataset.

### 4.4a Complete dataset



### 4.4b Impact 'T-extreme' >20 days



### 4.4c Impact 'T-extreme' >30 days

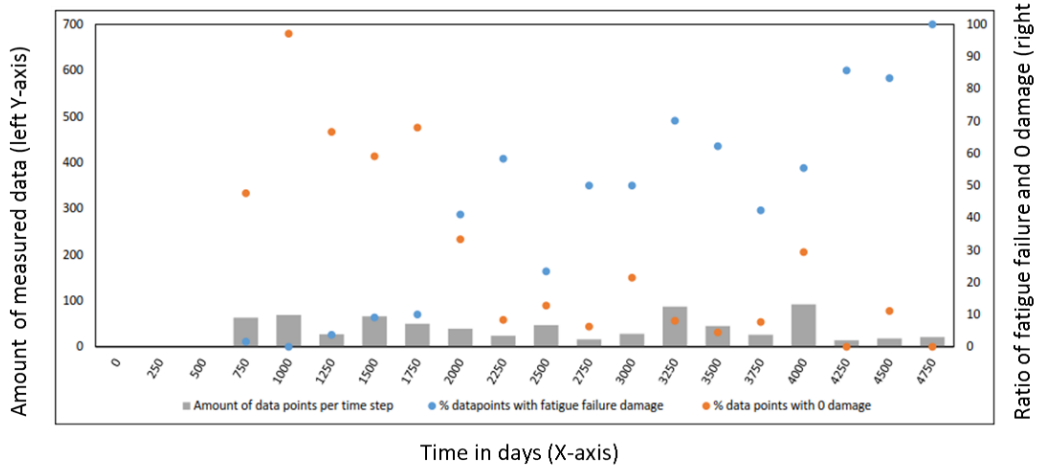


Figure 4.4: graphs complete dataset, and impact extreme cold days, with an average ratio of fatigue failure on the surface pavement.

#### 4.3.3 Impact of traffic and cold weather on surface pavement because of plotting fatigue failure ratio over time

This subchapter describes briefly the impact of traffic and cold weather on surface pavement expressed in a ratio. The impact of the variable 'TI' on the fatigue failure ratio and the 0 damage ratio is displayed in figure 4.5. Figure 4.5a shows the fatigue failure ratio of light traffic intensity. A similar trend can be observed in figure 4.4. The measured data depicts that when the surface pavement ages the fatigue failure increases and the 0 damage ratio decreases. As with figure 4.2a the histogram misses measured data when the fatigue failure ratio increases significantly. Therefore, men could argue that the fatigue failure will increase according to the trend that is perceived in the complete dataset. The impact of moderate 'TI' though, shown in figure 3.5b a fairly similar trend can be detected as in figure 4.4a. Next, the heavy 'TI' shown in figure 4.5c shows something else, a significant increase in fatigue failure ratio and a significant decrease in 0 damage ratio can be perceived in the early stage of the life-cycle of the pavement. This fairly similar trend can be depicted in figure 4.2c. Overall according to the measured data is the fatigue failure ratio approximately 90 %.

The impact of traffic and cold weather combined expressed in the ratio is displayed in figure 4.6. The measured data show that in figure 3.6a a fairly similar increase of fatigue ratio as in figure 4.5a. Furthermore the same could be said about the decreasing of 0 damage ratio. The influence of moderate 'TI' in combination with cold weather show in respect with figure 4.5b slightly increase of fatigue failure ratio when the pavement ages. However, 0 damage show no significant decrease in comparison to figure 4.5b. The impact of cold weather in combination with heavy traffic shows for fatigue failure ratio an earlier increase and for 0 damage ratio an earlier decrease in the life-cycle of the pavement. Overall from the measured data can be depicted that at time-step 2000 days the fatigue failure ratio is approximately 90 % and the 0 damage ratio 0 %.

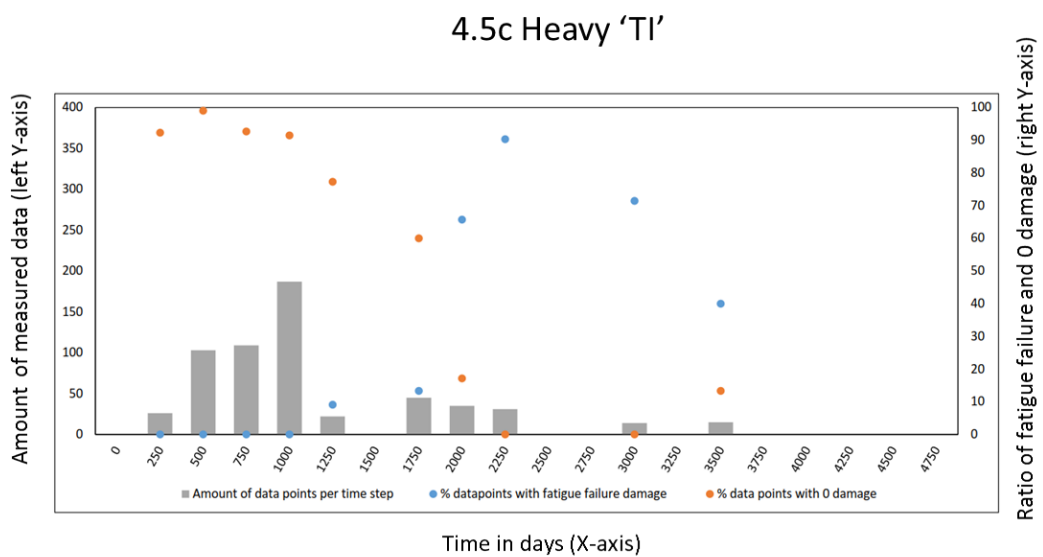
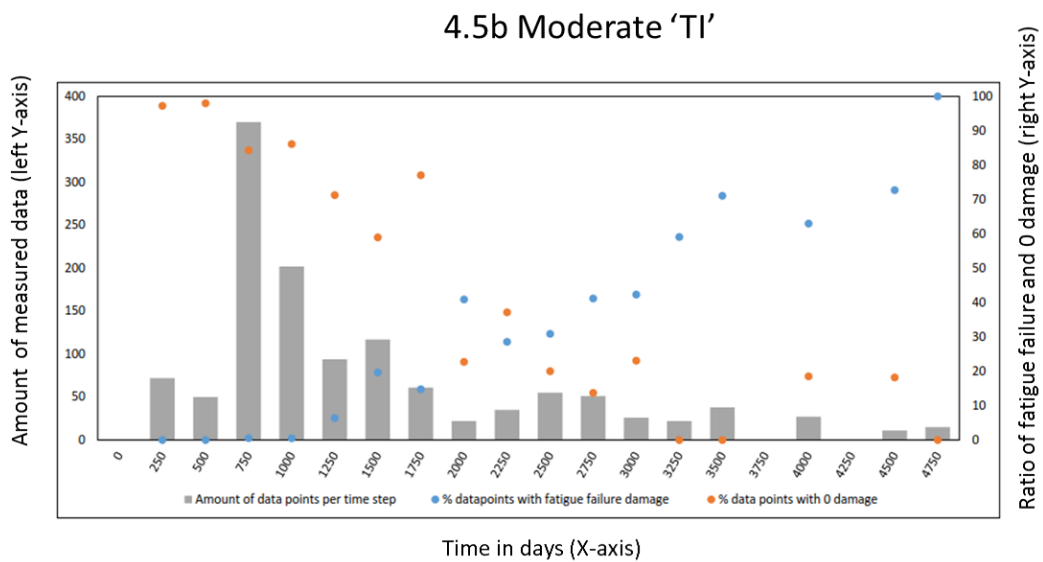
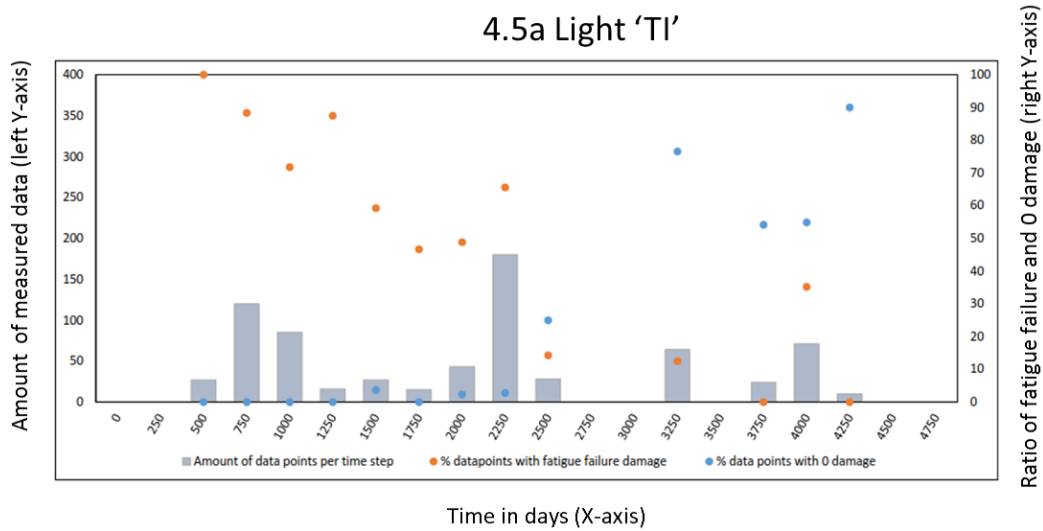
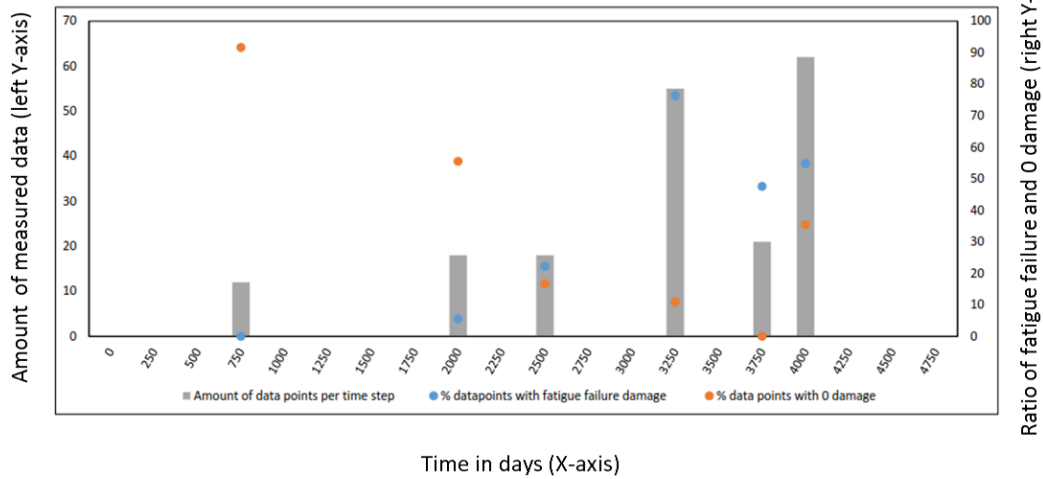
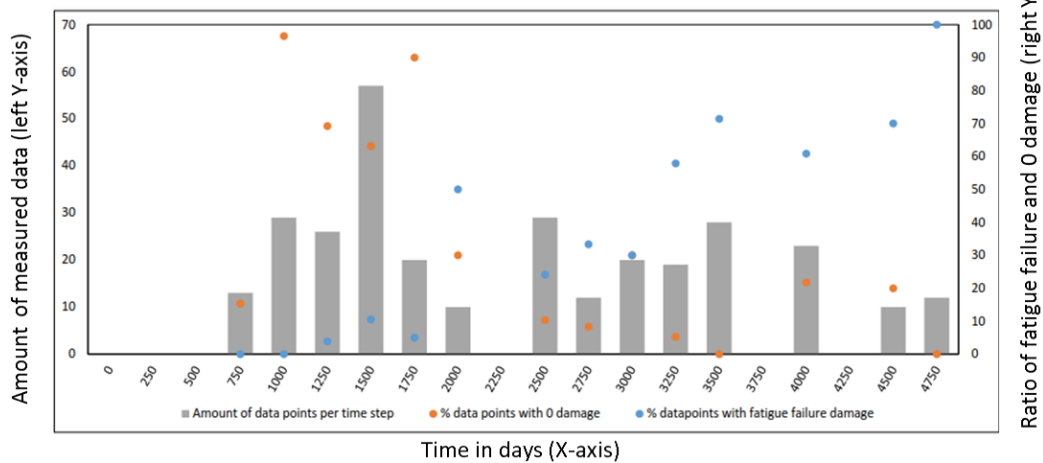


Figure 4.5: graphs with the influence of traffic intensity by trucks, with an average ratio of fatigue failure on the surface pavement.

### 4.6a Light 'TI' and 'T-extreme >30 days



### 4.6b Moderate 'TI' and 'T-extreme >30 days



### 4.6c Heavy 'TI' and 'T-extreme >30 days

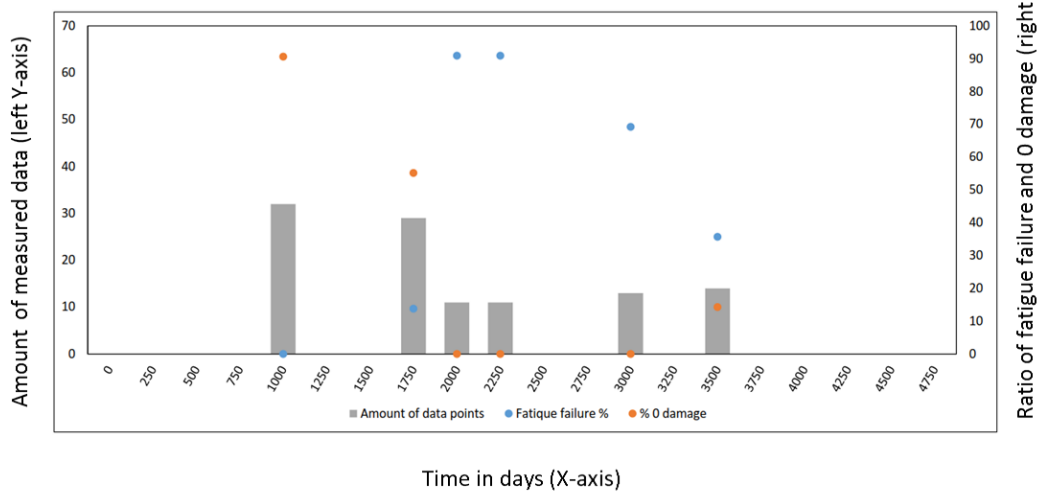


Figure 4.6: graphs, the impact of traffic intensity by trucks, and the influence of cold weather combined, with an average ratio of fatigue failure on the surface pavement.

#### 4.4 Best-fit curve

This subchapter describes the results of the best-fit curves. In order to produce a best-fit model, the CDF of the beta distribution is used (National Institute of Standards and Technology, 2013). We create a best-fit curve out of the empirical fatigue failure ratio graphs by using a linear regression analyzes (Razali & Wah, 2011). Razali & Wah 2011 used a linear regression analyzes aswell to find the best-fit CDF curve. The graph that is used as an example (see figure 4.9) the ‘complete dataset’ fatigue failure ratio graph. This plot is selected because of, the plot has the most measured data. The other best-fit curves can be observed in Appendix E. Furthermore, as earlier mentioned in subchapter 3.4 the X-axis ‘time in days’ is transformed into normalized time/time(max) due to the fact that the CDF has an output between 0 and 1. The maximum time of the pavement life-cycle plotted in all the histograms is 5000 days. The time-steps are 250 days, to plot the normalized time on the X-axis a calculation need to be made. To implement the normalized time a calculation of  $250/5000 = 0.05$  and  $5000/250 = 20$ ,  $20 * 0.05 = 1$  is needed. Next, to find the best-fit beta distribution curve a best-fit linear regression model is produced (Appendix E).

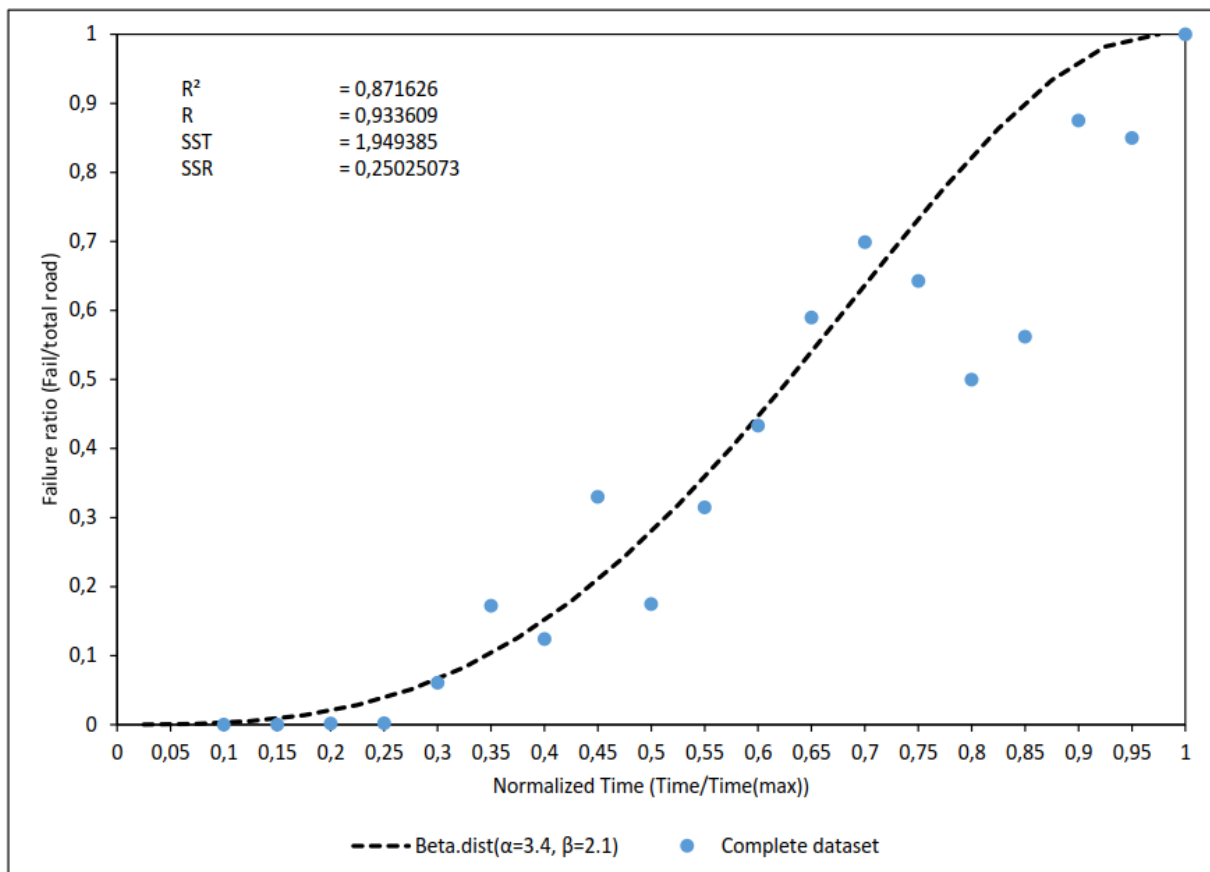


Figure 4.9: Best fit model fatigue failure ratio curve, of the complete dataset graph.

Figure 4.9 can be an  $R^2$  of 0,87 observed. The trend of the best-fit curve showed in the early stage higher significands, then in a later stage of the probability curve of the life-cycle. Furthermore, the same technique is used to predict the impact of the independent variables ‘TI’, and ‘T-extreme’. Figure 4.10 depicts 10 different scenarios that can be used to predict the fatigue failure ratio of surface pavement. The downside of these prediction models is that the filtering technique will lack measured data and will produce a low  $R^2$ .

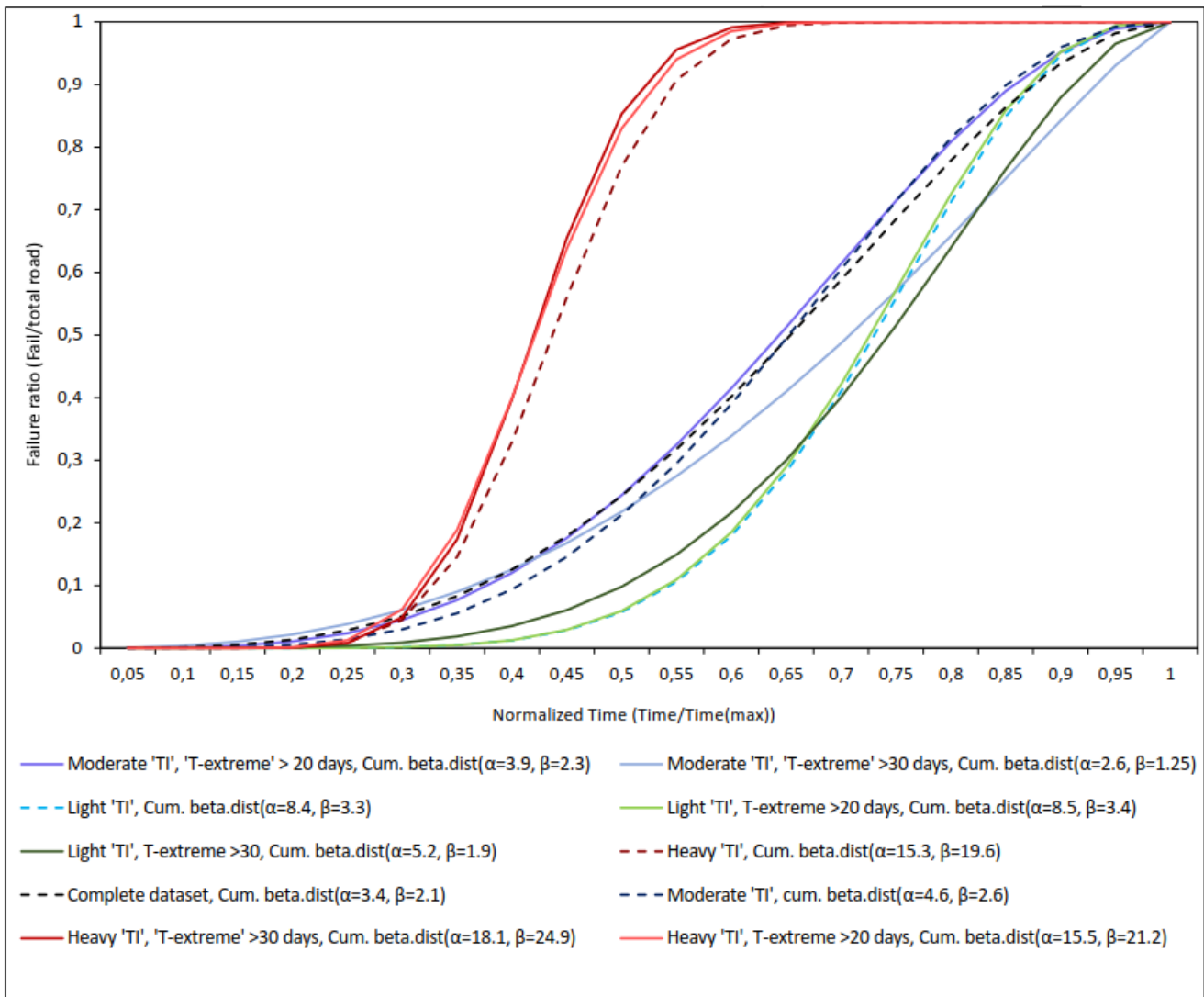


Figure 4.10: Scheme of the 10 different scenarios that predict the fatigue failure ratio of surface pavement.

The first best-fit curves that are described as a scenario are the scenarios with the independent variable heavy 'TI' (see figure 4.10). In these scenarios, the surface pavement will have the lowest hazard on a long life-cycle. The red dashed line is the scenario with, only heavy use of truck traffic. In the two scenarios where the impact of cold weather is included ('T-extreme' > 20 days, and > 30 days) have a slightly faster hazard on a short life-cycle. These three best-fit models show a 'coefficient of determination' of; (see Appendix D) only 'heavy 'TI',  $R^2= 0,541364$ ' (red dashed line), 'heavy 'TI', 'T-extreme' > 20 days,  $R^2= 0,319794$ ' (light red line), and 'heavy 'TI', 'T-extreme' > 30 days,  $R^2= 0,169399$ '. The scenarios with light use of truck traffic (see green lines figure 4.10); only 'light 'TI',  $R^2= 0,795076$ ' (green dashed line), 'light 'TI', 'T-extreme' > 20 days,  $R^2= 0,749961$ ' (light green line), and 'light 'TI', 'T-extreme' > 30 days,  $R^2= 0,534401$ ' (dark green line). The moderate use of trucks on surface pavement can be depicted as the blue lines figure 4.10. This group show the highest significance and is fairly similar in respect with the complete dataset curve; only 'moderate 'TI',  $R^2= 0,832657$ ' (dashed blue line), 'moderate 'TI', 'T-extreme' > 20 days,  $R^2= 0,759969$ ' (light blue line), and 'moderate 'TI', 'T-extreme' > 30 days,  $R^2= 0,74657$ '. For all graphs of the different scenarios see Appendix E. The used ' $\alpha$ ' and ' $\beta$ ' of the different best-

fit models are depicted in figure 4.11. This clear overview show of the different will be used for a simulation model.

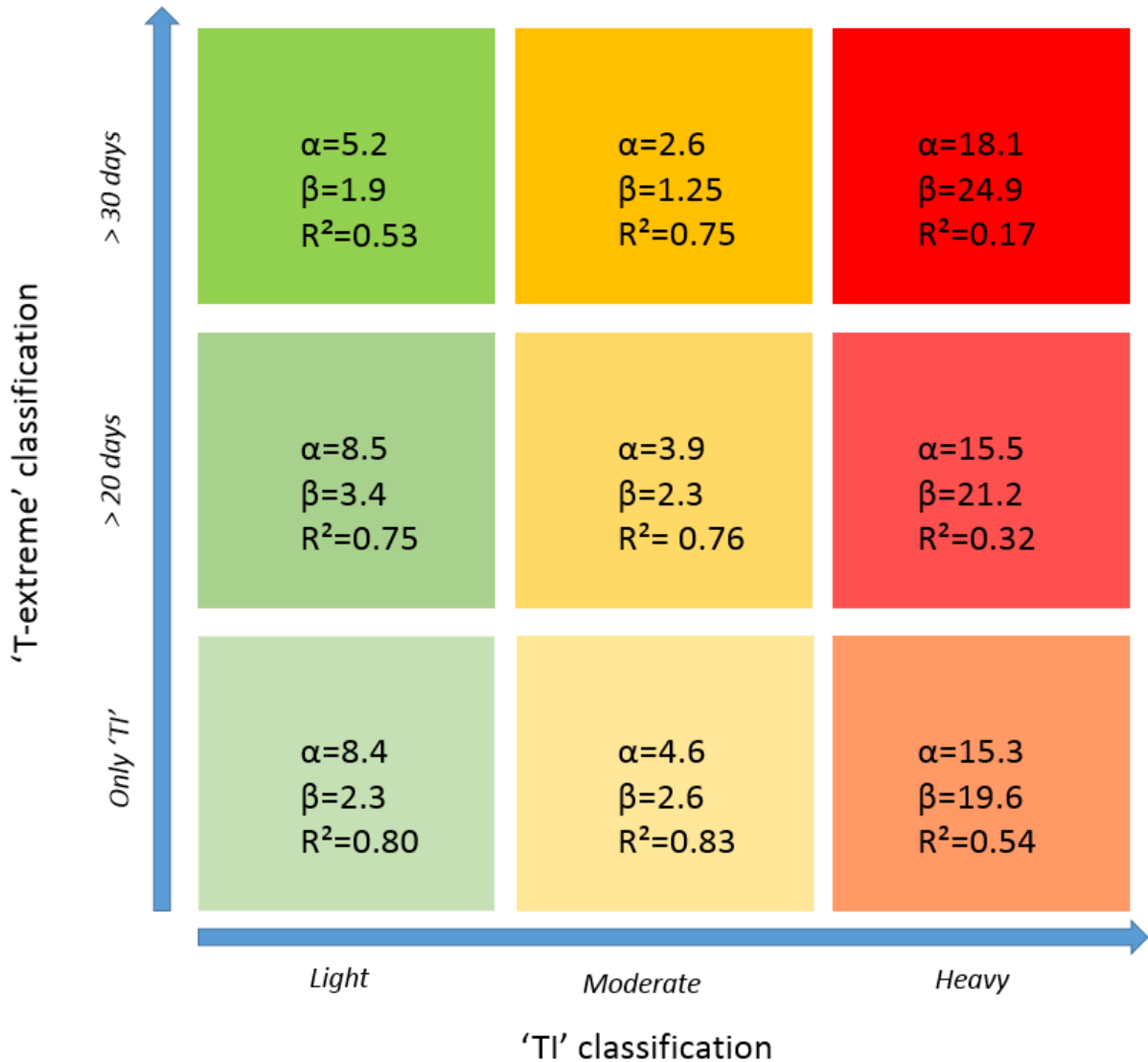


Figure 4.11: Overview of the figures of the cumulative beta distribution from the different scenarios.

The best-fit models will be used for a case study. This case study will be explained in the next subchapter (Case study of the project 'A12 VEG').

## 4.5 'Monte Carlo' simulation

This subchapter will describe the use of the Monte Carlo simulation model to predict the risk for fatigue failure of 10% during aging of the surface pavement. The Monte Carlo method is used because we want to capture error in the dataset for the three parameters 'TI' (light, moderate, and heavy). We will capture standard deviation of our dataset with respect to the best-fit beta distribution using the following equation (see figure 4.12). We will use the standard deviation to include the observed error in our predictive the risk over time model. As was observed in subchapter 3.3 and 3.4. There is practically no impact observed of the parameter 'temperature' (see figure 4.10) on the measured data and therefore, on the CDF. The impact of this variable is smaller than the measured standard deviation and is therefore captured by our error model and not used as input for the simulation.

$$VAR = \sum_i^N \frac{(f(beta\ dist.) - y_i)^2}{N}$$

$$Std. = \sqrt{VAR}$$

Figure 4.12: Function of error capturing for calculating the variance

The upper bound and a lower bound of the best fit beta distribution can be described by the following function as is shown in figure 4.13. See Appendix F for process description.

$$Upper\ bound = f((\alpha - std.), (\beta + std.))$$

$$Lower\ bound = f((\alpha + std.), (\beta - std.))$$

Figure 4.13: Function of the upper bound and the lower bound of the best fit beta distribution.

The simulation model is used to incorporate the error of the two shape parameters ( $\alpha$ ,  $\beta$ ) by producing more than 1000 simulations. For the process description of the Monte Carlo simulation see Appendix G. The result of the simulation model is depicted in figure 4.14. The figure shows three normal distributions of the three traffic intensity scenarios of the critical moment curve of the fatigue failure ratio of 10%. Due to the fact, that the best-fit cumulative beta distributions (see figure 4.10) are increasing rapidly when the fatigue failure ratio has reached 10%. Overall, men could argue that high 'TI' degrades faster than moderate and light 'TI'. High 'TI' will show a fatigue failure ratio of 10% at approximately of 1750 days (4.8 years), moderate 'TI' shows a fatigue failure ratio of 10% at approximately 2000 days (5.6 years), and light 'TI' will show a fatigue failure ratio of 10% at approximately 2600 days (7.1 years).

### Critical Moment Curve (10% of the road shows fatigue failure)

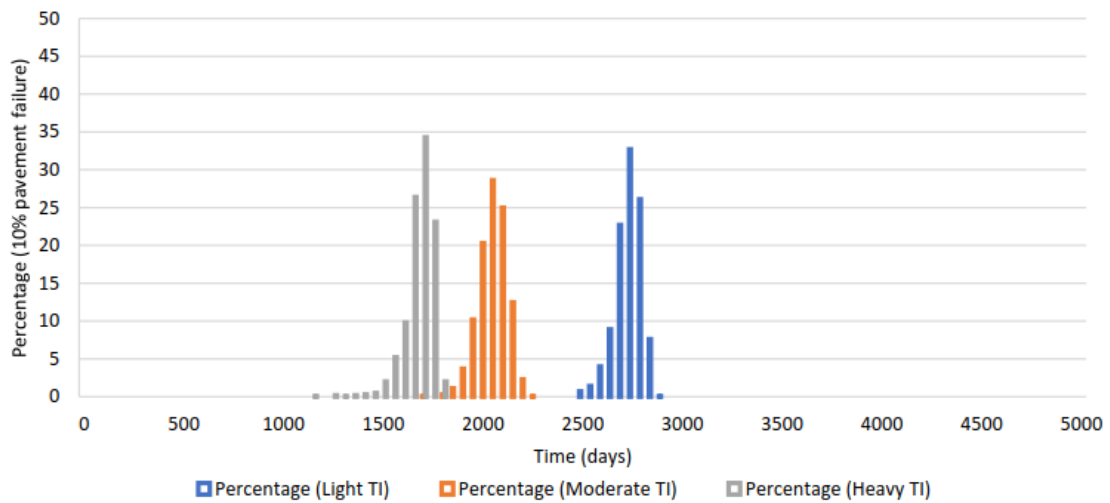


Figure 4.14: Normal distribution graph of the critical moment curve of 10 % pavement failure.

#### 4.5.1 Case study project ‘A12 VEG’

The case study is a project called ‘A12 VEG’ and is carried out by the contractor ‘Heijmans’, this contract is a DBFM contract construction with the agency RWS. The project is located between Ede and the junction Grijsoort in The Netherlands (see figure 4.15).

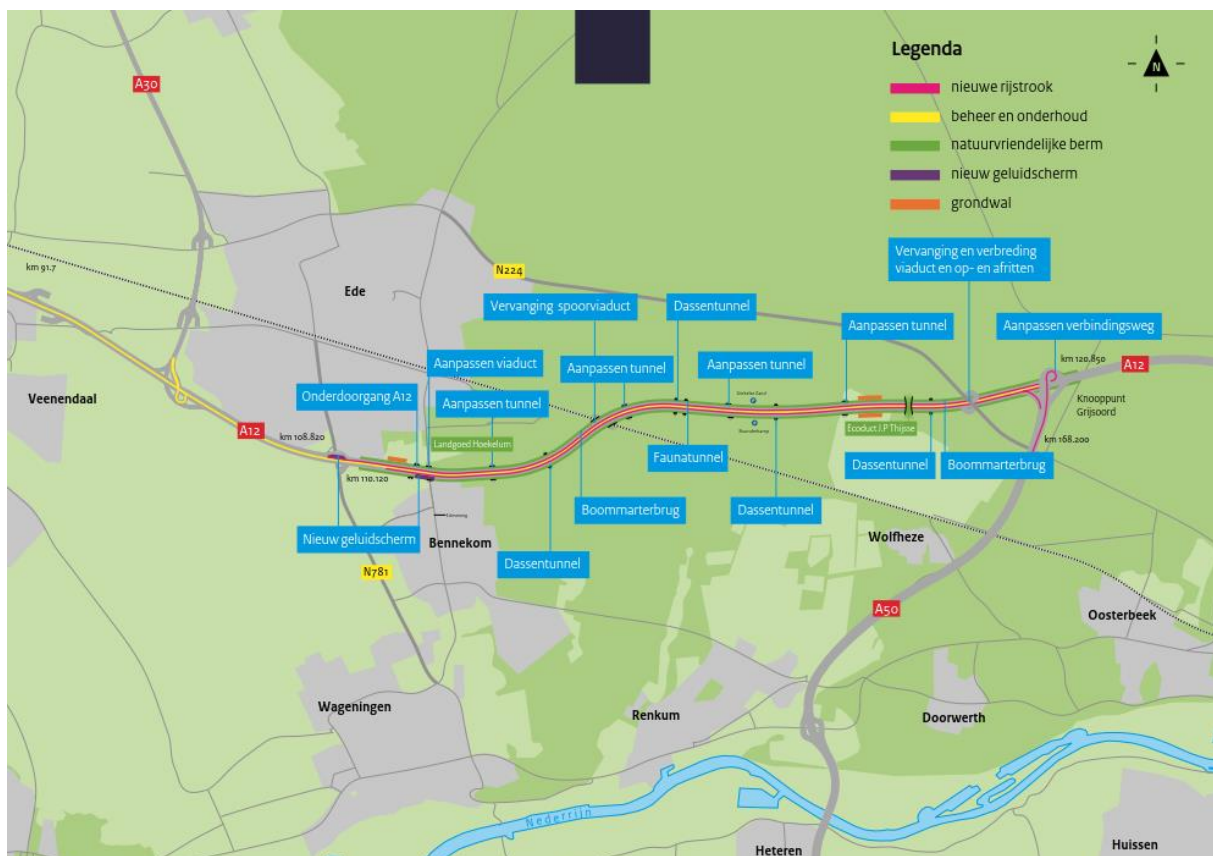


Figure 4.15: Location of the project named ‘A12 VEG’(Rijkswaterstaat, 2014)

‘Heijmans’ has constructed in this project 11 kilometer of 3\*3 lanes of PAC surface pavement construction and is as well responsible for the maintenance of the road construction. The contract period for maintenance of the road construction is 16 years.

For the case study, ‘INWEVA’ is consulted for choosing the probability model. The amount of trucks that passes per day is between 2500 and 3000 trucks a day. Therefore, a moderate ‘TI’ scenario probability model is picked. Furthermore, to produce a more accurate model, the method ‘Percentile’ is included in the model. Percentile is a method that is used to measure an indicating value below a given percentage. The percentage is depicted from a certain group.

The ‘Monte Carlo’ simulation model produces the following numbers that can be depicted from Table 4.1. The table shows 3 percentile groups. The range between the percentile groups is approximately 200 days for this case study. Furthermore, at 5.6 years the percentile of 50 % is reached, men could argue that the change on 10% fatigue failure is at this moment in the life-cycle of the surface pavement 5 %.

10 % of the surface pavement show fatigue failure due to raveling				
Average in days		Percentile 90%	Percentile 50%	Percentile 10%
2025,955775	Percentage	0,385835429	0,40624946	0,423013957
Max days 5000	Days	1929,177146	2031,247302	2115,069783
	Years	5,28541684	5,565061102	5,794711735
95 % of the surface pavement show fatigue failure due to raveling				
Average in days		Percentile 90%	Percentile 50%	Percentile 10%
4458,681017	Percentage	0,87711317	0,891196308	0,907207978
Max days 5000	Days	4385,565851	4455,981542	4536,039889
	Years	12,01524891	12,20816861	12,42750655

Table 4.1: The table shows the output of the probability ‘Monte Carlo’ simulation model for moderate ‘TI’ scenario.

## 4.6 Summary Results

This subchapter describes, in brief, the results of the two techniques that are used to analyze and filter the measured data over time, the results of the best-fit models, the results of the ‘Monte Carlo’ simulation, and the results of the case study ‘A12 VEG’.

- The degradation histograms show that traffic intensity has numerous significance in comparison to the cold weather histograms.
- The histograms of both factors combined shows only with heavy traffic intensity a significance.

- The standard deviation increases over time in the degradation histograms due to the fact of the scattering of the measured data.
- The fatigue failure histograms the same trend can be observed as in the degradation histograms. Traffic intensity has a numerous significance in comparison to the cold weather factor. Furthermore, the influence of both factors combined shows that only heavy traffic has a slight significance on fatigue failure to the surface pavement over time.
- The best-fit models show that the moderate scenario has the highest coefficient determination, because of, the amount of measured data. The scenario with heavy traffic intensity displays a trend line that the risk of fatigue failure increases numerous significance than the moderate scenario and light scenario.
- The output of the Monte Carlo simulation shows that predicting the risk of 10 % fatigue failure on the surface pavement increases over time when traffic intensity increases.
- The result of the case study shows that predicting the risk of 10 % fatigue failure over time at the percentile of 50 % approximately 2000 days is or 5.6 years. The complete fatigue failure of the road construction will be around 4500 days or 12.2 years.



## 5. Conclusions

The main goal of this research was to manage different databases and merge them together into one big database. This dataset was then used to produce a prediction model that could predict the risk of fatigue failure over time on surface pavement. To produce the dataset a FME model is made to link the pavement tills to the construction data, inspection data, classification of degradation, traffic intensity, and temperatures where the surface pavement was exposed to during its life-cycle. The merged database was plotted on a timeline with degradation classifications. The research aimed to find an answer for the research question; *'Which external factors have the highest impact on raveling that influences the degradation curve of surface pavement at highways in The Netherlands? And what is the risk impact of the external factors on the fatigue failure of the surface pavement?'*. By means of producing a reliable degradation curve in a prediction model.

The FME model that is produced, proves to be an accessible tool to tackle the automatization problem. The output of the spatial datasets that are merged with non-spatial datasets shows some flaws but is in general acceptable merged. The tool can easily be reproduced or fine-tuned in the future.

The database that is created out of the FME model shows a significant scattering. Therefore, it is not possible to produce a reliable risk degradation prediction model directly using the measured data. However, the acquired plots do show a trend with more degradation as time progresses. Furthermore, using several filtering techniques such as traffic intensity different trend lines can be observed. Therefore, the plots show the impact of the independent variable truck traffic intensity and slightly an impact of cold weather.

Because of the technique that is used to plot fatigue failure over time the scattering can be captured. This way the prediction model is produced. With the prediction model, it is still not possible to predict the impact of cold weather on the surface pavement over time. However, the prediction model can simulate the fatigue failure scenarios of the traffic intensity parameter with a certain accuracy. Even though an extra assumption is made that the best-fit curve is the truth. The error from the fatigue failure ratio measured data can be captured within the error bar (see subchapter 3.5). The prediction simulation model with a fatigue failure of 10 % can be used in practice for light 'TI' within a range of approximately 160 days and a lifespan of 7.1 years, moderate 'TI' within a range of approximately 200 days and a lifespan of 5.6 years, and heavy 'TI' within a range of approximately 160 days and 4.8 years. Furthermore, the model can be getting more accurate during the years by adding more measured data.



## 6. Discussion and recommendations

This chapter discusses this research and applies recommendations for further research. In this chapter, the following issues will be discussed for degradation of surface pavement, because of, the raveling; FME model, probability model, monitoring surface pavement, classify 'quality' of surface pavement, archiving the data, and the influence of the two used external parameters.

### 6.1 FME model

The FME model can be used in the near future as a tool for more integrated data that can be stored in the model. Measured data can efficiently add to the model. Furthermore, because of the automatization of the model, the model will generate always the same kind of output. Therefore, stakeholders can easily adapt the tool for practical purposes.

The downside of the model is the limitations of the input data. the visual inspection data is now only ones inspected, at the moment that RWS want to reconstruct the surface pavement. This gives a limitation that the road is not frequently inspected during its lifespan. Furthermore, the quality of the surface pavement during construction time need to be implemented as well to increase the accuracy of the prediction model.

### 6.2 predicting the risk model

The prediction the risk model is a support tool that gives an indication when the surface pavement starts to show fatigue failure at a certain time in the life-cycle of the pavement. According to the results of Henning & Roux (2012), low volume traffic load ravel faster than high volume roads. The results of this thesis though, show the opposite. The results show that heavy intensity of truck loading the probability to ravel increases and light intensity of truck loading the probability decreases. The conclusion of Henning & Roux (2012) was that the asphalt was more elastic due to the passing axle loads and therefore heals itself (L. T. Mo et al., 2008). However, Henning & Roux (2012) mention that their network pavement data was very limited and needed to increase for a better conclusion. Furthermore, the research was conducted in New Zealand where there is a lower environmental impact. The Netherlands have a colder climate and therefore the surface pavement will behave differently (M. Huurman et al., 2010). Hence, it is important to understand the impact of the environmental impact in The Netherlands. The results of this research show the opposite. Heavy traffic intensity has the most significant impact on fatigue failure on the surface pavement and light traffic intensity lower impact risk of fatigue failure on the surface pavement. Furthermore, the risk model can predict when the fatigue failure is starting to show during the life-cycle of the surface pavement. Henning & Roux (2012) developed a model that could predict the increasing risk of raveling during the life-cycle of the surface pavement.

Furthermore, the tool can be used for practical reasons and can support the perception of the experts. The experts can use the probability models for more specific research in the future, like way of monitoring, more specific research on parameters (traffic intensity, environmental impact, and quality of the surface pavement), archiving the right measured data.

Furthermore, stakeholders can use the prediction model for decision-making tools and models.

### 6.3 Monitoring surface pavement

There is a verity of important factors that cause the scattering. The first factor is the way the data is measured. The technique of visual inspections is in these days outdated. The data points are all independently observed points and or not monitored. Furthermore, the inspections are done visually. Even though it is done by experts who have the knowledge about the degradation of the surface pavement and classify these damages in a matrix, the inspection is not accurate. The classification is linked to a 100-meter tile and not to degradation spot. With this method, the scattering cannot be captured. The footage that is used by the third party (like, Cyclomedia), that is used by 'Heijmans' is not accurate enough. In traditional forms of contracts, the technique was usable for the contractors. But the new contract forms require a more accurate approach for maintaining roads. An accurate approach is necessary to farm the ride footage. Furthermore, monitoring roads need to be included during the life-cycle of the surface pavement (R. Kuppeveld, personal communication. March 13, 2017). To monitor the lane sections a measurement vehicle can be used. This vehicle is equipped with eight high-resolution cameras and can drive up to 90 km/h (see figure 6.1) (Opara et al., 2016).

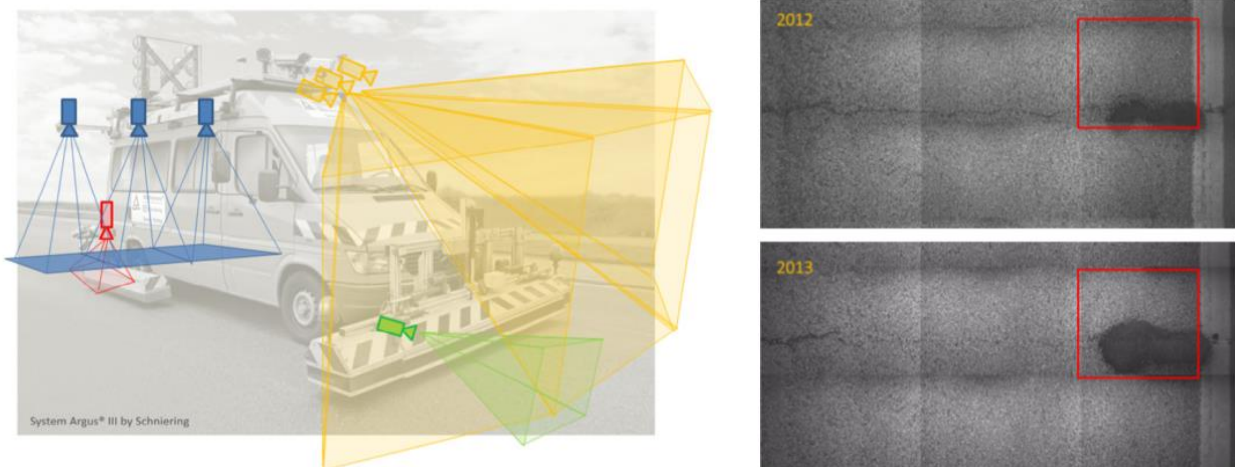


Figure 6.1 and 6.2: Cameras mounted on a measurement vehicle and top down footage (Opara et al., 2016)

This vehicle makes close up footage top down (see figure 6.2). Which is why, the footage can place adjacent to each other and therefore, better be monitored what the stage is of the surface pavement. The use these measurement vehicles are a more reliable, more secure measurement than visual inspection can be produced, and more data can be farmed.

Another factor in appointing is the moment of the visual inspections. The dataset exposes that the most visual inspections are performed around three years of the life-cycle of the surface pavement. In this period almost no degradation displays at that curtain moment. The visual inspections can be performed later in the life-cycle of the surface pavement. According to the probability simulation model the advice is to inspect, heavy 'TI' between 4 to 5 years, for

moderate 'TI' this can inspect between 5 to 6 years, and light 'TI' can be inspected around 7 years.

#### 6.4 'Quality' of the surface pavement

Due to the literature review, and the scattering in the dataset, men could argue that the 'quality' of the binder during construction has an important impact on the life-cycle of the surface pavement. The binder of the asphalt reduces the relaxation potentials. When asphalt aging more quickly, the binder loses this potential and the risk of fatigue failure increases (Hagos, 2008). The problem of this behavior is that aging asphalt is simulated in laboratories ages different than in the field. Furthermore, it can predict reliable up till three years of the life-cycle of the asphalt. Do so, to understand the 'quality' of the asphalt, monitoring during the construction period in the field is important, and during the life-cycle of the surface pavement as well. Furthermore, aged samples can be used to inspect the binder, to understand the quality at the moment when the surface pavement displays fatigue failure. This knowledge can be used in combination with external factors and the monitored construction data that have an influence on fatigue failure of the surface pavement. The measured data can be added to the probability model to make this model more accurate.

Another point of discussion is about to understand 'quality' of the binder is to produce x-rays (L. T. Mo et al., 2008). Contractors can harvest samples of asphalt, which no longer meet the requirements of the contract. If the degradation of the surface pavement does no longer meet the requirements, the binder can be analyzed by making scans of the samples. Due so, the contractor knows the 'quality' of the binder the moment that it does no longer meet the requirements of the contract.

#### 6.5 Archiving the data

Archiving the data could be a factor that could explain the scattering of the measured data is the archived construction date of the surface pavement. KernGIS is used for storing data. hence, the construction dates, where sometimes not mentioned, incorrect, or only a construction year was mentioned. These construction dates needed, therefore, to be clocked in by hand. This could give errors. Furthermore, emergency repairs are not archived in KernGIS during the life-cycle of the pavement. Therefore, people could argue that the construction type of the surface pavement is incorrectly archived, this could explain the old measured data with a high traffic intensity (see figure 4.2c).

For archiving the data, a better system needs to be produced. Therefore, it is important that 'Heijmans' produces a tool by themselves. In this tool the following data need to be stored of projects; the construction date of the surface pavement, emergency repairs, monitoring dates, condition of the surface pavement that is monitored, pavement type.

#### 6.6 The impact of the parameters traffic intensity and cold weather

The trend line of traffic intensity is observed in the plotted graphs (see Chapter 4, Results). The impact of cold weather with this technique shows a slight significance but could not be

included in the risk simulation model. However, according to the literature, is that cold weather has an impact on the low fatigue performance surface pavement (Hagos, 2008). Therefore, to understand the influence of cold weather on the surface pavement a different approach needs to be used to predict the impact of the cold weather. An approach that could be used is to monitor surface pavement during the winter to observe low fatigue performance of the surface pavement.

## Reverences

- Abraham, H. (1938). *ASPHALTS AND ALLIED SUBSTANCES Their Occurrence, Modes of Production, Uses in the dirts and Methods of Testing*. NEW YORK D. VAN NOSTRAND COMPANY, INC.
- Adlinge, S. S., & Gupta, P. a K. (2009). Pavement Deterioration and its Causes. *Mechanical & Civil Engineering*, 9–15. Retrieved from [www.iosrjournals.org](http://www.iosrjournals.org)
- Al-Jibouri, S., & Ogink, G. (2009). Proposed model for integrating RAMS method in the design process in construction. *Architectural Engineering and Design Management*, 5(4), 179–192. <http://doi.org/10.3763/aedm.2008.0100>
- Anastasopoulos, P. C., Florax, R. J. G. M., Labi, S., & Karlaftis, M. G. (2010). Contracting in highway maintenance and rehabilitation: Are spatial effects important? *Transportation Research Part A: Policy and Practice*, 44(3), 136–146. <http://doi.org/10.1016/j.tra.2009.12.002>
- Bertolini, M., Bevilacqua, M., & Massini, R. (2006). FMECA approach to product traceability in the food industry. *Food Control*, 17(2), 137–145. <http://doi.org/10.1016/j.foodcont.2004.09.013>
- Bowles, J. B., & Peláez, C. E. (1995). Fuzzy logic prioritization of failures in a system failure mode, effects and criticality analysis. *Reliability Engineering and System Safety*, 50(2), 203–213. [http://doi.org/10.1016/0951-8320\(95\)00068-D](http://doi.org/10.1016/0951-8320(95)00068-D)
- Chen, A., & Chen, C. (2016). Comparison of GUM and Monte Carlo methods for evaluating measurement uncertainty of perspiration measurement systems. *Measurement: Journal of the International Measurement Confederation*, 87, 27–37. <http://doi.org/10.1016/j.measurement.2016.03.007>
- Chen, D. H., & Won, M. (2015). Field performance with state-of-the-art patching repair material. *Construction and Building Materials*, 93, 393–403. <http://doi.org/10.1016/j.conbuildmat.2015.06.002>
- Ching, J., & Wang, J.-S. (2016). Application of the transitional Markov chain Monte Carlo algorithm to probabilistic site characterization. *Engineering Geology*, 203, 151–167. <http://doi.org/10.1016/j.enggeo.2015.10.015>
- D. Bouwmeester; M. Huurman; F. Tolman, A. A. A. M. (2004). PROBABILISTIC ANALYSIS OF FATIGUE CRACKING IN ASPHALT PAVEMENTS, 2(1), 8.
- D.J.R. (Dirk-Jan Rijke) Vinke. (2013). *Rijkswaterstaat from skilful technical specialist towards strategic professional procurer*. Delft University of Technology (TU Delft).
- Dong, Q., Huang, B., & Zhao, S. (2014). Field and laboratory evaluation of winter season pavement pothole patching materials. *International Journal of Pavement Engineering*. Taylor & Francis. <http://doi.org/10.1080/10298436.2013.814772>
- Doorduijn, J., Horst, R. van der, Kooij, J. van der, Nugteren, H. P., Verra, N., & Wit, L. B. de. (1994). *Ontwikkeling van een beoordelingsmethode voor rafeling van zeer open asfaltbeton*.

- E. Ray Brown, Stephen A. Cross, Gehler, J. G. (1991). Evaluation of Pavement Bleeding Problem on I-55 in Illinois. *NCAT Report 91-07*, (91).
- Eversdijk, A. W. ., & Korsten, A. F. . (2009). Concessionele publiek-private samenwerkingsrelaties; Feiten en fities bij op DBFM gebaseerd infrastructurele projecten. *Bestuurswetenschappen*, 3(3), 25–44.
- Francken, L., Vanelstraete, A., and Verhasselt, A. (1997). (1997). Francken, L., Vanelstraete, A., and Verhasselt, A. (1997). “Long term aging of pure and modified bitumen: Influence on the rheological properties and relation with the mechanical performance of asphalt mixtures.” 1259-1278. *TRB*, 1997.
- Hagos, E. T. (2008). *The Effect of Aging on Binder Properties of Porous Asphalt Concrete*.
- Han, J., Oztoprak, S., Parsons, R. L., & Huang, J. (2007). Numerical analysis of foundation columns to support widening of embankments. *Computers and Geotechnics*, 34(6), 435–448. <http://doi.org/10.1016/j.compgeo.2007.01.006>
- Haskett, J. D., Pachepsky, Y. A., & Acock, B. (1995). Use of the beta distribution for parameterizing variability of soil properties at the regional level for crop yield estimation. *Agricultural Systems*, 48(1), 73–86. [http://doi.org/10.1016/0308-521X\(95\)93646-U](http://doi.org/10.1016/0308-521X(95)93646-U)
- Henning, T. P. F. (University of A., & Roux, D. C. (New Z. L. (2012). A Probabilistic Approach for Modelling Deterioration. *Journal of the South African Institution of Civil Engineering*, 54(2), 36–44.
- Huurman, M., Mo, L. T., & Woldekidan, M. F. (2010). Porous Asphalt Ravelling In Cold Weather Conditions. *Pavement Research and Technology*, 3(3), 110–118.
- Huurman, R. M., Mo, L. T., & Medani, T. O. (2007). Advanced Pavement Analysis Techniques, (September).
- Kandhal, P. S., & Chakraborty, S. (1996). EFFECT OF ASPHALT FILM THICKNESS ON SHORT AND LONG TERM AGING OF ASPHALT PAVING, (January).
- Khosravi, H., Abtahi, S. M., Koosha, B., & Manian, M. (2013). An analytical-empirical investigation of the bleeding mechanism of asphalt mixes. *Construction and Building Materials*, 45, 138–144. <http://doi.org/10.1016/j.conbuildmat.2013.04.004>
- Koninklijk Nederlands Meteorologisch Instituut. (2016). KNMI. Retrieved from <http://www.knmi.nl/over-het-knmi/about>
- Kroese, D. P., Brereton, T., Taimre, T., & Botev, Z. I. (2014). Why the Monte Carlo Method is so important today Uses of the MCM. *WIREs Computational Statistics*, 6(6), 386–392. <http://doi.org/10.1002/wics.1314>
- Kuennen, T. (2013). Loss of Cover. *Better Roads*, 1–7.
- Lira, B., Jelagin, D., & Birgisson, B. (2013). Gradation-based framework for asphalt mixture. *Materials and Structures*, 46(8), 1401–1414. <http://doi.org/10.1617/s11527-012-9982-3>
- Miradi, M. (2004a). Development of intelligent models for ravelling using neural network. *2004 IEEE International Conference on Systems, Man and Cybernetics (IEEE Cat*.

- No.04CH37583), 4, 3599–3606. <http://doi.org/10.1109/ICSMC.2004.1400901>
- Miradi, M. (2004b). M. Miradi, Neural network models predict ravelling and analyse material/construction properties, in: Proceedings of Intelligent Systems and Control, Hawaii, USA, 2004, 2004.
- Mo, L., Huurman, M., Wu, S., & Molenaar, a. a. a. (2014). Mortar fatigue model for meso-mechanistic mixture design of ravelling resistant porous asphalt concrete. *Materials and Structures*, 47(6), 947–961. <http://doi.org/10.1617/s11527-013-0105-6>
- Mo, L. T., Huurman, M., Wu, S. P., & Molenaar, A. A. A. (2007). Investigation into stress states in porous asphalt concrete on the basis of FE-modelling, 43, 333–343. <http://doi.org/10.1016/j.finel.2006.11.004>
- Mo, L. T., Huurman, M., Wu, S. P., & Molenaar, A. A. A. (2008). 2D and 3D meso-scale finite element models for ravelling analysis of porous asphalt concrete. *Finite Elements in Analysis and Design*, 44(4), 186–196. <http://doi.org/10.1016/j.finel.2007.11.012>
- Mo, L. T., Huurman, M., Wu, S. P., & Molenaar, A. A. A. (2011). Bitumen-stone adhesive zone damage model for the meso-mechanical mixture design of ravelling resistant porous asphalt concrete. *International Journal of Fatigue*, 33(11), 1490–1503. <http://doi.org/10.1016/j.ijfatigue.2011.06.003>
- Murali Krishnan, J., & Lakshmana Rao, C. (2001). Permeability and bleeding of asphalt concrete using mixture theory. *International Journal of Engineering Science*, 39(6), 611–627. [http://doi.org/10.1016/S0020-7225\(00\)00064-1](http://doi.org/10.1016/S0020-7225(00)00064-1)
- National Institute of Standards and Technology. (2013). - Handbook of Statistical Methods. Retrieved from <http://www.itl.nist.gov/div898/handbook/>
- Nijssen, Wilfred A M G, Marc J.A. Stet, Wim A. Kramer, G. J. (n.d.). *Technical and Economical Feasibility of Pavement Widening in Cement. ?*
- Opara, K. R., Skakuj, M., & Stöckner, M. (2016). Factors affecting raveling of motorway pavements - A field experiment with new additives to the deicing brine. *Construction and Building Materials*, 113, 174–187. <http://doi.org/10.1016/j.conbuildmat.2016.03.039>
- Pearson, K. (1916). Ilat/ieinaticctl Contributions to the Theory of Eoolution. Second Supplement to a Memoir on Skew Variation. *The Royal Society*.
- Pelaez, C. E., & Bowles, J. B. (1994). Using fuzzy logic for system criticality analysis. *Proceedings of Annual Reliability and Maintainability Symposium (RAMS)*, 449–455. <http://doi.org/10.1109/RAMS.1994.291150>
- Perry, M. J. (2014). Role of aggregate petrography in micro-texture retention of greywacke surfacing aggregate. *Road Materials and Pavement Design*, 15(4), 791–803. <http://doi.org/10.1080/14680629.2014.923781>
- Razali, N. M., & Wah, Y. B. (2011). Power comparisons of Shapiro-Wilk , Kolmogorov-Smirnov, Lilliefors and Anderson-Darling tests. *Journal of Statistical Modeling and Analytics*, 2(1), 21–33. <http://doi.org/doi:10.1515/bile-2015-0008>
- Rijkswaterstaat. (2014). Verbreding A12 tussen Ede.

- Rijkswaterstaat. (2016a). INWEVA verkeersintenseiteiten.
- Rijkswaterstaat. (2016b). Spatial dataset KernGIS. Retrieved from <https://www.rijkswaterstaat.nl/zakelijk/zakendoen-met-rijkswaterstaat/werkwijzen/werkwijze-in-gww/data-eisen-rijkswaterstaatcontracten/kerngis-droog-en-beheerkaart-nat.aspx>
- Rijkswaterstaat. (2017). Kerngis Droog en Beheerkaart Nat. Retrieved from <https://www.rijkswaterstaat.nl/zakelijk/zakendoen-met-rijkswaterstaat/werkwijzen/werkwijze-in-gww/data-eisen-rijkswaterstaatcontracten/kerngis-droog-en-beheerkaart-nat.aspx> 20-03-2017  
Rijkswaterstaat
- Safe Software Inc. (2015). FME<sup>®</sup> Desktop Training Manual. Vancouver: Safe Software Inc.
- Salt, M., & Fog, S. (2007). Standard Practice for. *Evaluation*, 1–14. <http://doi.org/10.1520/C0305-06.2>
- Suh, Y. C., Cho, N. H., & Mun, S. (2011). Development of mechanistic-empirical design method for an asphalt pavement rutting model using APT. *Construction and Building Materials*, 25(4), 1685–1690. <http://doi.org/10.1016/j.conbuildmat.2010.10.014>
- syndeks. (2017). DBFMO constructie. Retrieved from [http://www.syndeks.nl/dbfmo/crm\\_sub\\_index.htm](http://www.syndeks.nl/dbfmo/crm_sub_index.htm)
- US Department of Defence. (1949). *Procedures for performing a failure mode, effects and criticality analysis. MIL-STD-1629, November, AMSC Number N3074* (Vol. 11). <http://doi.org/10.1016/j.cardfail.2005.06.223>
- Vargas-Nordbeck, A., & Timm, D. H. (2012). Rutting characterization of warm mix asphalt and high RAP mixtures. *Road Materials and Pavement Design*, 13(January), 1–20. <http://doi.org/10.1080/14680629.2012.657042>
- Vervoort, D. (2013). *The effect of asphalt maintenance regimes on inflation correction in Dutch DBFM contracts*.
- Zamora-Barraza, D., Calzada-Pérez, M. A., Castro-Fresno, D., & Vega-Zamanillo, A. (2011). Evaluation of anti-reflective cracking systems using geosynthetics in the interlayer zone. *Geotextiles and Geomembranes*, 29(2), 130–136. <http://doi.org/10.1016/j.geotexmem.2010.10.005>
- Zhang, X., & Briaud, J.-L. (2010). Coupled water content method for shrink and swell predictions. *International Journal of Pavement Engineering*, 11(1), 13–23. <http://doi.org/10.1080/10298430802394154>
- Zhang, Y., van de Ven, M., Molenaar, A., & Wu, S. (2016). Preventive maintenance of porous asphalt concrete using surface treatment technology. *Materials & Design*, 99, 262–272. <http://doi.org/10.1016/j.matdes.2016.03.082>



## Appendix A

In 'Appendix A' gives a brief overview of the damage types that could occur on pavement constructions due to internal and external factors.

### *Groups of fatigue pavement failures*

There are four categories of common asphalt pavement surface distresses (Adlinge & Gupta, 2009):

- A. Cracking
- B. Surface deformation
- C. Disintegration
- D. Surface defects

#### *A. Types Cracking*

Cracking can be divided in seven types of cracking (Adlinge & Gupta, 2009):

- 1. Fatigue cracking (alligator cracking)
- 2. Longitudinal cracking
- 3. Transverse cracking
- 4. Block cracking
- 5. Slippage cracking
- 6. Reflective cracking
- 7. Edge cracking

Cracks appear on the surface of asphalt pavement. The cracks in the pavement are mainly caused by an upward extension of the cracks in the lower layers of the asphalt. Cracks occur due to, fatigue, shrinkage, consolidation process, construction joints, and age (Zamora-Barraza, Calzada-Pérez, Castro-Fresno, & Vega-Zamanillo, 2011).

#### *1. Fatigue cracking*

Fatigue cracking or alligator cracking is an of interconnected cracks. It creates small, irregular shaped pieces in the pavement. The cause of the cracks is that the surface layer or base fails, due to traffic loading (fatigue). If the road in this phase of the fatigue level the road will start to get potholes (see below, C.1. paragraph potholes). Drainage problems is a result of alligator cracking. To resolve the drainage problem larger areas require reclamation or reconstruction (Adlinge & Gupta, 2009).

#### *2. Longitudinal cracking*

Longitudinal cracking has several causes. The cracks can occur due to frost, joint failure, consolidation and/ or settlements, these failures may be load induced (Adlinge & Gupta, 2009), (Han, Oztoprak, Parsons, & Huang, 2007). Consolidation is caused by widening the road

construction. Widening the road is due to the increased traffic volume. By adding an embankment for widening the road, the pavement will get distressed due to the different foundation and soil mix beneath the pavement (Han et al., 2007).

### 3. *Transverse cracking*

Transverse cracks are right angle cracks that form to the centre line of the roadway. The cracks have the same causes as longitudinal cracks. The cracks start as hairline or very narrow cracks and widen with age (Adlinge & Gupta, 2009).

### 4. *Block cracking*

Block cracks occur into irregular pieces due to lack of compaction during construction or it is the result of transverse and longitudinal cracks intersecting (Adlinge & Gupta, 2009).

### 5. *Slippage cracking*

Slippage cracks are crescent shaped cracks. The end point cracks are pointed towards the oncoming vehicles. The cracks are caused by horizontal forces due to traffic that is braking. Poor bonding between asphalt surface and the layer below is often the cause of the failure. Mainly no tack coat is used (Adlinge & Gupta, 2009).

### 6. *Reflective cracking*

Reflective cracking is caused by cracks that are in the old pavement below due to consolidation and/ or ground contraction. The upper new layer deforms caused by traffic loads. This causes new cracks in the upper layer. The cracks follow the pattern of the pavement below (Zamora-Barraza et al., 2011).

### 7. *Edge cracking*

As the name shows edge cracking starts at the edge of the pavement. At a certain moment in time edge cracking transforms into alligator cracking. The cracks are a result of lack of support of the shoulder of the pavement caused by excess moisture that erodes the foundation at the shoulder of the pavement (Adlinge & Gupta, 2009).

### B. *Surface deformation*

The pavement deformation comes from weakness in one or more layers of the pavement. The layers have to experience flexible movement due to loads. The deformation may accompany by cracking. The surface distortions can have a negative influence on the safety of the traffic (Adlinge & Gupta, 2009).

The basic types of the surface deformation are:

1. Rutting
2. Corrugations

3. Shoving
4. Depressions
5. Swell

#### 1. *Rutting*

Rutting, or permanent deformation, is a typical deterioration type of AC pavement for characterizing a failure fatigue in the life cycle of the pavement (Suh, Cho, & Mun, 2011). It can be circumscribed as an accumulation of small amounts of irredeemable strain in the pavement layers, due to loads. Higher traffic volumes, axle loads and truck tire pressures are the main parameters that cause rutting (Vargas-Nordbeck & Timm, 2012).

#### 2. *Corrugations*

Corrugation is a pavement failure where the surface has become distorted like a washboard, that is why people refer to wash boarding. It is caused by too much AC, too much fine aggregate, or too smooth/ rounded textured aggregate. Corrugation occurs most of the time at places where vehicles stop and accelerate (Adlinge & Gupta, 2009).

#### 3. *Shoving*

Shoving looks like corrugation, it also a form of plastic movement in the AC upper layer. The fatigue failure is that there from local bulges at the surface. It is caused by the same parameters as corrugation (Adlinge & Gupta, 2009).

#### 4. *Depressions*

Depressions are small local areas that have bowl-shaped form. The areas may also include cracks. It is due to consolidation or movement of the supporting layers or instability in the foundation. Depression can cause dangerous situations for the passing traffic. Furthermore, the bowled shape form holes collect water (Adlinge & Gupta, 2009).

#### 5. *Swell*

Swells are upward bulges at the surface of the pavement. The bulges are caused by expansive soil in combination with frost. Expansive soils are soils absorb water, it works like a sponge. After the soil layer is drained and it starts freezing the stress on the lower layer of the asphalt gets too high and starts to bulge. Swells can cause like depressions dangerous situations for passing traffic (X. Zhang & Briaud, 2010).

#### C. *Disintegration*

Disintegration is a type of distress in the pavement. The distress that occurs is breaking up of the pavement into small, loose pieces. Furthermore, if the disintegration is not repaired on time, a complete reconstruction of the pavement is needed (Adlinge & Gupta, 2009). There are two types of disintegration:

1. Potholes
2. Patches

### 1. *Potholes*

Potholes are like depressions bowl-shaped holes. The potholes are located on the surface of the AC. The shape of the potholes exists of sharp edges and vertical sides. The vertical sides are from top to a depth that can be beyond five centimeters. mentioned in the paragraph alligator cracking, potholes are a result of alligator cracking. The surface of the pavement is a type of service fatigue failure of the AC. At a moment in time, the interconnected cracks cause the pavement surface break into small pieces. The traveling wheels then pulling the broken pieces out of the AC. Furthermore, Freezing accelerates the cycle of cracks and broken pieces that slam out of the pavement due to traveling wheels. Due to, the water inside the pavement that expand during the frost period. The ice forces higher stress on the cracks. Therefore, the wheels of the passed by traffic can more easily slam out the pieces that occur due to the frost. Furthermore, Potholes reduce the pavement performance and the life-cycle of the pavement and, it has a high influence on the road safety (Dong, Huang, & Zhao, 2014).

### 2. *Patches*

Patch is a technique that removes a part of the defect pavement and replaces with new pavement material. When the patched location fails, surrounding pavement will fail as well (Adlinge & Gupta, 2009). Furthermore, patching is an expensive and extensive way of repairing pavement (D. H. Chen & Won, 2015). Shortly said patching is a cover to protect the old failure of the pavement (Adlinge & Gupta, 2009).

### *D. Surface defects*

Surface defects are failures that occur in the surface layer of the pavement. The most common types are as followed:

1. Ravelling
2. Bleeding
3. Polishing

#### 1. *Ravelling*

Raveling is a failure where the aggregate particles get loose of the adhesion composition of bitumen and aggregate. The failure mechanism is due to the axle load in a combination of the stress of the tires that scull on the surface layer of the pavement (L. T. Mo et al., 2008). This failure mechanism is a very common failure in PAC constructions (L. Mo et al., 2014). It occurs because of the void content in the construction of the PAC, approximately a percentage of twenty.

#### 2. *Bleeding*

Bleeding is a shiny film at the surface of the pavement. The film of the surface becomes usually sticky (Salt & Fog, 2007). The phenomenon happens when the aggregate voids start to fill with the asphalt binder in the pavement. Furthermore, asphalt binder expands and appears on the surface of the pavement due to, hot weather. The failure is that this phenomenon has highly influence on the skid resistance of the pavement, especially when the pavement surface is wet. Bleeding occurs due to, poor construction practices (Khosravi, Abtahi, Koosha, & Manian, 2013). Furthermore, for understanding the mechanism of bleeding, other than, only empirical and qualitative observations is carried out (Murali Krishnan & Lakshmana Rao, 2001). This is due to the fact that research on AC mostly has been done with a phenomenological way of thinking and, bleeding is a micro-mechanical activity. This phenomenon has rarely been investigated analytically (E.Ray Brown, Stephen A. Cross, Gehler, 1991).

### 3. *Polishing*

Polishing is a failure mechanism where the aggregate of the pavement gets polished, due to trafficking. The outcome is that the skid resistance of the pavement fails. which, is crucial for the safety performance of the pavement (Perry, 2014). (Anastasopoulos, Florax, Labi, & Karlaftis, 2010)

## Appendix B

The interviews are stored on a USB-stick and can be looked up on the USB-stick.

## Appendix C

This appendix shows the 'DWW-Wijzer' provided by RWS.

**Tabel 1: Richtlijnen en richtwaarden voor de indeling van schade in ernstklassen**

Schade	Ernstklasse		
	1 Lichte schade	2 Matige schade	3 Ernstige schade
<b>Rafeling</b>			
Op niet ZOAB-deklaag (per schadeplek)	Hier en daar mortel uit het oppervlak en/ of af en toe een steentje weg	Meer dan af en toe een steentje weg en/of de eerste steenlaag is duidelijk uitgereden	Grotere plekken uit het oppervlak verdwenen en/ of de tweede steenlaag is uitgereden
Op ZOAB-deklagen (per m <sup>2</sup> uit rijspoor)	5-10% van het oorspronkelijk aantal stenen in de oppervlaktelaag is uitgereden	11-20% van het oorspronkelijk aantal stenen in de oppervlaktelaag is uitgereden	Meerdan 20% van het oorspronkelijk aantal stenen in de oppervlaktelaag is uitgereden
<b>Scheurvorming</b> (perschadeplek)			
<b>Dwarsscheuren</b>			
Wijde en/of Hoogteverschil	< 3mm < 2mm	3 t/m 20 mm 2 t/m 10 mm	> 20mm >10 mm
<b>Langsscheuren</b>			
Wijde en/of Hoogteverschil	< 3mm < 2mm	3 t/m 20 mm 2 t/m 10 mm	> 20mm >10 mm
Craquelé	Scheuren niet verbonden	Scheuren verbonden, zonder losse elementen	Scheuren verbonden, met losse elementen
<b>Onvlakheid</b> (gem. Waarde over 100 meter)			
Dwarsonvlakheid			
Rijspoordiepte	≤ 14mm	15 t/m 17 mm	≥ 18 mm*1
Langsonvlakheid (IRI)	≤ 2.5	2.6 t/m 3.4	≥ 3.5
<b>Stroefheid</b> (gem. waarde over 100 meter)	≥ 0.45	0.35 t/m 0.44	≤ 0.37
<b>Dwarshelling</b> (gem. Waarde over 100 meter)*2	≥ 1.6%	1.1 t/m 1.5%	≤ 1.0%

\*1 En/of de rijspoor diepte is over een lengte van tenminste 50 meter gemiddeld ≥23mm  
 \*2 De vermelde waarden gelden voor rechtstanden en voor bogen met een grote straat.  
 Voor bogen met een krappe straat en voor verkantingsovergangen gelden andere waarden.

**Tabel 2: Richtlijnen voor de omvangscategorieën van de diverse schade**

Schade	Omvangscategorieën		
	A Geringe omvang	B Beperkte omvang	C Grote omvang
<b>Rafeling</b>			
(% lengte van 100m- vak)	<15%	15 t/m 25%	>25%
<b>Samenhang- scheurvorming</b>			
Dwarsscheuren (aantal binnen 100m-vak)	<3	3 t/m 7	>7
Langsscheuren en/of craquelé (% lengte van 100 m-vak)	<10%	10 t/m 30%	> 30%
<b>Combinatie van rafeling, langsscheuren en craquelé op niet ZOAB-deklagen</b>			
(% lengte van 100m-vak)	<15%	15 t/m 30%	>30%

Table Appendix C1: DWW-Wijzer matrix

## Appendix D

This Appendix captures the output of the FME model that is translated into degradation histograms. A flow chart (see figure D1) of the analyses filter technique shows the flow to produce the different impact histograms. Table 3.2 shows the output of the FME model this measured data then is filtered in Excel by using a **IF-statement** for the two independent variables and the time steps of 250 days (see IF-statement functions D1 for examples). Furthermore the age of the 100-meter tile is calculated by using the date of inspection – the date of the construction = number of days (age pavement).

*'TI' Heavy traffic intensity = (IF(Excelcel < 6300; (IF(Excelcel > 4200; 1; 0)); 0)*

*'T – extreme' > 20 days = IF(Excelcel > 20; 1; 0)*

*Capture datapoint in timestep = IF(Excelcel < 1500; (IF(Excelcel = 1250; 1; 0)); 0)*

*Age datapoint = Inspection date (Excelcel) – Construction date (Excelcel)*

*IF-statement functions D1: The three If-statement that are used to capture the impact of the independent variables and the timestep of the datapoint. Furthermore, the age of the datapoint is calculated.*

After this filtering technique the timestep datasets are transported in to tables the average is calculated and the standard deviation of the average (see average function D1 for an example).

*Average damage per timestep = SUM(total FMECA risk points)/n*

*Standard deviation per timestep = STDEV(SUM of total FMECA risk points)*

*Average function D1: To plot the impact of the independent variables tables are formed. These two functions are used to realize the plots.*

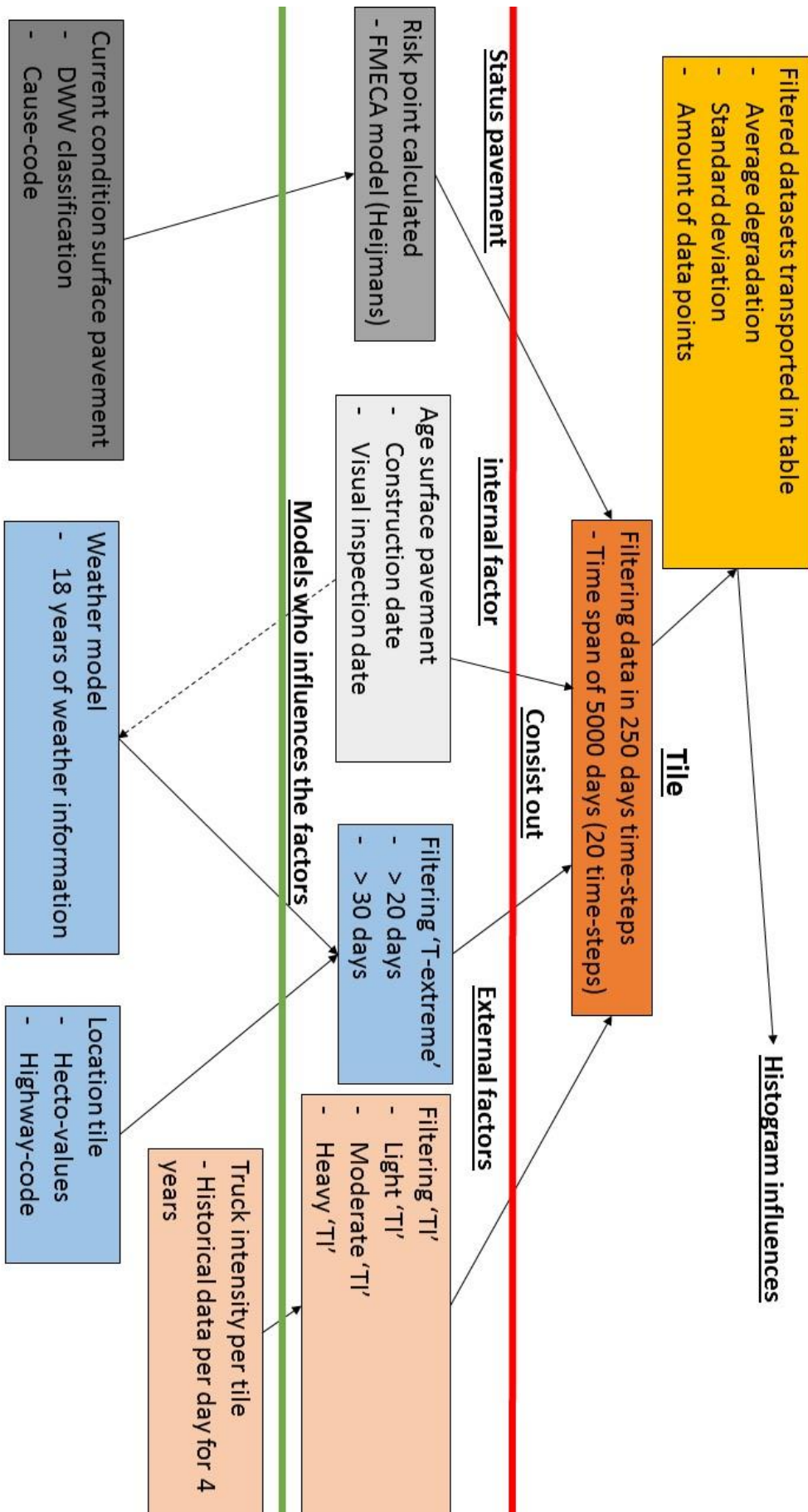


Figure Appendix D1: flow-chart of the filtering technique that is used to plot the histograms.

## Appendix E

This Appendix gives an overview of all plotted best-fit curve of the cumulative beta distribution models of the two independent impact variables traffic intensity and cold weather. To realize the best-fit curves the tables of the fatigue failure ratio were used (see Appendix F). The best-fit curves are made by using a linear regression analyzes to find  $R^2$  by hand. The functions that are used to produce the best-fit curve explained below in linear regression function Appendix E1. The functions are put in a table (see all table Appendixes E) for producing plots of the different best-fit curves (See all figures Appendixes E).

$$CDF \text{ per timestep} = BETA.DISTR(normalized\ time(X); \alpha; \beta; TRUE)$$

$$Fatigue\ failure\ ratio\ per\ timestep = \% \text{ fatigue failure of dataset per timestep}$$

$$SST = SUM((Fatigue\ failure\ ratio\ per\ timestep - mean\ fatigue\ failure\ ratio)^2)$$

$$SSR = SUM((Fatigue\ failure\ ratio\ per\ timestep - BETA.DISTR\ per\ timestep)^2)$$

$$R^2 = 1 - \left(\frac{SSR}{SST}\right)$$

$$R = \sqrt{R^2}$$

*Linear regression functions Appendix E1: To find the best-fit curve by hand the highest  $R^2$  needs to be find.*

Light 'TI'

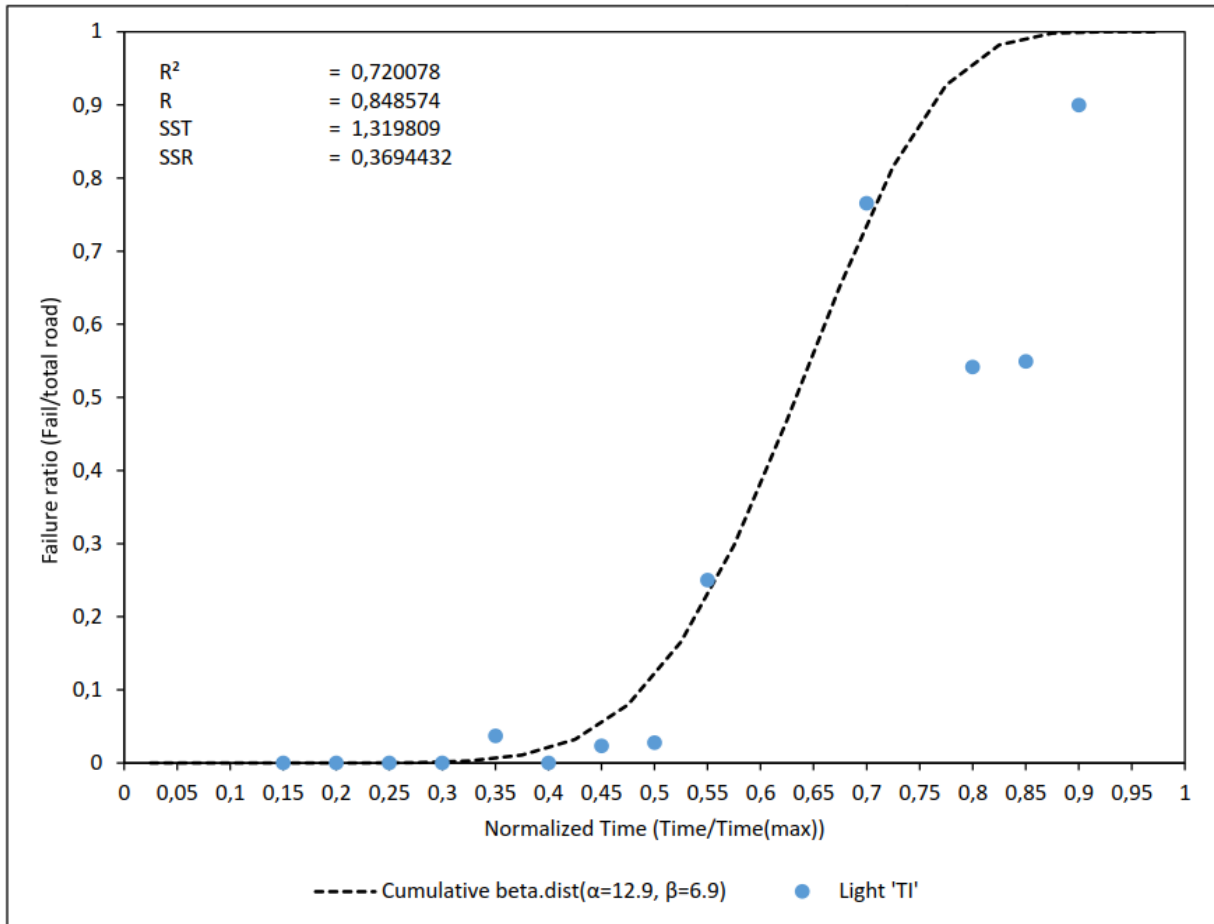


Figure Appendix E1: Best-fit model light 'TI' scenario

Normalized time	CDF ( $\alpha=8.4, \beta=3.3$ )	Fatigue failure ratio	Fatigue failure ratio		sst	ssr	R <sup>2</sup>	R
0,05	7,94739E-10						0,7950758	0,89167
0,1	2,40484E-07							
0,15	6,45812E-06	0	0		0,056668	4,17E-11		
0,2	6,40987E-05	0	0		0,056668	4,11E-09		
0,25	0,00036752	0	0		0,056668	1,35E-07		
0,3	0,001484561	0	0		0,056668	2,2E-06		
0,35	0,00469438	3,703703704	0,037037037		0,040406	0,001046		
0,4	0,012368769	0	0		0,056668	0,000153		
0,45	0,028254382	2,325581395	0,023255814		0,046137	2,5E-05		
0,5	0,057459103	2,777777778	0,027777778		0,044215	0,000881		
0,55	0,105934969	25	0,25		0,000143	0,020755		
0,6	0,179305879							
0,65	0,281029838							
0,7	0,410124268	76,5625	0,765625		0,278335	0,126381		
0,75	0,559016869							
0,8	0,712488537	54,1666667	0,541666667		0,092183	0,02918		
0,85	0,849078901	54,92957746	0,549295775		0,096874	0,08987		
0,9	0,946561395	90	0,9		0,438177	0,002168		
0,95	0,992720726							
1	1							
		Mean	0,238050621	Total	1,319809	0,270461		

Table Appendix E1: Best-fit model light 'TI' scenario

Light 'TI', T-extreme' >20 days

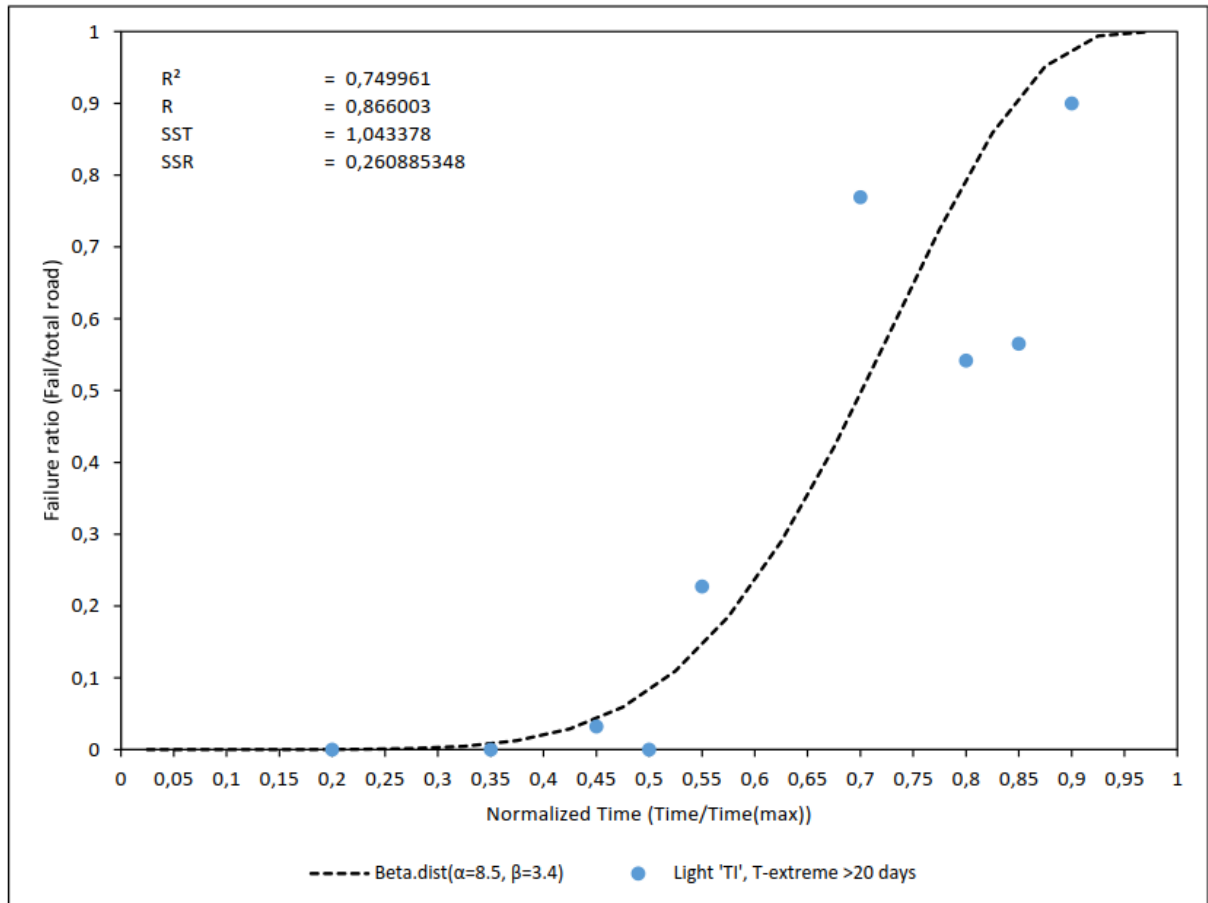


Figure Appendix E2: Best-fit model light 'TI' and 'T-extreme'>20 days scenario

Normalized time	CDF ( $\alpha=8.5, \beta=3.4$ )	Fatigue failure ratio	Fatigue failure ratio		sst	ssr	R <sup>2</sup>	R
0,05	6,88359E-10						0,749961	0,866003
0,1	2,22146E-07							
0,15	6,18043E-06							
0,2	6,27902E-05	0	0		0,113767	3,94E-09		
0,25	0,000366034							
0,3	0,001496653							
0,35	0,004775325	0	0		0,113767	2,28E-05		
0,4	0,012664311							
0,45	0,029059701	3,225806452	0,032258065		0,093047	1,02E-05		
0,5	0,059259156	0	0		0,113767	0,003512		
0,55	0,1093819	22,72727273	0,227272727		0,012105	0,013898		
0,6	0,185087317							
0,65	0,289605895							
0,7	0,421369666	76,92307692	0,769230769		0,186569	0,121007		
0,75	0,571896559							
0,8	0,724998802	54,16666667	0,541666667		0,041768	0,033611		
0,85	0,858742386	56,52173913	0,565217391		0,051949	0,086157		
0,9	0,9516476	90	0,9		0,316638	0,002667		
0,95	0,993815592							
1	1							
		Mean	0,337293958	Total	1,043378	0,260885		

Table Appendix E2: Best-fit model light 'TI' and 'T-extreme'>20 days scenario

Light 'TI', 'T-extreme' > 30 days

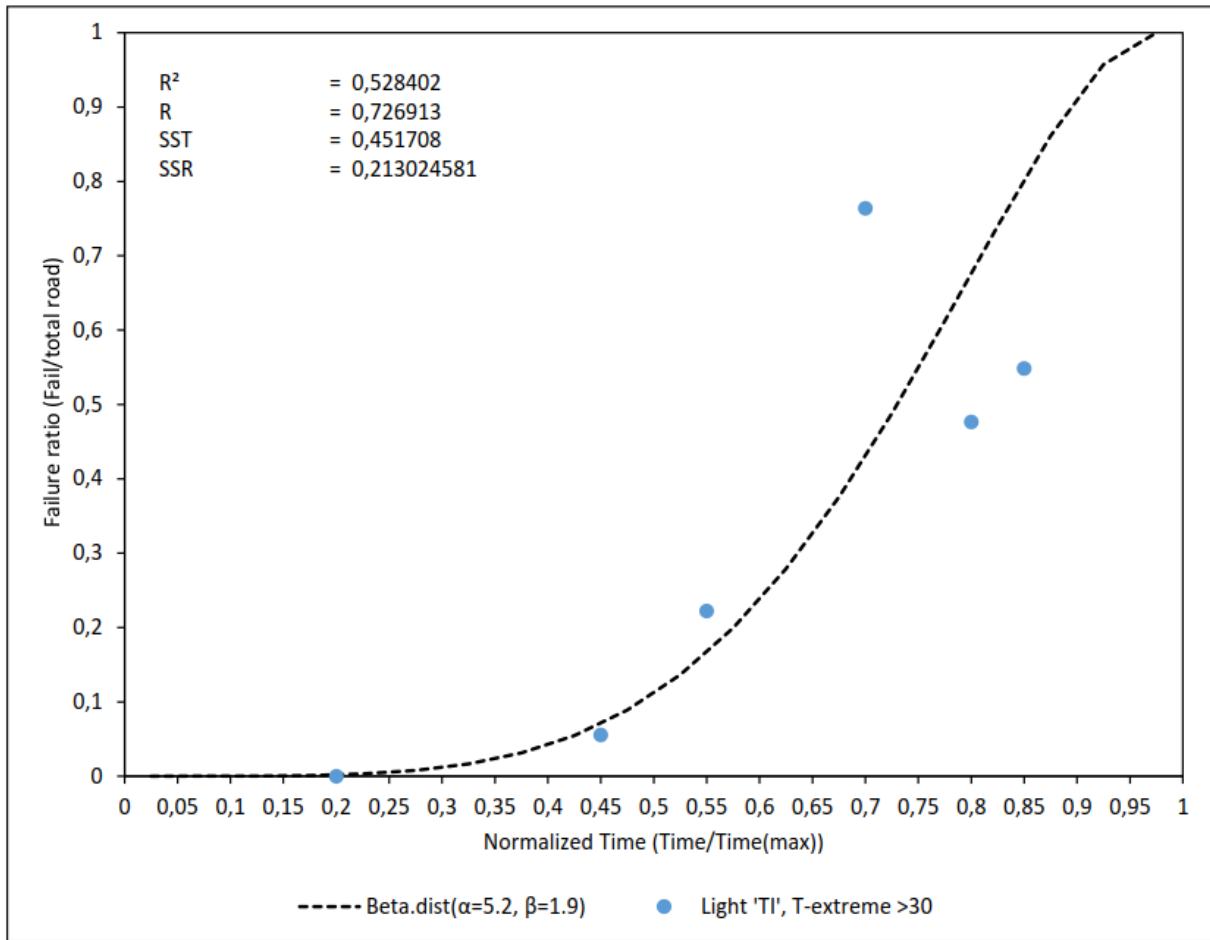


Figure Appendix E3: Best-fit model light 'TI' and 'T-extreme'>30 days scenario

Normalized time	CDF ( $\alpha=5.2, \beta=1.9$ )	Fatigue failure ratio	Fatigue failure ratio		sst	ssr	R <sup>2</sup>	R
0,05	8,80842E-07						0,528402487	0,726913
0,1	3,10997E-05							
0,15	0,000245533							
0,2	0,001048497	0	0		0,118564	1,1E-06		
0,25	0,003193565							
0,3	0,007846687							
0,35	0,016605047							
0,4	0,031465735							
0,45	0,05473891	5,555555556	0,055555556		0,083392	6,67E-07		
0,5	0,088900212							
0,55	0,136376902	22,22222222	0,222222222		0,014911	0,007369		
0,6	0,199261349							
0,65	0,278944064							
0,7	0,375655819	76,36363636	0,763636364		0,175816	0,150529		
0,75	0,487903553							
0,8	0,611775195	47,61904762	0,476190476		0,017387	0,018383		
0,85	0,74006724	54,83870968	0,548387097		0,041639	0,036741		
0,9	0,861132535							
0,95	0,957145862							
1	1							
Mean				0,344331952	Total	0,451708	0,213025	

Table Appendix E3: Best-fit model light 'TI' and 'T-extreme'>30 days scenario

Moderate 'TI'

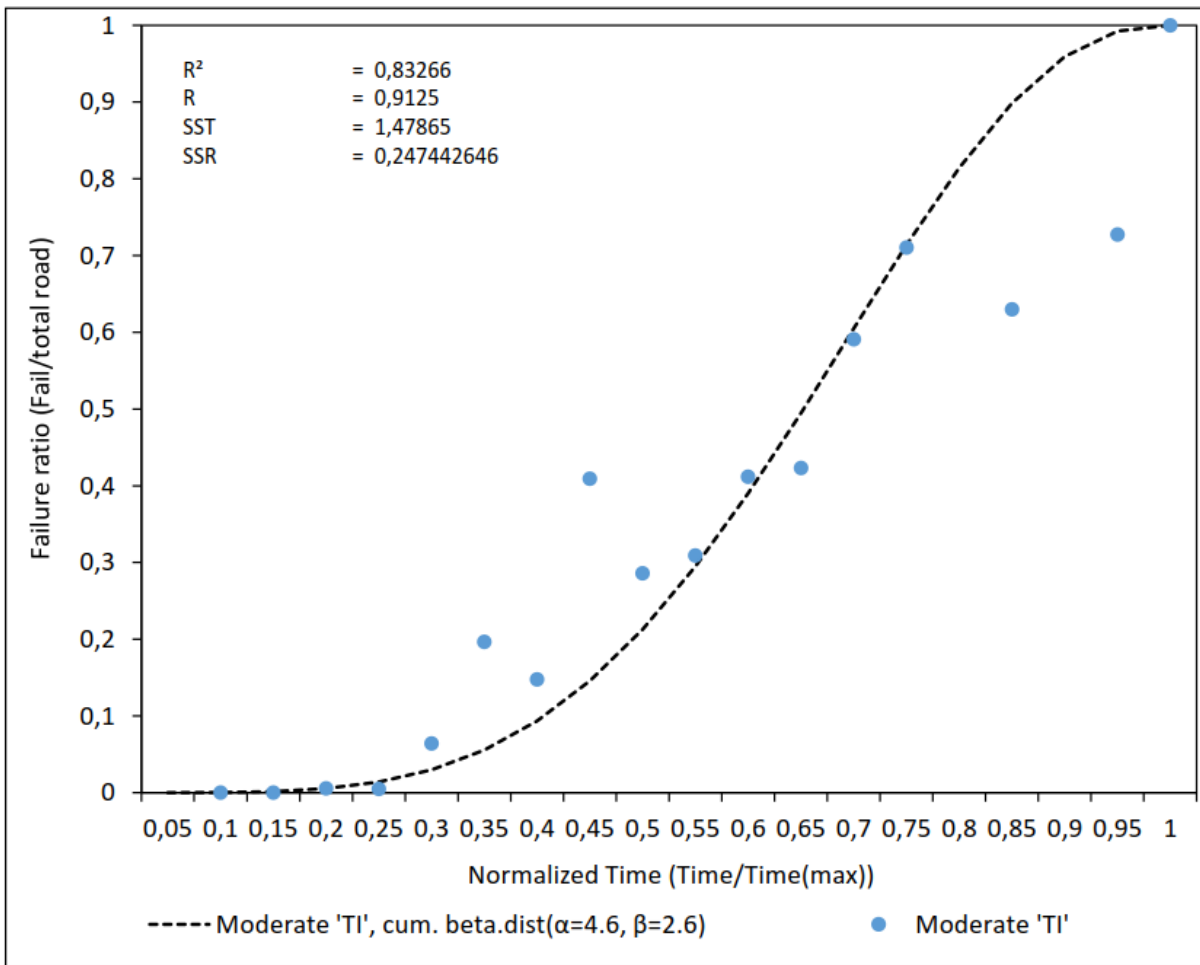


Figure Appendix E4: Best-fit model moderate 'TI' scenario

Normalized time	CDF ( $\alpha=4.6, \beta=2.6$ )	Fatigue failure ratio	Fatigue failure ratio		sst	ssr	R <sup>2</sup>	R
0,05	1,15605E-05						0,832656536	0,9125
0,1	0,00026142	0	0		0,121079	6,83E-08		
0,15	0,001569016	0	0		0,121079	2,46E-06		
0,2	0,005459306	0,540540541	0,005405405		0,117346	2,91E-09		
0,25	0,014063633	0,495049505	0,004950495		0,117658	8,3E-05		
0,3	0,029903872	6,382978723	0,063829787		0,080732	0,001151		
0,35	0,055605411	19,65811966	0,196581197		0,022917	0,019874		
0,4	0,093570748	14,75409836	0,147540984		0,040169	0,002913		
0,45	0,145639984	40,90909091	0,409090909		0,003737	0,069406		
0,5	0,212762219	28,57142857	0,285714286		0,003875	0,005322		
0,55	0,294701568	30,90909091	0,309090909		0,001511	0,000207		
0,6	0,389802651	41,17647059	0,411764706		0,004071	0,000482		
0,65	0,494843372	42,30769231	0,423076923		0,005642	0,00515		
0,7	0,605008008	59,09090909	0,590909091		0,059022	0,000199		
0,75	0,714022822	71,05263158	0,710526316		0,131452	1,22E-05		
0,8	0,814512929							
0,85	0,898671541	62,96296296	0,62962963		0,079336	0,072384		
0,9	0,959405809							
0,95	0,992331928	72,72727273	0,727272727		0,143875	0,070256		
1	1	100	1		0,425151	0		
Mean		0,347963727		Total	1,478651	0,247443		

Table Appendix E4: Best-fit model moderate 'TI' scenario

Moderate 'TI', 'T-extreme' > 20 days

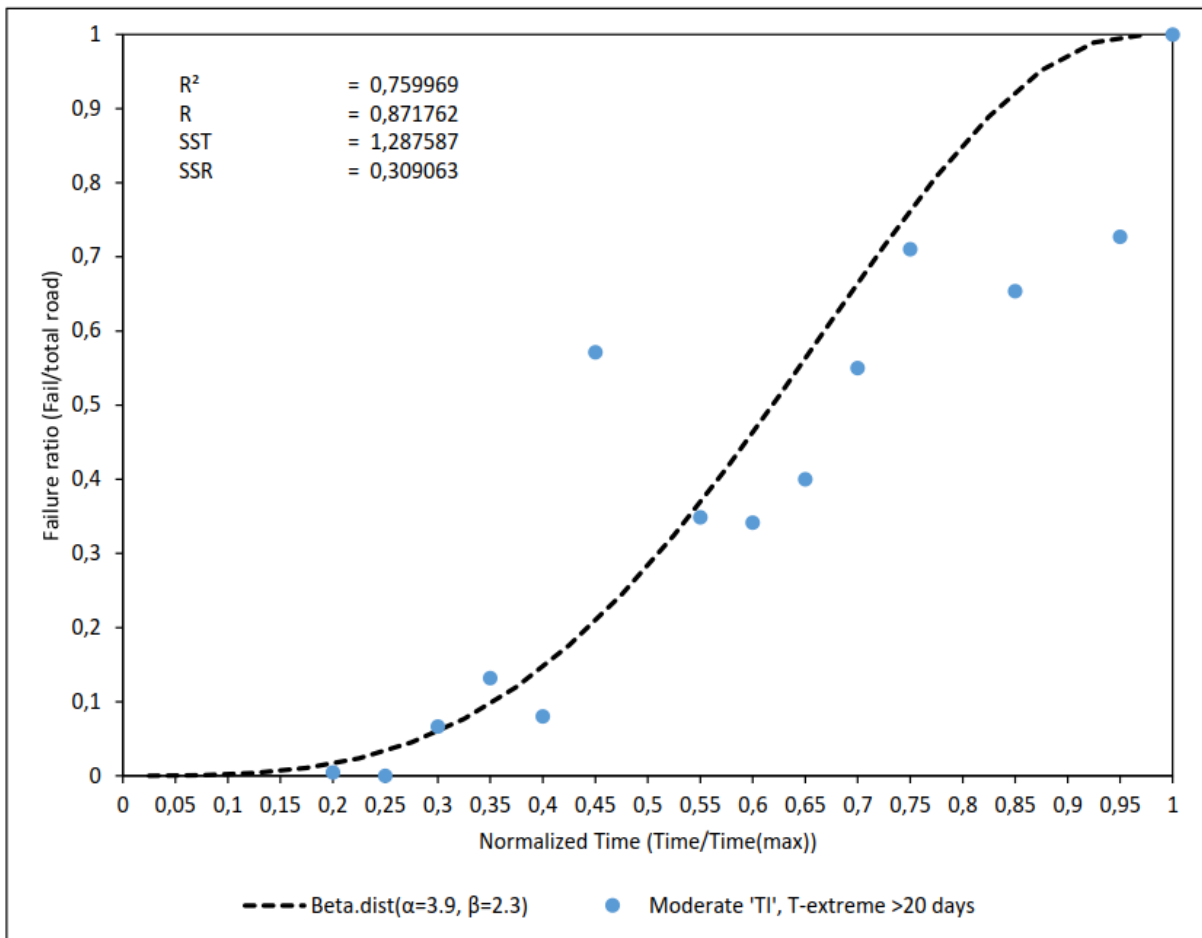


Figure Appendix E5: Best-fit model moderate 'TI' and 'T-extreme'>20 days scenario

Normalized time	CDF ( $\alpha=3.9, \beta=2.3$ )	Fatigue failure ratio	Fatigue failure ratio		sst	ssr	R <sup>2</sup>	R
0,05	5,62007E-05						0,759969	0,871762
0,1	0,000794112							
0,15	0,003645215							
0,2	0,010542389	0,465116279	0,004651163		0,155543	3,47E-05		
0,25	0,023637796	0	0		0,159233	0,000559		
0,3	0,045058436	6,666666667	0,066666667		0,110472	0,000467		
0,35	0,076689432	13,18681319	0,131868132		0,071381	0,003045		
0,4	0,119981729	8	0,08		0,101787	0,001599		
0,45	0,175783459	57,14285714	0,571428571		0,029718	0,156535		
0,5	0,244195676							
0,55	0,324454457	34,88372093	0,348837209		0,00252	0,000595		
0,6	0,414842764	34,14634146	0,341463415		0,003315	0,005385		
0,65	0,512637379	40	0,4		9,22E-07	0,012687		
0,7	0,614099159	55	0,55		0,022789	0,004109		
0,75	0,714519855	71,05263158	0,710526316		0,097024	1,59E-05		
0,8	0,808348067							
0,85	0,889436707	65,38461538	0,653846154		0,064926	0,055503		
0,9	0,951503629							
0,95	0,989057095	72,72727273	0,727272727		0,107737	0,068531		
1	1	100	1		0,361153	0		
<b>Mean</b>		0,399040025		<b>Total</b>	1,287597	0,309063		

Table Appendix E5: Best-fit model moderate 'TI' and 'T-extreme'>20 days scenario

Moderate 'TI', 'T-extreme' > 30 days

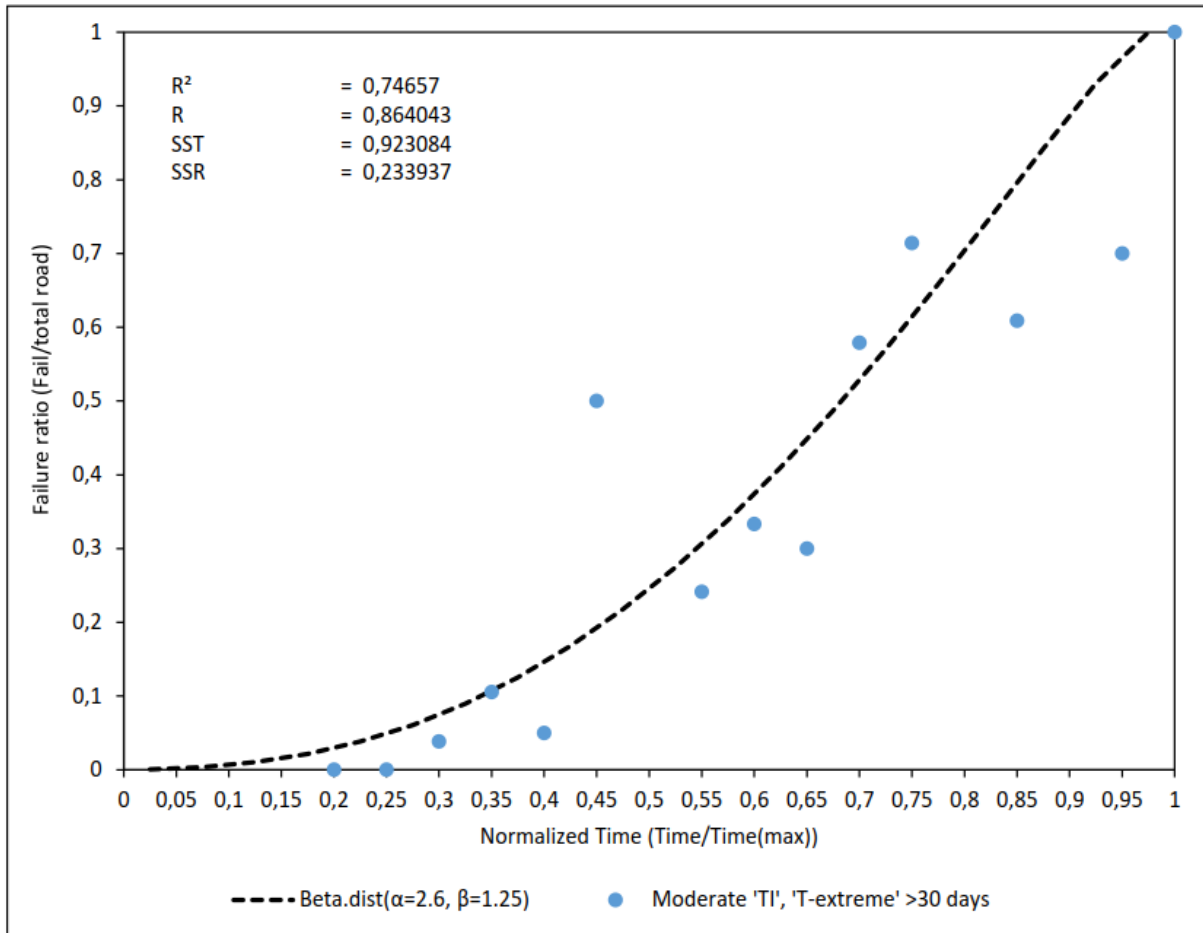


Figure Appendix E6: Best-fit model moderate 'TI' and 'T-extreme'>30 days scenario

Normalized time	CDF ( $\alpha=2.6, \beta=1.25$ )	Fatigue failure ratio	Fatigue failure ratio		sst	ssr	R <sup>2</sup>	R
0,05	0,000607487						0,74657	0,864043
0,1	0,003647987							
0,15	0,010364566							
0,2	0,021669935	0	0		0,136391	0,00047		
0,25	0,038289114	0	0		0,136391	0,001466		
0,3	0,060808133	3,846153846	0,038461538		0,109462	0,000499		
0,35	0,089696498	10,52631579	0,105263158		0,069722	0,000242		
0,4	0,125317719	5	0,05		0,10196	0,005673		
0,45	0,167932671	50	0,5		0,017079	0,110269		
0,5	0,217697467							
0,55	0,274656047	24,13793103	0,24137931		0,016367	0,001107		
0,6	0,338726539	33,33333333	0,333333333		0,001294	2,91E-05		
0,65	0,409679123	30	0,3		0,004804	0,01203		
0,7	0,487100827	57,89473684	0,578947368		0,043947	0,008436		
0,75	0,570338231	71,42857143	0,714285714		0,119007	0,020721		
0,8	0,658398636							
0,85	0,749762767	60,86956522	0,608695652		0,057305	0,0199		
0,9	0,841971377							
0,95	0,93042466	70	0,7		0,109355	0,053096		
1	1	100	1			0		
<b>Mean</b>			0,369311862	<b>Total</b>	<b>0,923084</b>	<b>0,233937</b>		

Table Appendix E6: Best-fit model moderate 'TI' and 'T-extreme'>30 days scenario

Heavy 'TI'

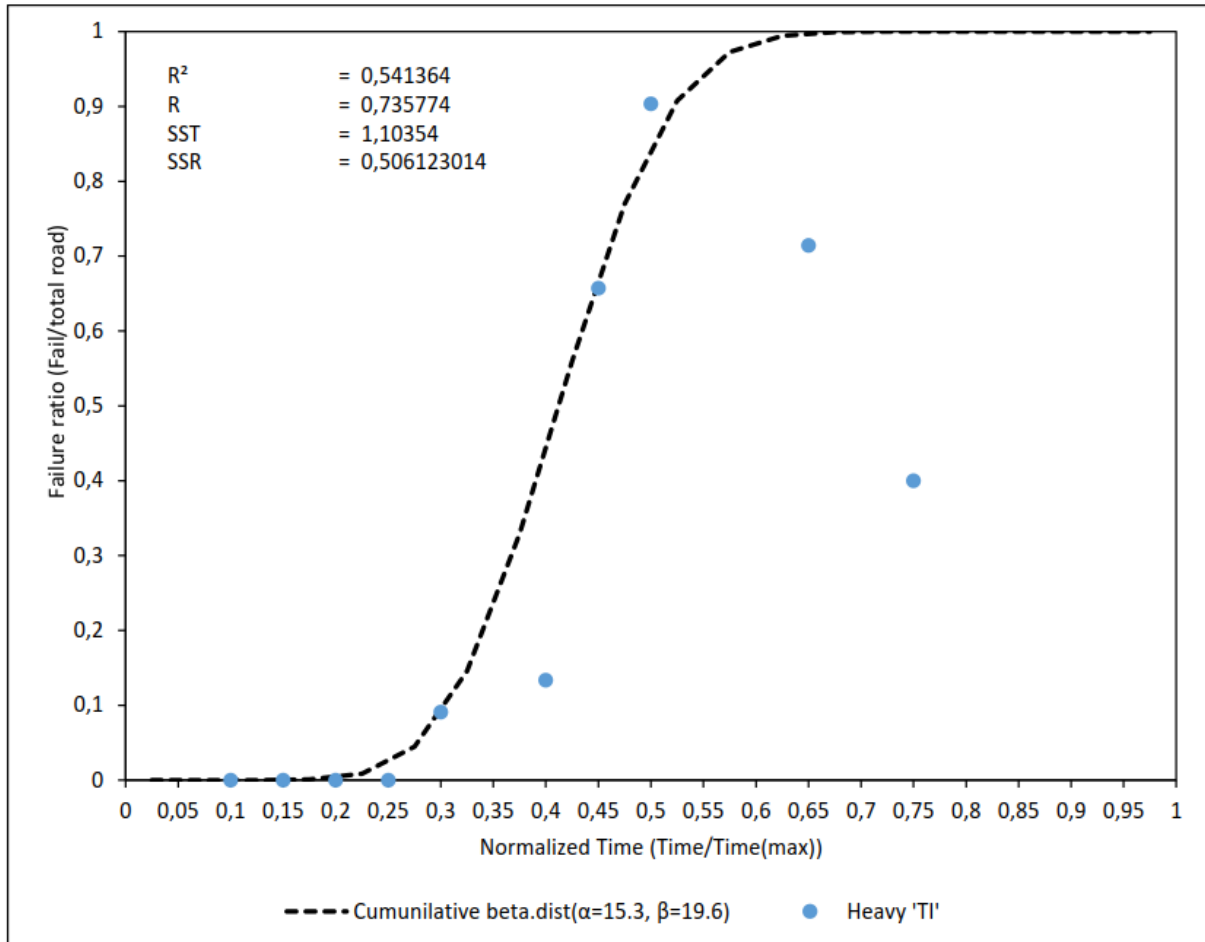


Figure Appendix E7: Best-fit model heavy 'TI' scenario

Normalized time	CDF ( $\alpha=15.3, \beta=19.6$ )	Fatigue failure ratio	Fatigue failure ratio		sst	ssr	R^2	R
0,05	9,49129E-12						0,541363996	0,735774
0,1	1,50508E-07	0	0		0,084036	2,27E-14		
0,15	2,79906E-05	0	0		0,084036	7,83E-10		
0,2	0,000819025	0	0		0,084036	6,71E-07		
0,25	0,008492374	0	0		0,084036	7,21E-05		
0,3	0,044768046	9,090909091	0,090909091		0,039593	0,002129		
0,35	0,145574317							
0,4	0,328729091	13,33333333	0,133333333		0,02451	0,03818		
0,45	0,560009785	65,71428571	0,657142857		0,134875	0,009435		
0,5	0,769629693	90,32258065	0,903225806		0,376181	0,017848		
0,55	0,907495192							
0,6	0,972801526							
0,65	0,994495028	71,42857143	0,714285714		0,180112	0,078517		
0,7	0,9992995							
0,75	0,999951423	40	0,4		0,012124	0,359942		
0,8	0,99999856							
0,85	0,999999988							
0,9	1							
0,95	1							
1	1							
		Mean	0,28988968	Total	1,10354	0,506123		

Table Appendix E7: Best-fit model heavy 'TI' scenario

Heavy 'TI', 'T-extreme' > 20 days

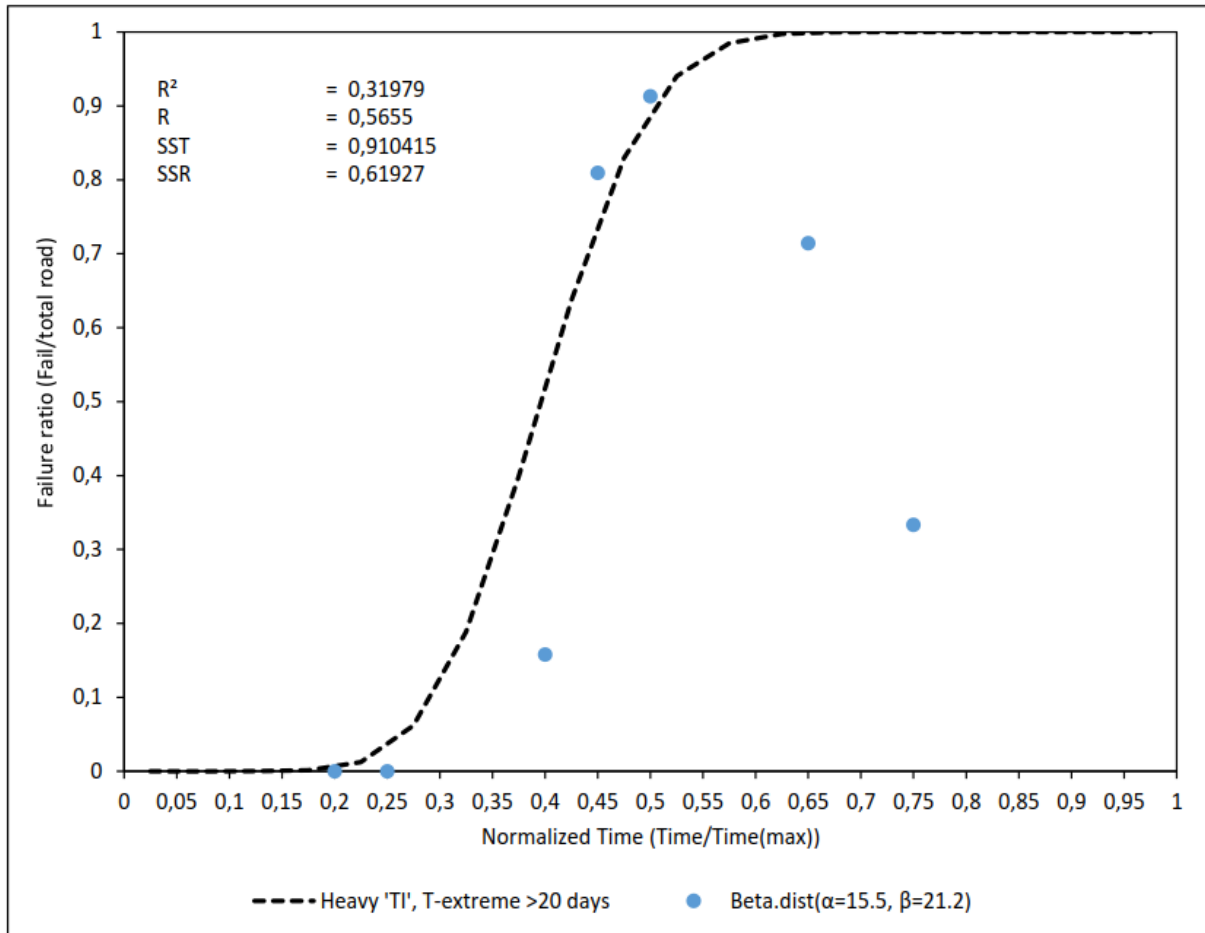


Figure Appendix E8: Best-fit model heavy 'TI' and 'T-extreme'>20 days scenario

Normalized time	CDF (α=15.5, β=21.2)	Fatigue failure ratio	Fatigue failure ratio		sst	ssr	R^2	R
0,05	1,41604E-11						0,319794	0,565503
0,1	2,37927E-07							
0,15	4,41133E-05							
0,2	0,001252689	0	0		0,174973	1,57E-06		
0,25	0,012405623	0	0		0,174973	0,000154		
0,3	0,06180285							
0,35	0,188660975							
0,4	0,398885193	15,78947368	0,157894737		0,067809	0,058076		
0,45	0,637787268	80,95238095	0,80952381		0,153058	0,029493		
0,5	0,829881775	91,30434783	0,913043478		0,244774	0,006916		
0,55	0,940197302							
0,6	0,984999507							
0,65	0,997485353	71,42857143	0,714285714		0,087609	0,080202		
0,7	0,999744413							
0,75	0,999986501	33,33333333	0,333333333		0,007219	0,444426		
0,8	0,999999715							
0,85	0,999999999							
0,9	1							
0,95	1							
1	1							
Mean			0,418297296	Total	0,910415	0,61927		

Table Appendix E8: Best-fit model heavy 'TI' and 'T-extreme'>20 days scenario

Heavy 'TI', 'T-extreme' > 30 days

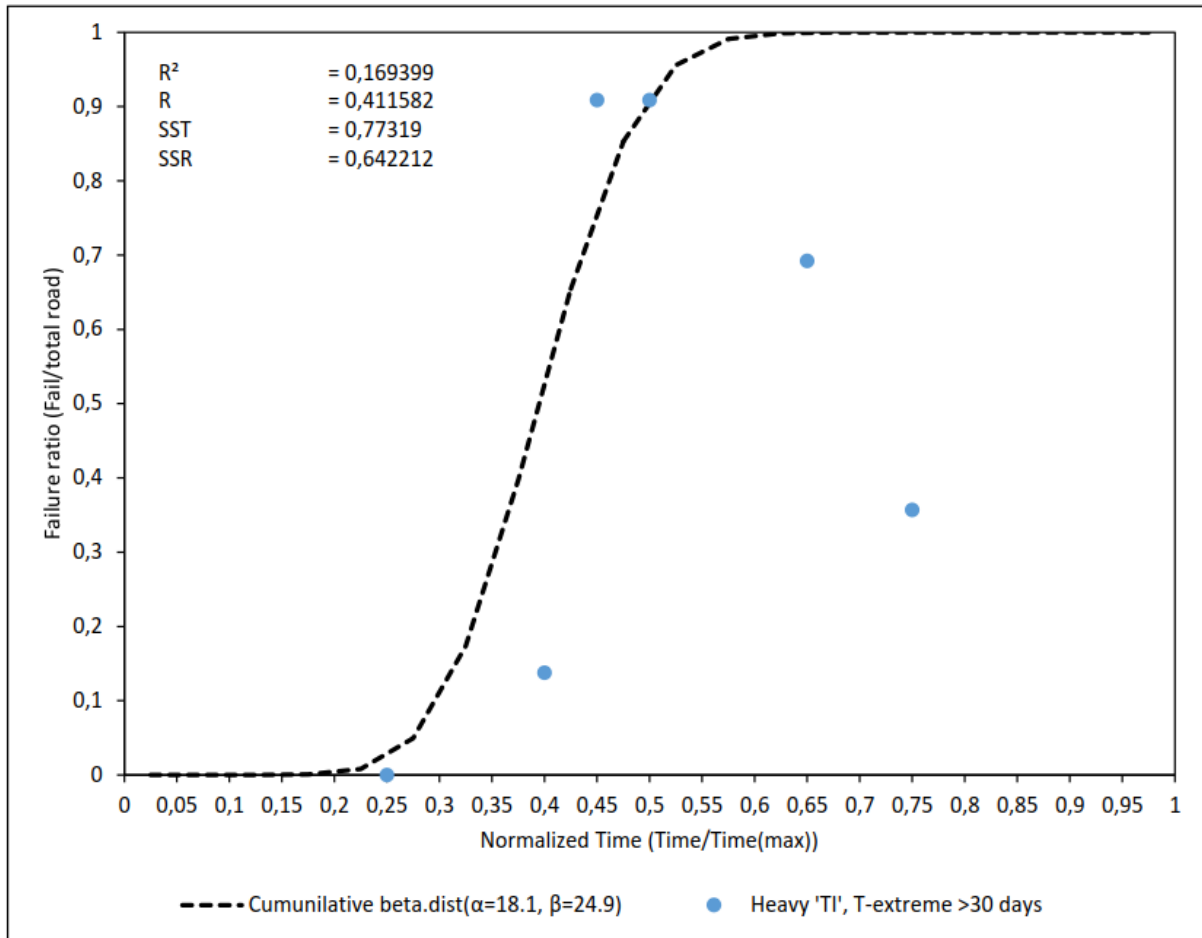


Figure Appendix E9: Best-fit model heavy 'TI' and 'T-extreme'>30 days scenario

Normalized tim	CDF ( $\alpha=18.1, \beta=24.9$ )	Fatigue failure ratio	Fatigue failure ratio		sst	ssr	R^2	R
0,05	3,22828E-13						0,169399	0,411582
0,1	2,69814E-08							
0,15	1,16541E-05							
0,2	0,000561114							
0,25	0,007868601	0	0		0,250928	6,19E-05		
0,3	0,049280715							
0,35	0,17355241							
0,4	0,396885474	13,79310345	0,137931034		0,131766	0,067057		
0,45	0,654727795	90,90909091	0,909090909		0,166598	0,064701		
0,5	0,853005265	90,90909091	0,909090909		0,166598	0,003146		
0,55	0,955664612							
0,6	0,991041804							
0,65	0,998876474	69,23076923	0,692307692		0,036626	0,093984		
0,7	0,999921939							
0,75	0,999997492	35,71428571	0,357142857		0,020674	0,413262		
0,8	0,999999973							
0,85	1							
0,9	1							
0,95	1							
1	1							
<b>Mean</b>		0,500927234		<b>Total</b>	<b>0,77319</b>	<b>0,642212</b>		

Table Appendix E9: Best-fit model heavy 'TI' and 'T-extreme'>30 days scenario

## Appendix F

Appendix F shows the tables of all the histograms that are used for fatigue failure technique over time. The tables are produced by using the tables from that are used to plot the degradation curves. The tables then are transformed into ratio tables per timestep as is shown in all the tables below. Then the fatigue failure ratio and 0 damage ratio are used for the histograms as is shown in chapter 4 Result model.

	0> and <250 days	250> and <500 days	500> and <750 days	750> and <1000 days	1000> and <1250 days	1250> and <1500 days	1500> and <1750 days	1750> and <2000 days	2000> and <2250 days	2250> and <2500 days	2500> and <2750 days	2750> and <3000 days	3000> and <3250 days	3250> and <3500 days	3500> and <3750 days	3750> and <4000 days	4000> and <4250 days	4250> and <4500 days	4500> and <4750 days	4750> and <5000 days	
Complete dataset																					
Amount of data points	4	101	182	599	521	132	151	121	100	246	89	60	39	103	56	30	105	16	20	24	
Amount of damage 0	4	94	180	520	453	98	89	81	32	131	13	9	6	9	2	2	30	0	2	0	
Amount of damage 5	0	6	2	73	59	20	19	22	25	52	36	14	3	8	10	1	9	1	1	0	
Amount of damage 12	0	1	0	5	8	6	17	3	10	19	12	11	7	14	8	12	7	1	0	0	
Amount of damage 18	0	0	0	0	0	0	0	0	0	1	0	0	0	0	0	0	0	0	0	0	
Amount of damage 21	0	0	0	1	1	4	13	4	11	2	7	3	3	3	1	1	2	0	4	4	
Amount of damage 28	0	0	0	0	0	2	8	5	17	18	9	12	16	33	7	7	18	5	6	6	
Amount of damage 40	0	0	0	0	0	2	4	5	5	15	10	10	3	12	13	5	29	2	3	9	
Amount of damage 55	0	0	0	0	0	0	1	1	0	3	2	1	1	8	3	3	7	2	4	4	
Amount of damage 70	0	0	0	0	0	0	0	0	0	5	0	0	0	12	1	1	7	0	2	1	
% 0 damage	100	93,06930693	98,9010989	86,81135225	86,94817658	74,24242424	58,94039735	66,94214876	32	53,25203252	14,60674157	15	15,38461538	8,737864078	3,571428571	6,666666667	28,57142857	0	10	0	
% 5 damage	0	5,940594059	1,098901099	12,1869783	11,3243762	15,15151515	12,58278146	18,18181818	25	21,13821138	40,4494382	23,33333333	7,692307692	7,766990291	17,85714286	3,333333333	8,571428571	6,25	5	0	
% 12 damage	0	0,99009901	0	0,834724541	1,535508637	4,545454545	11,25827815	2,479338843	10	7,723577236	13,48214607	18,33333333	17,94871795	13,59223301	14,28571429	40	6,666666667	6,25	0	0	
% 18 damage	0	0	0	0	0	0	0	0	0	0,406504065	0	0	0	0	0	0	0	0	0	0	
% 21 damage	0	0	0	0,166944908	0,19193858	3,03030303	8,609271523	3,305785124	11	0,81300813	7,865168539	5	7,692307692	12,62135922	1,785714286	3,333333333	1,904761905	0	20	16,66666667	
% 28 damage	0	0	0	0	0	1,515151515	5,298013245	4,132231405	17	7,317073171	10,11235955	20	41,02564103	32,03883495	12,5	23,33333333	17,14285714	31,25	30	25	
% 40 damage	0	0	0	0	0	1,515151515	2,649006623	4,132231405	5	6,097560976	11,23595506	16,66666667	7,692307692	11,65048544	23,21428571	16,66666667	27,61904762	12,5	15	37,5	
% 55 damage	0	0	0	0	0	0,662251656	0,826446281	0	0	1,219512195	2,247191011	1,666666667	2,564102564	7,766990291	5,357142857	3,333333333	2,857142857	43,75	10	16,66666667	
% 70 damage	0	0	0	0	0	0	0	0	0	2,032520325	0	0	0	5,825242718	21,42857143	3,333333333	6,666666667	0	10	4,166666667	
total %	100	100	100	100	100	100	100	100	100	100	100	100	100	100	100	100	100	100	100	100	
Fatigue failure %	0	0	0	0,166944908	0,19193858	6,060606061	17,21854305	12,39669421	33	17,4796748	31,46067416	43,33333333	58,97435897	69,90291262	64,28571429	50	56,19047619	87,5	85	100	

Table Appendix F1: Measured data complete dataset divided in time-steps

	0> and <250 days	250> and <500 days	500> and <750 days	750> and <1000 days	1000> and <1250 days	1250> and <1500 days	1500> and <1750 days	1750> and <2000 days	2000> and <2250 days	2250> and <2500 days	2500> and <2750 days	2750> and <3000 days	3000> and <3250 days	3250> and <3500 days	3500> and <3750 days	3750> and <4000 days	4000> and <4250 days	4250> and <4500 days	4500> and <4750 days	4750> and <5000 days	
T-extreme > 20 days																					
Amount of data points				278	374	57	117	65	66	43	68	47	35	99	56	30	102	16	20	24	
Amount of damage 0				249	352	35	75	45	24	6	6	7	6	8	2	2	29	0	1	0	
Amount of damage 5				27	22	12	16	11	12	7	31	11	2	8	10	1	8	0	1	0	
Amount of damage 12				1	0	5	13	1	4	3	8	10	7	13	8	12	6	1	0	0	
Amount of damage 18				0	0	0	0	0	0	1	0	0	0	0	0	0	0	0	0	0	
Amount of damage 21				1	0	4	8	3	7	0	7	2	3	13	1	1	2	0	4	4	
Amount of damage 28				0	0	1	2	2	16	13	6	6	13	31	7	7	18	5	6	6	
Amount of damage 40				0	0	0	3	3	3	7	8	10	3	12	3	5	29	2	3	9	
Amount of damage 55				0	0	0	0	0	0	0	2	1	1	8	3	3	7	2	4	4	
Amount of damage 70				0	0	0	0	0	0	5	0	0	0	6	12	1	7	0	2	1	
% 0 damage				89,56834532	94,11764706	61,40350877	64,1025641	69,23076923	36,36363636	13,95348837	8,823529412	14,89361702	17,14285714	8,080808081	3,571428571	6,666666667	28,43137255	0	10	0	
% 5 damage				9,712230216	5,882352941	21,05263158	13,67521368	16,92307692	18,18181818	16,27806977	45,58823529	23,40425532	5,714285714	8,080808081	17,85714286	3,333333333	7,843137255	6,25	5	0	
% 12 damage				0,35971223	0	8,771929825	11,11111111	1,538461538	6,060606061	6,976744186	11,76470588	21,27659574	20	13,13131313	14,28571429	40	5,882352941	6,25	0	0	
% 18 damage				0	0	0	0	0	0	2,325581395	0	0	0	0	0	0	0	0	0	0	
% 21 damage				0,35971223	0	7,01754386	6,837606838	4,615384615	10,60606061	0	10,29411765	4,255319149	8,571428571	13,13131313	1,785714286	3,333333333	1,960784314	0	20	16,66666667	
% 28 damage				0	0	1,754385965	1,709401709	3,076923077	24,24242424	30,23255814	8,823529412	12,76595745	37,14285714	31,31313131	12,5	23,33333333	17,64705882	31,25	30	25	
% 40 damage				0	0	2,564102564	4,545454545	4,545454545	16,27806977	11,76470588	21,27659574	8,571428571	12,12121212	23,21428571	16,66666667	28,43137255	28,43137255	12,5	15	37,5	
% 55 damage				0	0	0	0	0	0	2,325581395	2,941176471	2,127659574	2,857142857	8,080808081	5,357142857	3,333333333	2,941176471	43,75	10	16,66666667	
% 70 damage				0	0	0	0	0	0	11,62790698	0	0	0	6,060606061	21,42857143	3,333333333	6,862745098	0	10	4,166666667	
total %				100	100	100	100	100	100	100	100	100	100	100	100	100	100	100	100	100	
Fatigue failure %				0,35971223	0	8,771929825	11,11111111	12,30769231	39,39393939	60,46511628	33,82352941	40,42553191	57,14285714	70,70707071	64,28571429	50	57,84313725	87,5	85	100	

Table Appendix F2: Measured data influence 'T-extreme' > 20 days, divided in time-steps

	0> and <250 days	250> and <500 days	500> and <750 days	750> and <1000 days	1000> and <1250 days	1250> and <1500 days	1500> and <1750 days	1750> and <2000 days	2000> and <2250 days	2250> and <2500 days	2500> and <2750 days	2750> and <3000 days	3000> and <3250 days	3250> and <3500 days	3500> and <3750 days	3750> and <4000 days	4000> and <4250 days	4250> and <4500 days	4500> and <4750 days	4750> and <5000 days	
T-extreme > 30 days																					
Amount of data points				63	69	27	66	50	39	24	47	16	28	87	45	26	92	14	18	21	
Amount of damage 0				30	67	18	39	34	13	2	6	1	6	7	2	2	27	0	2	0	
Amount of damage 5				30	2	7	11	11	8	4	24	4	2	4	9	1	8	1	1	0	
Amount of damage 12				2	0	1	10	0	2	3	6	2	6	13	6	12	6	1	0	0	
Amount of damage 18				0	0	0	0	0	0	1	0	0	0	0	0	0	0	0	0	0	
Amount of damage 21				1	0	1	3	1	5	0	2	0	2	11	0	1	2	0	4	4	
Amount of damage 28				0	0	0	0	1	8	6	4	3	9	25	6	16	5	6	5	9	
Amount of damage 40				0	0	0	3	3	3	5	4	5	2	12	9	3	26	2	2	9	
Amount of damage 55				0	0	0	0	0	0	0	1	0	1	8	2	1	5	1	3	3	
Amount of damage 70				0	0	0	0	0	0	3	0	0	0	5	11	6	0	2	0	0	
% 0 damage				47,61904762	97,10144928	66,66666667	59,09090909	68	33,33333333	8,333333333	12,76595745	6,25	21,42857143	8,045977011	4,444444444	7,692307692	29,34782609	0	11,11111111	0	
% 5 damage				47,61904762	2,898550725	25,92592593	16,66666667	22	20,51282051	16,66666667	51,06382979	25	7,142857143	4,597701149	20	3,846153846	8,695652174	7,142857143	5,555555556	0	
% 12 damage				3,174603175	0	3,703703704	15,15151515	0	5,128205128	12,5	12,76595745	12,5	21,42857143	14,94252874	13,33333333	46,15384615	6,52173913	7,142857143	0	0	
% 18 damage				0	0	0	0	0	0	4,166666667	0	0	0	0	0	0	0	0	0	0	
% 21 damage				1,587301587	0	3,703703704	4,545454545	2	12,82051282	0	4,255319149	0	7,142857143	12,64367816	0	3,846153846	2,173913				

	0> and <250 days	250> and <500 days	500> and <750 days	750> and <1000 days	1000> and <1250 days	1250> and <1500 days	1500> and <1750 days	1750> and <2000 days	2000> and <2250 days	2250> and <2500 days	2500> and <2750 days	2750> and <3000 days	3000> and <3250 days	3250> and <3500 days	3500> and <3750 days	3750> and <4000 days	4000> and <4250 days	4250> and <4500 days	4500> and <4750 days	4750> and <5000 days	
TI moderate																					
Amount of data points	72	50	370	202	94	117	61	22	35	55	51	26	22	38							15
Amount of damage 0	70	49	312	174	67	69	47	5	13	11	7	6	0	0							0
Amount of damage 5	2	1	51	19	16	12	4	5	7	21	13	2	3	5							0
Amount of damage 12	0	0	5	8	5	13	1	3	5	6	10	7	6	6							0
Amount of damage 18	0	0	0	0	0	0	0	0	0	0	0	0	0	0							0
Amount of damage 21	0	0	1	1	4	11	2	7	0	6	3	2	3	0							0
Amount of damage 28	0	0	1	0	2	8	3	2	3	5	11	5	5	5							0
Amount of damage 40	0	0	0	0	0	4	3	0	6	5	6	3	3	11							5
Amount of damage 55	0	0	0	0	0	0	1	0	1	1	1	1	2	1							4
Amount of damage 70	0	0	0	0	0	0	0	0	0	0	0	0	0	10							1
% 0 damage	97,2222222	98	84,3243243	86,13861386	71,27659574	58,97435897	77,04918033	22,72727273	37,14285714	20	13,7254902	23,07692308	0	0							0
% 5 damage	2,777777778	2	13,78378378	9,405940594	17,0212766	10,25641026	6,557377049	22,72727273	20	38,18181818	25,49019608	7,692307692	13,63636364	13,15789474							0
% 12 damage	0	0	1,351351351	3,96039604	5,319148936	11,11111111	1,639344262	13,63636364	14,28571429	10,90909091	19,60784314	26,92307692	27,27272727	15,78947368							0
% 18 damage	0	0	0	0	0	0	0	0	0	0	0	0	0	0							0
% 21 damage	0	0	0,27027027	0,495049505	4,255319149	9,401709402	3,278688525	31,81818182	0	10,90909091	5,882352941	7,692307692	13,63636364	0							0
% 28 damage	0	0	0,27027027	0	2,127659574	6,837606838	4,918032787	9,090909091	8,571428571	9,090909091	21,56862745	19,23076923	22,72727273	13,15789474							0
% 40 damage	0	0	0	0	0	3,418803419	4,918032787	0	17,14285714	9,090909091	11,76470588	11,53846154	13,63636364	28,94736842							0
% 55 damage	0	0	0	0	0	0	1,639344262	0	2,857142857	1,818181818	1,960784314	3,846153846	9,090909091	2,631578947							0
% 70 damage	0	0	0	0	0	0	0	0	0	0	0	0	0	26,31578947							0
total %	100	100	100	100	100	100	100	100	100	100	100	100	100	100	100	100	100	100	100	100	100
Fatigue failure %	0	0	0,540540541	0,495049505	6,382978723	19,65811966	14,75408936	40,90909091	28,57142857	30,90909091	41,17647059	42,30769231	59,09090909	71,05263158							0

Table Appendix F5: Measured data influence moderate 'TI', divided in time-steps

	0> and <250 days	250> and <500 days	500> and <750 days	750> and <1000 days	1000> and <1250 days	1250> and <1500 days	1500> and <1750 days	1750> and <2000 days	2000> and <2250 days	2250> and <2500 days	2500> and <2750 days	2750> and <3000 days	3000> and <3250 days	3250> and <3500 days	3500> and <3750 days	3750> and <4000 days	4000> and <4250 days	4250> and <4500 days	4500> and <4750 days	4750> and <5000 days	
TI heavy																					
Amount of data points	26	103	109	187	22			45	35	31				14							15
Amount of damage 0	24	102	101	171	17			27	6	0				0							2
Amount of damage 5	2	1	8	16	2			10	3	1				0							5
Amount of damage 12	0	0	0	0	1			2	3	2				4							2
Amount of damage 18	0	0	0	0	0			0	0	0				0							0
Amount of damage 21	0	0	0	0	0			2	3	2				1							1
Amount of damage 28	0	0	0	0	0			2	15	13				4							0
Amount of damage 40	0	0	0	0	2			2	5	6				3							2
Amount of damage 55	0	0	0	0	0			0	0	2				2							1
Amount of damage 70	0	0	0	0	0			0	0	5				0							2
% 0 damage	92,30769231	99,02912621	92,6605046	91,44385027	77,27272727			60	17,14285714	0				0							13,33333333
% 5 damage	7,692307692	0,970873786	7,339449541	8,556149733	9,090909091			22,22222222	8,571428571	3,225806452				0							33,33333333
% 12 damage	0	0	0	0	4,545454545			4,444444444	8,571428571	6,451612903				28,57142857							13,33333333
% 18 damage	0	0	0	0	0			0	0	0				0							0
% 21 damage	0	0	0	0	0			4,444444444	8,571428571	6,451612903				7,142857143							6,666666667
% 28 damage	0	0	0	0	0			4,444444444	42,85714286	41,93548387				28,57142857							0
% 40 damage	0	0	0	0	9,090909091			4,444444444	14,28571429	19,35483871				21,42857143							13,33333333
% 55 damage	0	0	0	0	0			0	0	6,451612903				14,28571429							6,666666667
% 70 damage	0	0	0	0	0			0	0	16,12903226				0							13,33333333
total %	100	100	100	100	100			100	100	100				100							100
Fatigue failure %	0	0	0	0	9,090909091			13,33333333	65,71428571	90,32258065				71,42857143							40

Table Appendix F6: Measured data influence heavy 'TI', divided in time-steps

	0> and <250 days	250> and <500 days	500> and <750 days	750> and <1000 days	1000> and <1250 days	1250> and <1500 days	1500> and <1750 days	1750> and <2000 days	2000> and <2250 days	2250> and <2500 days	2500> and <2750 days	2750> and <3000 days	3000> and <3250 days	3250> and <3500 days	3500> and <3750 days	3750> and <4000 days	4000> and <4250 days	4250> and <4500 days	4500> and <4750 days	4750> and <5000 days	
TI light, T-extreme >20																					
Amount of data points			17				23		31	12	22				65						
Amount of damage 0			16				14		18	5	3				7						
Amount of damage 5			1				5		9	4	12				5						
Amount of damage 12			0				4		3	2	2				4						
Amount of damage 18			0				0		0	1	0				0						
Amount of damage 21			0				0		1	0	1				9						
Amount of damage 28			0				0		0	0	2				24						
Amount of damage 40			0				0		0	0	1				6						
Amount of damage 55			0				0		0	0	1				0						
Amount of damage 70			0				0		0	0	0				7						
% 0 damage			94,11764706				60,86956522		58,06451613	41,66666667	13,63636364			10,76923077							0
% 5 damage			5,882352941				21,73913043		29,03225806	33,33333333	54,54545455			7,692307692							0
% 12 damage			0				17,39130435		9,677419355	16,66666667	9,090909091			6,153846154							0
% 18 damage			0				0		0	8,333333333	0			0							0
% 21 damage			0				0		3,225806452	0	4,545454545			13,84615385							0
% 28 damage			0				0		0	0	9,090909091			36,92307692							50
% 40 damage			0				0		0	0	4,545454545			9,230769231							0
% 55 damage			0				0		0	0	4,545454545			6,153846154							40
% 70 damage			0				0		0	0	0			10,76923077							0
total %			100				100		100	100	100			100							100
Fatigue failure %			0				0		3,225806452	0	22,72727273			76,92307692							90

Up-Table Appendix F7: Measured data influence light 'TI' and 'T-extreme' > 20 days, divided in time-steps, down-Table Appendix E8: Measured data influence moderate 'TI' and 'T-extreme' > 20 days divided in time-steps.

	0> and <250 days	250> and <500 days	500> and <750 days	750> and <1000 days	1000> and <1250 days	1250> and <1500 days	1500> and <1750 days	1750> and <2000 days	2000> and <2250 days	2250> and <2500 days	2500> and <2750 days	2750> and <3000 days	3000> and <3250 days	3250> and <3500 days	3500> and <3750 days	3750> and <4000 days	4000> and <4250 days	4250> and <4500 days	4500> and <4750 days	4750> and <5000 days	
TI moderate, T-extreme >20																					
Amount of data points		215	123	45	91	25	14			43	41	25	20	38			26			11	15
Amount of damage 0		191	114	28	60	21	4														

	0> and <250 days	250> and <500 days	500> and <750 days	750> and <1000 days	1000> and <1250 days	1250> and <1500 days	1500> and <1750 days	1750> and <2000 days	2000> and <2250 days	2250> and <2500 days	2500> and <2750 days	2750> and <3000 days	3000> and <3250 days	3250> and <3500 days	3500> and <3750 days	3750> and <4000 days	4000> and <4250 days	4250> and <4500 days	4500> and <4750 days	4750> and <5000 days	
Tl heavy, T-extreme >20																					
Amount of data points				11	139				38	21	23				14	15					
Amount of damage 0				11	128				23	2	0				0	2					
Amount of damage 5				0	11				9	2	1				0	5					
Amount of damage 12				0	0				0	0	1				4	2					
Amount of damage 18				0	0				0	0	0				0	0					
Amount of damage 21				0	0				2	0	0				1	1					
Amount of damage 28				0	0				2	14	10				4	0					
Amount of damage 40				0	0				2	3	5				3	1					
Amount of damage 55				0	0				0	0	1				2	1					
Amount of damage 70				0	0				0	0	5				0	2					
% 0 damage				100	92.08633094				60.52631579	9.523809524	0				0	13.33333333					
% 5 damage				0	7.913669065				23.68421053	9.523809524	4.347826087				0	33.33333333					
% 12 damage				0	0				0	0	4.347826087				28.57142857	13.33333333					
% 18 damage				0	0				0	0	0				0	0					
% 21 damage				0	0				5.263157895	0	0				7.142857143	6.666666667					
% 28 damage				0	0				5.263157895	66.66666667	43.47826087				28.57142857	0					
% 40 damage				0	0				5.263157895	14.28571429	21.73913043				21.42857143	6.666666667					
% 55 damage				0	0				0	0	4.347826087				14.28571429	6.666666667					
% 70 damage				0	0				0	0	21.73913043				0	13.33333333					
total %				100	100				100	100	100				100	93.33333333					
Fatigue failure %				0	0				15.78947368	80.95238095	91.30434783				71.42857143	33.33333333					

Table Appendix F9: Measured data influence heavy 'TI' and 'T-extreme' > 20 days divided in time-steps

	0> and <250 days	250> and <500 days	500> and <750 days	750> and <1000 days	1000> and <1250 days	1250> and <1500 days	1500> and <1750 days	1750> and <2000 days	2000> and <2250 days	2250> and <2500 days	2500> and <2750 days	2750> and <3000 days	3000> and <3250 days	3250> and <3500 days	3500> and <3750 days	3750> and <4000 days	4000> and <4250 days	4250> and <4500 days	4500> and <4750 days	4750> and <5000 days	
Tl light, T-extreme >30																					
Amount of data points				12					18		18			55		21	62				
Amount of damage 0				11					10		3			6		0	22				
Amount of damage 5				1					6		10			3		0	0				
Amount of damage 12				0					1		1			4		11	6				
Amount of damage 18				0					0		0			0		0	0				
Amount of damage 21				0					1		1			7		1	0				
Amount of damage 28				0					0		2			19		6	15				
Amount of damage 40				0					1		1			6		3	17				
Amount of damage 55				0					0		0			4		0	1				
Amount of damage 70				0					0		0			6		0	1				
% 0 damage				91.66666667					55.55555556		16.66666667			10.90909091		0	35.48387097				
% 5 damage				8.333333333					33.33333333		55.55555556			5.454545455		0	0				
% 12 damage				0					5.555555556		5.555555556			7.272727273		52.38095238	9.677419355				
% 18 damage				0					0		0			0		0	0				
% 21 damage				0					5.555555556		5.555555556			12.72727273		4.761904762	0				
% 28 damage				0					0		11.11111111			34.54545455		28.57142857	24.19354839				
% 40 damage				0					0		5.555555556			10.90909091		14.28571429	27.41935484				
% 55 damage				0					0		0			7.272727273		0	1.612903226				
% 70 damage				0					0		0			10.90909091		0	1.612903226				
total %				100					100		100			100		100	100				
Fatigue failure %				0					5.555555556		22.22222222			76.36363636		47.61904762	54.83870968				

Table Appendix F10: Measured data influence Light 'TI' and 'T-extreme' > 30 days divided in time-steps

	0> and <250 days	250> and <500 days	500> and <750 days	750> and <1000 days	1000> and <1250 days	1250> and <1500 days	1500> and <1750 days	1750> and <2000 days	2000> and <2250 days	2250> and <2500 days	2500> and <2750 days	2750> and <3000 days	3000> and <3250 days	3250> and <3500 days	3500> and <3750 days	3750> and <4000 days	4000> and <4250 days	4250> and <4500 days	4500> and <4750 days	4750> and <5000 days	
Tl moderate, T-extreme >30																					
Amount of data points				13	29	26	57	20	10		29	12	20	19	28		23			10	12
Amount of damage 0				2	28	18	36	18	3		3	1	6	1	0		5			2	0
Amount of damage 5				11	1	6	8	1	1		14	5	2	2	4		4			1	0
Amount of damage 12				0	0	1	7	0	1		5	2	6	5	4		0			0	0
Amount of damage 18				0	0	0	0	0	0		0	0	0	0	0		0			0	0
Amount of damage 21				0	0	1	3	0	4		1	0	1	3	0		0			1	1
Amount of damage 28				0	0	0	3	0	1		2	2	2	3	4		2			2	3
Amount of damage 40				0	0	0	0	1	0		3	2	2	3	7		9			2	5
Amount of damage 55				0	0	0	0	0	0		1	0	1	2	0		0			0	3
Amount of damage 70				0	0	0	0	0	0		0	0	0	0	9		5			2	0
% 0 damage				15.38461538	96.55172414	69.23076923	63.15789474	90	30		10.34482759	8.333333333	30	5.263157895	0		21.73913043			20	0
% 5 damage				84.61538462	3.448275862	23.07692308	14.03508772	5	10		48.27586207	41.66666667	10	10.52631579	14.28571429		17.39130435			10	0
% 12 damage				0	0	3.846153846	12.28070175	0	10		17.24137931	16.66666667	30	26.31578947	14.28571429		0			0	0
% 18 damage				0	0	0	0	0	0		0	0	0	0	0		0			0	0
% 21 damage				0	0	3.846153846	5.263157895	0	40		3.448275862	0	5	15.78947368	0		0			8.333333333	0
% 28 damage				0	0	0	5.263157895	0	10		6.896551724	16.66666667	10	15.78947368	14.28571429		0			20	25
% 40 damage				0	0	0	0	5	0		10.34482759	16.66666667	10	15.78947368	25		39.13043478			20	41.66666667
% 55 damage				0	0	0	0	0	0		3.448275862	0	5	10.52631579	0		0			0	25
% 70 damage				0	0	0	0	0	0		0	0	0	0	32.14285714		21.73913043			20	0
total %				100	100	100	100	100	100		100	100	100	100	100		100			100	100
Fatigue failure %				0	0	3.846153846	10.52631579	5	50		24.13793103	33.33333333	30	57.89473684	71.42857143		60.86956522			70	100

Up-Table Appendix F11: Measured data influence moderate 'TI' and 'T-extreme' > 30 days, divided in time-steps, down-Table Appendix F12: Measured data influence heavy 'TI' and 'T-extreme' > 30 days divided in time-steps.

## Appendix G

This Appendix gives the process description of the prediction the risk model the simulation 'Monte Carlo' method that is produced in Excel. The flow-chart is shown in two parts on the next two pages (figure Appendix G1 and G2). To produce the simulation the observed errors that are shown in all the scenarios needs to be captured. This is done by finding the variance (see function Appendix G1).

$$VAR = \sum_i^N \frac{(f(beta\ dist.) - y_i)^2}{N}$$
$$Std. = \sqrt{VAR}$$

*Function Appendix G1: Function of error capturing for calculating the variance*

The upper bound and a lower bound of the best fit beta distribution can be described by the following function as is shown in function Appendix G2.

$$Upper\ bound = f((\alpha - std.), (\beta + std.))$$

$$Lower\ bound = f((\alpha + std.), (\beta - std.))$$

*Function Appendix G2: Function of the upper bound and the lower bound of the best fit beta distribution.*

Now the error is captured the scenarios can be implemented in the simulation model. The simulation will be runned a 1000 times and first a random probability number is produced between 0 and 1 (see figure Appendix G2). Then the cumulative normal distribution of the shape parameter  $\alpha$  and  $\beta$  (between the upper bound and lower bound) are implemented in the simulation model (see function Appendix G3).

$$CDF(\alpha\ or\ \beta) = (RANDOM(between\ 0\ and\ 1), \alpha\ or\ \beta, std.*(\alpha\ or\ \beta))$$

*Function Appnedix G3: Cumulative normal distribution the function calculates in Excel the cumulative normal distribution of the shape parameters  $\alpha$  and  $\beta$  with the error captured.*

Furthermore CDF can not be below 0 so an IF-statement is used to filter out the calculations that show below 0. The next step is to calculate the fatigue failure shows a ratio of 10 % due to the fact that at this moment all the curves of the scenarios are rapit increases. The CDF of the beta distribution is used to expres all the simulations in a normal distribution plot (see function Appendix G1).

$$CDF\ of\ the\ Beta\ distribution = (fatigue\ failure\ ratio\ at\ 10\ \%, CDF\ \alpha, CDF\ \beta)$$

*Function Appendix G4: CDF of the Beta distribution he function calculates in Excel the risk when the CDF  $\alpha$  and  $\beta$  at a certain moment in normalized time a fatigue failure ratio of 10 %.*

Then the simulations runs the model a 1000 times so a normal distribution can be plotted what the possibility is when the road show fatigue failure of 10 % during aging at the impact of the independent variable ('TI', light, moderate, heavy). This can be observed in figure Appendix G2.

Process description prediction the risk simulation 'Monte Carlo' model, Part 1

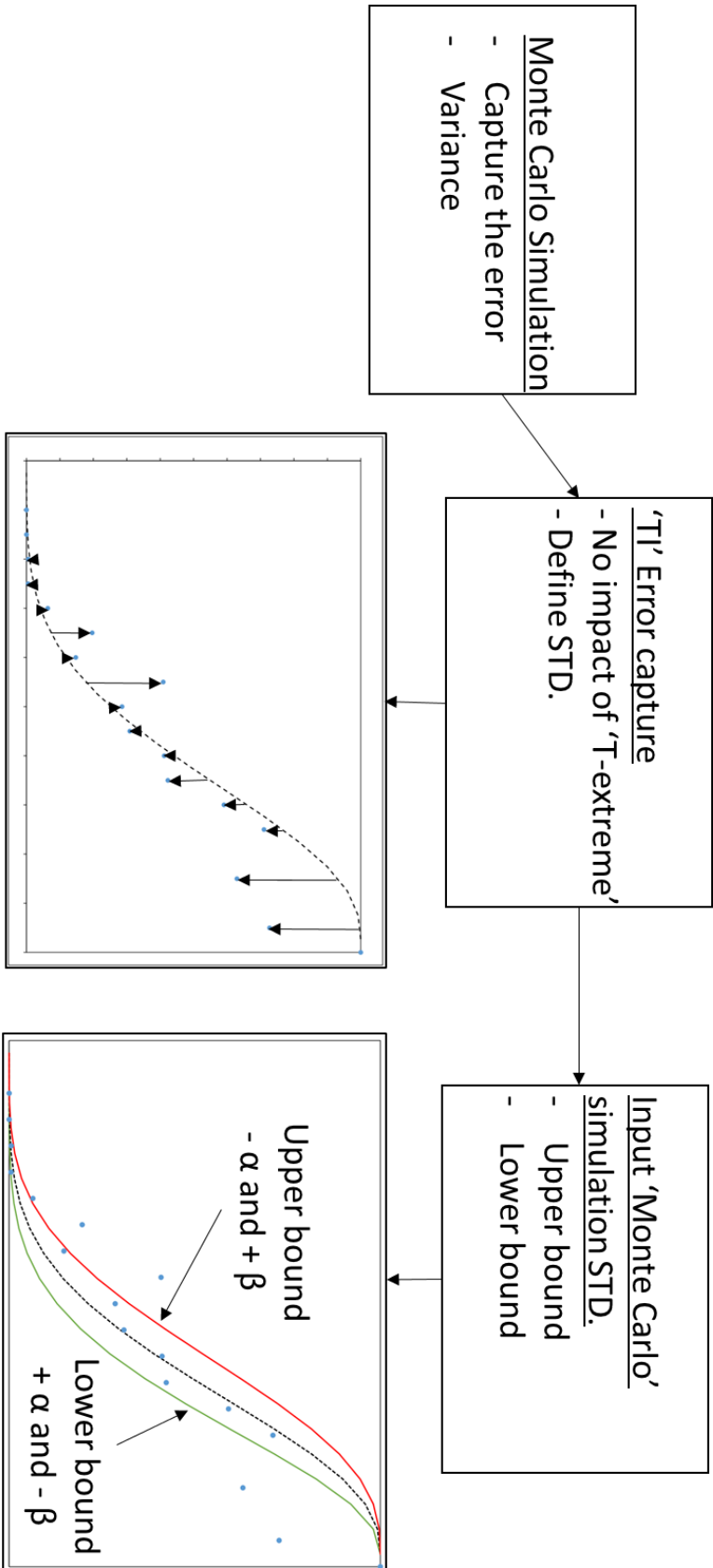


Figure Appendix G1: Process description part 1 of the Monte Carlo simulation model

**Process description prediction the risk simulation 'Monte Carlo' model, Part 2**

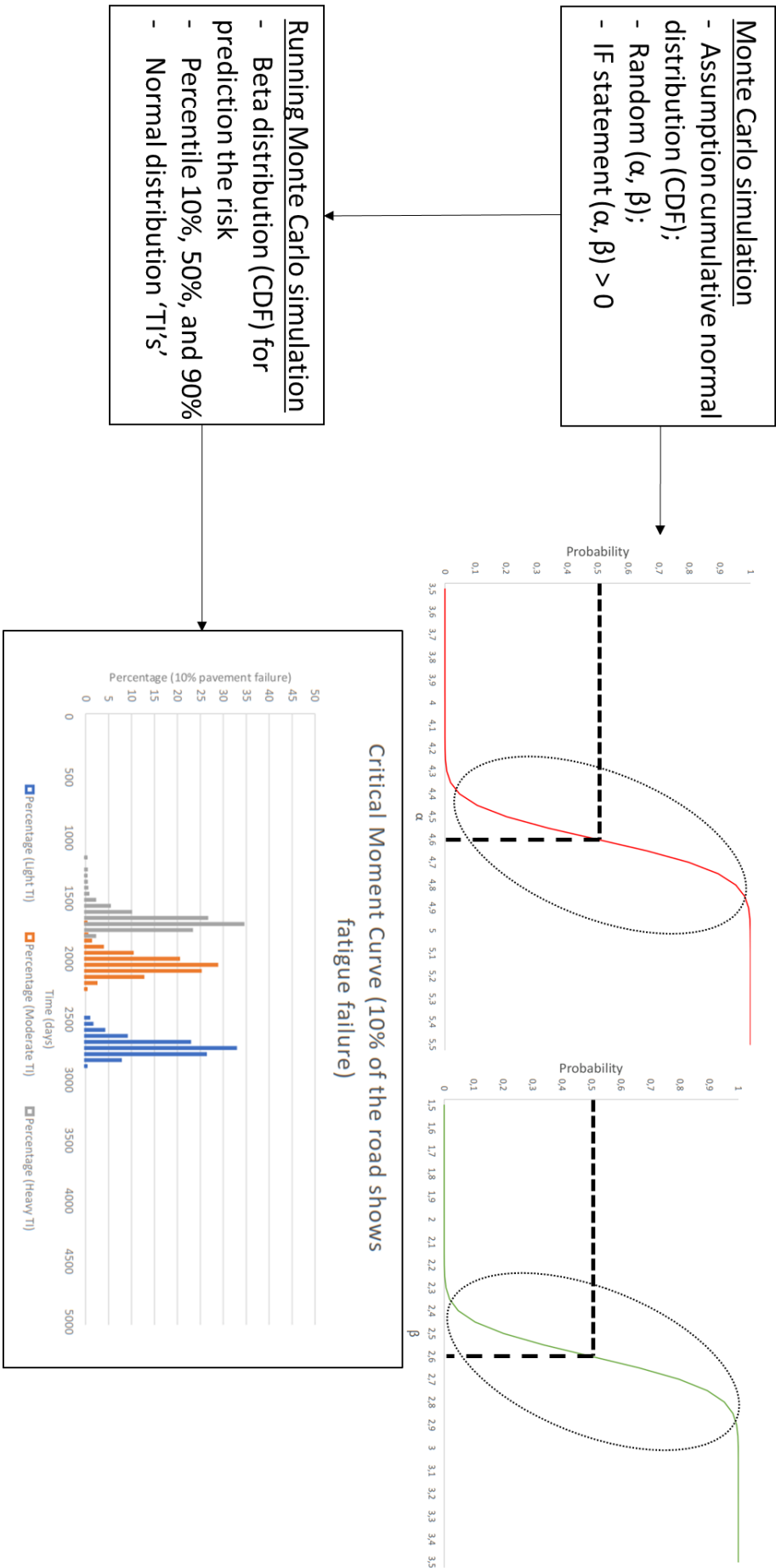


Figure Appendix G2: Process description part 2 of the Monte Carlo simulation model

